Progress in Oceanography 85 (2010) 137–170

Contents lists available at ScienceDirect

Progress in Oceanography

journal homepage: www.elsevier.com/locate/pocean

Review

Biological pump processes in the cryopelagic and hemipelagic Arctic Ocean: Canada Basin and Chukchi Rise

Susumu Honjo [a,b,*], Richard A. Krishfield [a], Timothy I. Eglinton [a], Steven J. Manganini [a], John N. Kemp [a], Kenneth Doherty [a,b], Jeomshik Hwang [a,c], Theresa K. McKee [a], Takatoshi Takizawa [d]

[a] Woods Hole Oceanographic Institution, Woods Hole, MA 02543, USA
[b] McLane Research Laboratories, Inc., East Falmouth, MA 02536, USA
[c] Pohang University of Science and Technology, Pohang 790-784, South Korea
[d] Japan Marine Science and Technology Center, Yokosuka 237-0061, Japan

ARTICLE INFO

Article history:
Received 20 March 2009
Received in revised form 2 February 2010
Accepted 7 February 2010
Available online 19 February 2010

ABSTRACT

The object of this study was to clarify the characteristics of the biological pump system operating in permanently or seasonally ice-covered ocean (cryopelagic) conditions by examining the export of particulate organic carbon (POC) and other components of oceanic particles in the Canada Basin at 120, 200, and 3067 m and in hemipelagic Chukchi Rise waters at 120 m. The first time-series sediment trap (TS-trap), B96-200m, was tethered to an Ice Ocean Environmental Buoy (IOEB) and deployed at 79.1°N, 132.2°E in March 1996; it was recovered in July 1997 at 76.7°N, 131.8°E, having drifted exclusively in the cryopelagic environment. The second TS-trap, S97-120m, also tethered to an IOEB, was launched at 75.2°N, 142.5°E in October 1997 and recovered at 80.0°N 155.9°E, having first traversed the cryopelagic Canada Basin to the west and then the hemipelagic Chukchi Rise. The third TS-trap, CD04-3067m, was deployed in August 2004 beneath the cryopelagic drift route of S97-120m at a water depth of 3067 m on a mooring in the interior of the 3824-m-deep Canada Abyssal Plain. All three TS-traps intercepted marine particles in 21 time-series sets of 17-day intervals for a total of 357 days each. The TMF (annual dried mass flux) intercepted by TS-trap B96-200m was only 0.4 g m^{-2} yr^{-1}, and the FC_{org} (mole annual export flux of POC) was 7.0 mmol C m^{-2} yr^{-1}. The export of FSi_{bio} (mole Si in diatom frustules) and lithogenic particles (in mole Al) were both extremely small. Ballast particle flux was three orders of magnitude smaller than in global epipelagic areas where the biological pump represents an important vehicle for carbon export to depth. The FC_{org} and ballast particles were rather small in the second drifting TS-trap, S97-120m. We conclude that the biological pump is currently ineffective in the cryopelagic Canada Basin so that, instead of removal to deep waters, carbon from primary production (2–4 mmol C m^{-2} yr^{-1}) is remineralized or converted to dissolved organic carbon (DOC) within the surface layer. At 4.3 gm^{-2} yr^{-1}, the TMF sampled by moored TS-trap CD04-3067m was an order of magnitude larger than the mass flux to the traps drifting at 120 and 200 m. The lithogenic particle flux was about 18 times larger than that in S97-120m. FC_{org} sampled by the moored trap was 14.2 mmol C m^{-2} yr^{-1}, 1.4–2 times larger than the POC fluxes encountered by the 120-m and 200-m drifting TS-traps. The $\Delta^{14}C$ values in the POC collected at 120 m indicated that the POC was mostly autochthonous. In contrast, the POC exported to 3067 m had an apparent ^{14}C age of 1900 years, indicating it was predominantly derived from aged, allochthonous carbon. The particle composition was largely invariant throughout the annual cycle, suggesting that the upper ocean ecosystem plays a minimal role in transporting POC and other marine particles. Instead, the majority of POC and other particulate matter is transported laterally to deep ocean layers from the shelf/slope reservoir. On the Chukchi Rise, we found a mosaic of environmental regimes, ranging from the intermittent development of a polynya in some locations where an efficient biological pump operates, to an area characterized by re-suspended allochthonous POC with an exceptionally high *F*Al. Such spatial heterogeneity, and associated sensitivity to the various physical and biogeochemical forcing factors, are distinctive characteristics of hemipelagic Arctic environments.

* Corresponding author. Address: Woods Hole Oceanographic Institution, Woods Hole, MA 02543, USA. Tel.: +1 508 540 1162; fax: +1 508 540 9439.
E-mail address: shonjo@whoi.edu (S. Honjo).

0079-6611/$ - see front matter © 2010 Elsevier Ltd. All rights reserved.
doi:10.1016/j.pocean.2010.02.009

Contents

1. Introduction

Oceanic primary production (PP) that escapes metabolism in surface waters is removed from the euphotic zone and transported by gravitational settling and zooplankton migration to the oceanic interior in the form of particulate organic carbon (POC). There it may feed mesopelagic ecosystems and the benthic community, or it may be buried in underlying sediments. This "biological pump" (called the "ocean carbon pump" by Volk and Hoffert (1985)) is ubiquitous in all pelagic oceans studied so far (reviewed by Honjo et al. (2008)), and is a crucial biogeochemical process for maintaining the ocean's carbon cycles in a steady state. Better knowledge about the functioning of the Arctic biological pump, especially in light of recent significant warming and melting of Arctic sea ice (e.g., Maslanik et al., 1999; Johannessen et al., 1995; Parkinson et al., 1999; Comiso et al., 2003; Stroeve et al., 2007; McGuire et al., 2009, is critical to understanding the far broader changes that are taking place in the current Arctic Ocean (e.g., reviews by Carmack et al. (1995), Macdonald (1996), Morison et al. (2000), Macdonald et al. (2004a,b), ACIA (2004), Rothrock et al. (1999), and Richter-Menge (2008)).

During most of the year, the vast polar pelagic ocean (occupying approximately 4.5 M km^2, including most of the Beaufort Gyre) is covered by sea ice except for small areas of open water (Fig. 1) (e.g., Sakshaug, 2004). We call this region, the coldest open ocean environment on Earth, the "cryopelagic ocean." In the cryopelagic ocean, solar radiation, air-sea exchange, particle fallout from the atmosphere along with its upper ocean dynamics are suppressed, filtered, insulated, and damped by the ice cover. A number of ice-camp expeditions in the Beaufort Gyre and the Central Arctic (reviews by Jones et al. (1990), Carmack (1990), Moritz and Perovich (1996)), particularly the SHEBA (Surface Heat Budget of the Arctic Ocean) study aboard the drifting CCGS *Des Groseilliers* (1997–1998), provided a wide range of critical time-series chemical and physical oceanographic observations spanning almost a year (e.g., Perovich et al., 1999; Uttal et al., 2002). However, investigating the biological pump in the vast expanse of the cryopelagic ocean throughout the High Arctic seasons remains a formidable task.

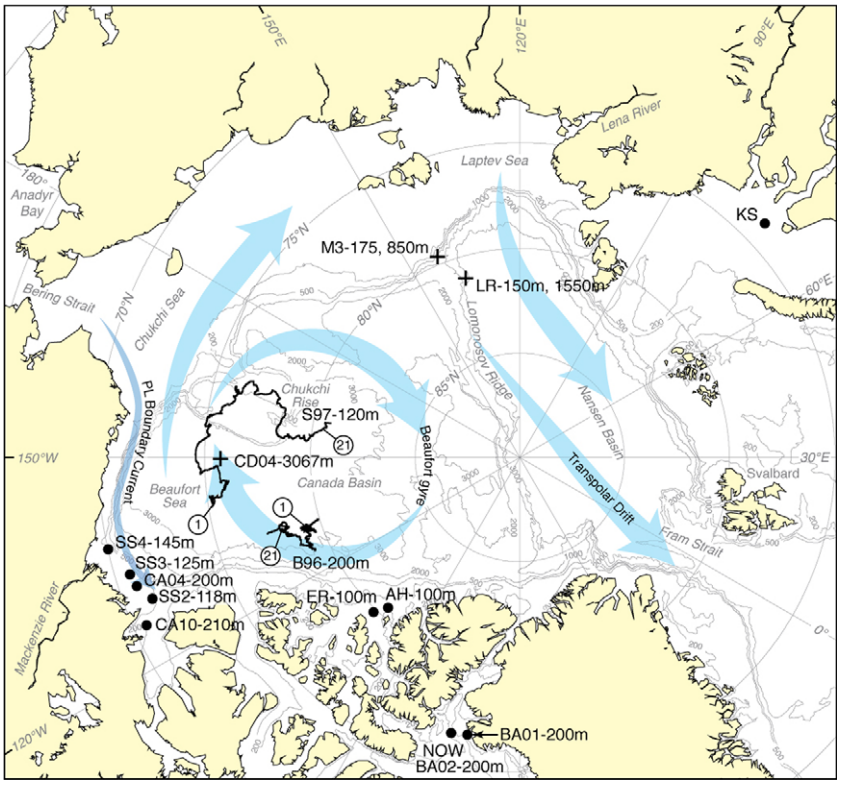

Fig. 1. Yearlong or near-yearlong time-series sediment trap stations in the western Arctic Ocean referenced in this study. Drift tracks of IOEB-tethered TS-traps B96-200m and S97-120m are projected over the Canada Basin and Chukchi Rise. Locations of deep-ocean, bottom-tethered moorings that include TS-trap(s) are indicated by (+). Filled circles indicate TS-trap stations anchored on shelf margins. KS: Kara Sea long-term deployment station (Lisitzin, 1995). NOW: Northern Water Polynya (Hargrave et al., 2002). SS2, SS3, SS4: Canadian Beaufort Sea Shelf stations (O'Brien et al., 2006). LR-150, 1550m: Lomonosov Ridge station (Fahl and Nöthig, 2007). CD04-3067: described in this paper. Blue arrows indicate the general ice drift pattern for the years with a low AO^- index (anti-cyclonic conditions) during 1989–1996. The year 1997 was the transition year to a high AO^+ index (Stein and Macdonald, 2004, Fig. 1.2.9). Details regarding the distribution of trap stations in the Eastern Arctic Ocean is available in Wassmann, 2004, Fig. 5.2 (p. 104) and Fig. 5.7 (p. 115). (For interpretation of the references to color in this figure legend, the reader is referred to the web version of this article.)

Despite these technical challenges, we took on the goal of developing a field system to collect data to enhance understanding of the biogeochemical cycles in the cryopelagic ocean. The specific task was to use time-series sediment traps (TS-traps) mounted on ice-tethered or bottom-anchored moorings. With respect to the former, we developed the Ice Ocean Environmental Buoy (IOEB) for suspending TS-traps beneath the ice (Honjo et al., 1995a,b). The first buoy, deployed in 1996–1997 operated successfully, gathering useful data while drifting in the eastern Canada Basin. Fortuitously, a second IOEB deployed in 1997–1998 drifted not only through a portion of the Beaufort cryopelagic ocean but also traversed the Chukchi Rise for 7 months, thus yielding particle export and other oceanographic time-series data for this significant hemipelagic region in the Arctic Ocean (Krishfield et al., 1999).

We also developed a method for deploying a long-term, seafloor-tethered TS-trap through thick sea ice. Only a few limited studies had described using TS-traps in this environment (e.g., Hargrave et al., 1989; Wassmann, 2004; O'Brien et al., 2006; Fahl and Nöthig, 2007; Forest et al., 2008) (Fig. 1). By applying improved polar ocean mooring technology, we successfully collected a set of annual export particle time-series samples from the abyssal Canada Basin. These samples were collected below the drift track of one of the buoy-tethered TS-traps mentioned above (Krishfield and Proshutinsky, unpublished, WHOI).

Our investigations, based on these three TS-trap deployments and previously published data, show clearly that the biological cycle in the Arctic Ocean is highly unique in both cryopelagic and hemipelagic environments compared to carbon cycles operating in the rest of the world's pelagic oceans, including the High Southern Ocean. We propose two major hypotheses and a paradigm regarding the operation of the biological pump in the Arctic Ocean: *Hypothesis 1*: What we consider to be a normal POC biological pump is strongly limited or ineffective in upper cryopelagic layers (which are equivalent to epipelagic zones of non-Arctic oceans), resulting in negligible export of POC derived from primary production to the interior of the cryopelagic ocean. *Hypothesis 2*: The carbon cycle is maintained in an entirely different manner from that we envision in all other world oceans. Specifically, allochthonous inputs dominate POC supply to the abyssal interior of the Canada Basin. *Paradigm*: Radiocarbon contents, C/N signatures, and temporal variations in particle fluxes suggest that the allochthonous POC is derived from the adjacent margins and may reflect carbon eroded either from the continents or reworked from the continental shelves (Hwang et al., 2008).

When compared to the Canada Basin cryopelagic ocean, an IOEB-based TS-trap that drifted across the hemipelagic Chukchi Plateau (the west side of the Chukchi Rise; Fig. 1) revealed dramatic geographical and seasonal differences in the quantity, nature, and age of POC, as well as sedimentary processes. Moreover, our observation on the hemipelagic Arctic Ocean supports the warning by Wassmann (2004) that our current understanding of changes in the biogeochemical environments of all Arctic Ocean geographic regions is particularly poor. Development of accurate pan-Arctic biogeochemical models is not possible based upon episodic POC export data from sporadic trap stations. The sea ice over the southern Chukchi Plateau now frequently disappears during a large part of the year, replaced by an extensive hemipelagic polynya. Thus, it is likely that this region may have

undergone dramatic changes in particle export processes since our last experiment.

Biogeochemical investigations of the Arctic Ocean have not kept pace with the rapidity of "Arctic change" that is underway, resulting in a woefully insufficient understanding of carbon cycling in the Arctic Ocean. Better knowledge of this critical ocean environment is imperative given the major changes that have been set in motion, such as the drastic reduction of cryopelagic ocean area and the replacement of the ice-edge environment with polynya conditions. We missed a very significant early changes in the Arctic that was linked to switching to the strong positive AO conditions in the late 1980s–early 1990s (Macdonald, 1996). The gap in data collection between the 1997 and 1998 drift of the second IOEB-tethered TS-trap and the 2004–2005 deployment of the anchored TS-trap resulted from general funding limitations shortly before wholesale changes in Arctic conditions were observed. Though it is difficult to assess the consequences of this gap, it seems likely that we may have missed critical events important to understanding the relationship between the upper cryopelagic carbon cycle and that of the abyssal ocean interior.

This review represents our best effort to present what we have learned so far.

2. Stations, field studies, and instrumentation

In late March 1996, B96-200m TS-trap was deployed 200 m below an IOEB set in a large multi-year ice floe at 79.1°N, 132.2°E. It began drifting toward the south in the eastern Canada Basin and was recovered at 76.7°N, 131.8°E in mid April 1997. In early October 1997, we deployed another IOEB with TS-trap at 120 m (S97-120m) in the northern Beaufort Sea, Canada Basin, at 75.2°N, 142.2°E (Table 1). This trap traveled over the Canada Abyssal Plain and the hemipelagic Chukchi Rise (Figs. 2 and 3). Both of these traps operated for 357 days. A third TS-trap was moored to a deep sea, stationary mooring to intercept particles in the interior of the Canada Basin on the Canada Abyssal Plain at 3067 m (CD04-3067m), for 357 days beginning in August 2004. This bottom-tethered mooring was located beneath the drift track of S97-120m's Phase 1 (Figs. 2 and 3). The time-series sediment traps we used were PARFLUX Mark 7-21, manufactured by McLane Research Laboratories, MA USA. These three TS-traps were constructed using titanium alloy and non-water absorbing engineering plastic materials to secure the greater strength and to prevent metallic contamination during long and unpredictable deployments www.mclanelabs.com/sediment.htm.

2.1. IOEB and IOEB-tethered TS-trap deployments, 1996–1998

Woods Hole Oceanographic Institution's (WHOI's) Ice Ocean Environmental Buoy (IOEB) was designed to meet the need for a highly reliable autonomous observatory to continuously collect atmospheric, ice, and underwater data for investigation of the cryopelagic environment that currently occupies a vast region of the Central Arctic Ocean. An IOEB, complete with underwater mooring and all instrumentation, can be deployed either from an icebreaker or supported by air-transport from an ice camp Krishfield et al., 1999; Krishfield et al., http://ioeb.whoi.edu. The IOEB accommodates many sensors to monitor characteristics of the air, sea ice, and the upper ocean, and it transmits the data to the scientific community via satellite in quasi-real time for a year or more (Krishfield et al., 1999). The sensors (with the TS-trap at the deepest point) are mounted along a robust mooring cable tethered to the IOEB and deployed through a 1-m-diameter hole augured into the ice by a

Table 1
Annual export fluxes of elemental ratios: summary and comparison.

	B96-200m	S97-120m	CD04-3067m	LR-150m	LR-1550m	SS4-145m	SS3-125m	SS2-118m
Source	(This article)	(This article)	(This article)	Fahl and Nöthig (2007)	Fahl and Nöthig (2007)	O'Brien et al. (2006)	O'Brien et al. (2006)	O'Brien et al. (2006)
Geographic area	Canada Basin	C.B., Chukchi Rasie	Canada Abyss Plain	Lomanosov Ridge	Lomanosov Ridge	Mackenzie Est.	Off-Tuktoyaktuk	Amundsen Gulf
General environment	Cryopelagic Upp. Oce.	C. pelagic/ over raise	Abyssal Plain interior	Cryopelagic Upp. Oce.	Abyssal slope	Near estuaty	Cont. shelf	Cont. shelf
TS-trap setting	Sea-ice tethered	Sea-ice tethered	Deep ocean interior	Cryopelagic, upper	Deep ocean interior	Plume head	Shelf edge	Shelf edge
Platform	IOEB	IOEB	Mooring	Mooring	Mooring	Mooring	Mooring	Mooring
Location	Table 3	Table 3	75.2°N 150.0°W	81.1°N 138.9°E	81.1°N 138.9°E	69.9°N 138.5°W	71.0°N 134.5°W	71.5°N–128.7°W
Water depth (m)	ap. 3600-3800	ap. 273-3850	3824	1712	1712	200	180	173
Opening date	04/27/1996	10/08/1997	08/13/2004	9/9/1995	9/9/1995	5/4/1987	8/4/1987	6/3/1987
Closing date	04/19/1997	09/30/1998	7/15/2005	8/16/1996	8/16/1996	8/12/1988	7/13/1988	8/22/1998
Days open	357	357	357	336	336	260	292	240
TS-increments #(days)	21 (17)	21 (17)	21 (17)	20 (variable)	20 (variable)	20 (10, 15)	22 (10)	18 (14)
*F*TDW $gm^{-2}\ yr^{-1}$	0.4	3.8	4.3	7.8	14.0	199.9	21.4	81.4
*F*OM $gm^{-2}\ yr^{-1}$	0.4	3.0	0.7	5.0	4.5	16.3	2.8	9.8
*F*Litho $gm^{-2}\ yr^{-1}$	0.0	0.8	3.6	2.9	9.6	196.3	96.0	73.5
%POC	21.8	15.4	4.0	15.1	6.0	4.4	7.1	6.4
%OM (%C × 1.87)	40.8	28.9	7.4	63.6	31.8	8.3	13.3	11.8
%AI	0.1	1.8	6.9	3.0	5.6	8.1	7.9	6.1
%Litho (%AI × 12.15)	0.7	21.4	83.4	36.4	63.2	92.4	97.2	88.2
*F*Corg mmol C $m^{-2}\ yr^{-1}$	7.0	49.0	14.2	98.2	69.8	724.3	126.1	436.9
*F*Norg mmol N $m^{-2}\ yr^{-1}$	0.7	6.4	1.2	n/a	n/a	n/a	n/a	n/a
*F*Cinorg mmol C $m^{-2}\ yr^{-1}$	2.0	2.4	1.4	7.0	4.2	70.5	6.8	3.2
*F*Sibio mmol Si $m^{-2}\ yr^{-1}$	0.3	17.7	1.8	32.0	39.4	237.9	33.6	135.1
*F*AI mmol AI $m^{-2}\ yr^{-1}$	Trace	2.5	10.9	8.7	29.1	598.6	62.6	182.2
Co/N (mol/mol)	9.7	7.7	12.0	n/a	n/a	n/a	n/a	n/a
Co/Ci	3.4	20.5	10.1	14.0	16.5	10.3	18.5	117.6
Co/Si_{bio}	27.2	2.8	7.7	3.1	1.8	3.0	3.7	3.2
Si_{bio}/Ci	0.1	7.4	1.3	4.6	9.3	3.4	4.9	36.4
Co/AI	>875	19.8	1.3	11.3	2.4	1.2	2.0	2.4
% Ternary ratio	75:22:03	71:03:26	81:08:11	72:05:23	62:04:35	70:07:23	76:04:20	76:01:23

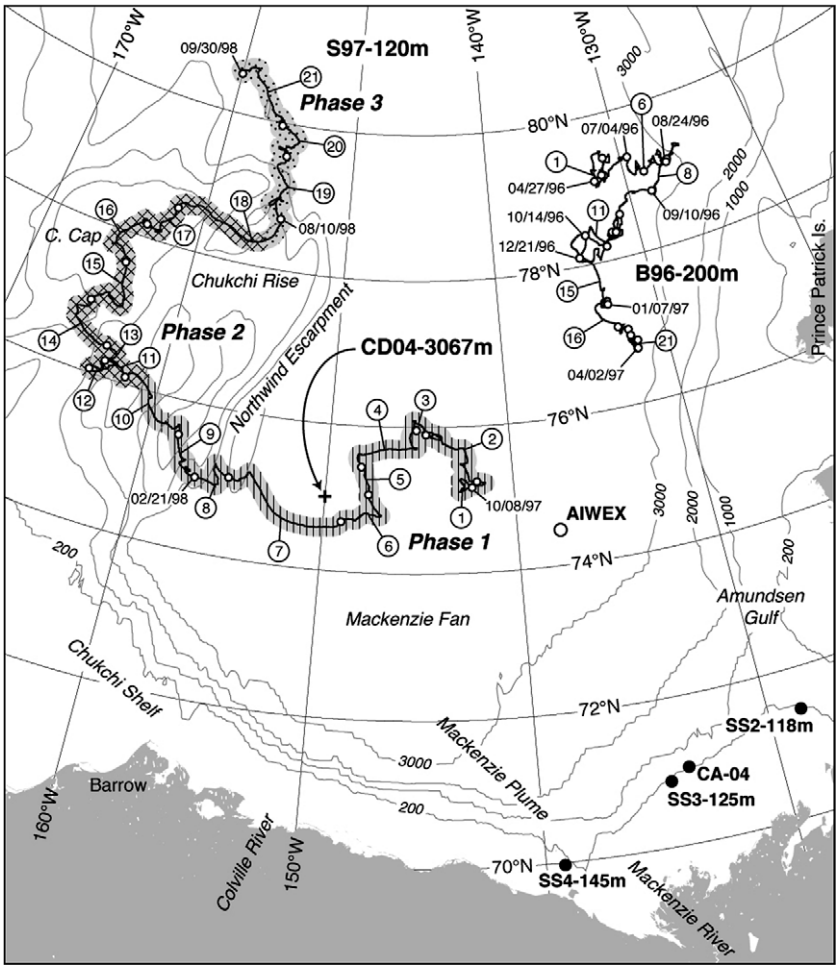

Fig. 2. Detailed drift tracks and trap opening-closing locations for TS-traps B96-200m and S97-120m (both marked by open circles) in the Canada Basin and over the Chukchi Rise. TS-trap CD04-3067m (+ symbol) was moored 757 m above the 3824-m-deep seafloor on the Canada Abyssal Basin. The numbers in circles are period numbers that correspond to Tables 3 and 4. Not all period numbers are indicated for the B96-200 m drift; refer to Krishfield, since 1996, at http://ioeb.whoi.edu for further information. Stations on the Mackenzie Shelf Edge (SS-2, SS-3, and SS-4) are major moored TS-trap stations (O'Brien et al., 2006). SS-4-145m was deployed in the area of the Mackenzie plume head. For detailed information on this experiment conducted by the Institute of Ocean Sciences, Sydney, Canada, see O'Brien et al. (2006). CD-04 near SS-3 was deployed by Québec-Océan, Université Laval, Canada (Forest et al., 2007).

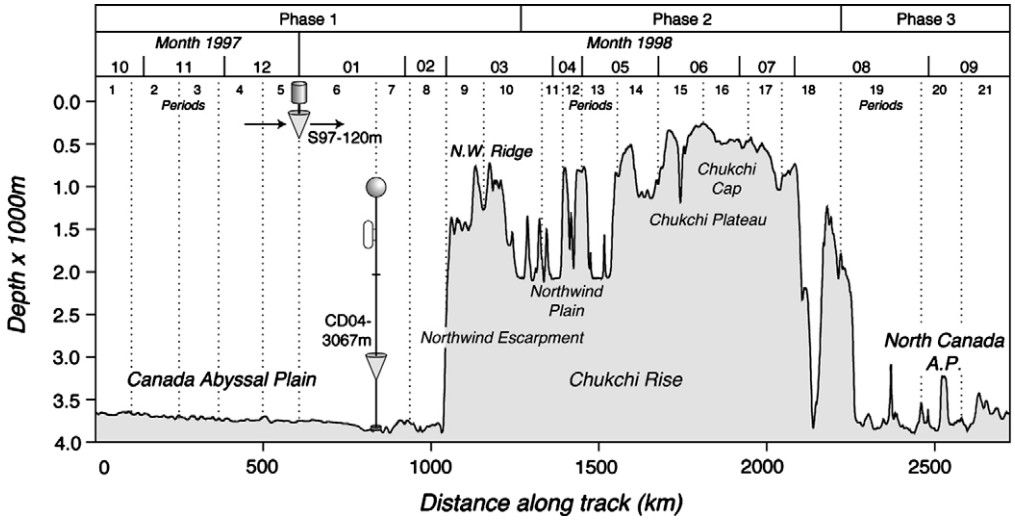

Fig. 3. Topographic profile along the drift route of TS-trap S97-120m. The top four lines show boundaries of IOEB S97 phases, years, and months, and open-close period numbers for TS-trap S97-120 during this passage. The authors compiled this topographic profile from ETOPO5 bathymetry data (National Geophysical Data Center, 2006). Digital relief was obtained by averaging the ocean depth over a 2-min diameter around a GPS location every 3 h throughout the drift of IOEB S97. The location of the seafloor-tethered CD04-3067m mooring is approximate.

hot-water ring jet. A 135-kg iron anchor attached below the TS-trap keeps the wire taut. In order to monitor the strain on the mooring under the ice, particularly during ice ridge or lead formation, an electronic stress gauge and a tilt-detector is installed at the upper end of mooring, and data from these sensors are transmitted to WHOI every 24 h throughout the IOEB deployment.

Both IOEB-tethered TS-traps (and the moored TS-trap described below) intercepted settling particles during uniform, 16.81-day intervals (rounded up to 17 days in this paper) for 21 periods totaling 357 days. The exact start and end dates of this schedule differed due to the particular deployment opportunity; the trap schedules were recorded electronically. All three TS-traps worked flawlessly; the internal electronics of the Mark 7-21 TS-trap recorded consistent open/close commands and successful execution of all other program components.

To preserve the intercepted organic matter, each TS-trap sample bottle was filled with a 0.3% *in situ* seawater solution of $HgCl_2$ immediately before deployment. This preservative has been applied successfully for long-term deployment of TS-traps with a buffered seawater solution of formalin, particularly in the JGOFS Southern Ocean experiments as one of that program's standard practices (Honjo et al., 2000). $HgCl_2$ and the samples contaminated by $HgCl_2$ solution are highly toxic and must be handled carefully by following proper chemical hygiene plans.

2.2. Location and drift vectors of the IOEB-tethered TS-traps

IOEB locations were updated 24–28 times per day via ARGOS satellite. Thus, we have precise locations for TS-traps during sampling-period openings and closings (http://ioeb.whoi.edu, Fig. 2). The drift tracks of five independent IOEBs deployed in this area (e.g., Krishfield et al., 1999), including IOEBs B96 and S97, demonstrate the Beaufort Gyre circulation that prevails over the Canada Basin and the Chukchi Plateau (Fig. 1; e.g., Stein and Macdonald, 2004). IOEB B96 drifted 250.8 km in 357 days (an average daily displacement of 703 m d^{-1}) between its first opening and its last closing. IOEB S97 traveled 722.42 km for an average daily displacement of 2023 m d^{-1} at a speed almost three times that of IOEB B96. However, the total drift distance for IOEB B96 (the sum of the IOEB's detailed movements calculated hourly) was 1809.94 km, compared to 2723.63 km for IOEB S97, suggesting that B96's movements contained higher frequency variability (Table 2 and Fig. 2). B96 was deployed off the Queen Elizabeth Islands in multi-year ice in 1996–1997. The ice thickness along the S97 route was less than half that of B96 (Krishfield et al., 1999), suggesting that S97 was in second-year ice.

The average drifting rates of IOEBs B96 and S97, equivalent to 5.6 and 8.8 cm s^{-1}, respectively, are comparable to deeper-ocean current velocities where export flux measurements of particles have been made in many other lower-latitude ocean areas. However, the exact movements of the TS-traps at 200 m and 120 m relative to the water is uncertain because the relationship between IOEB drift and deeper-ocean currents is not clear.

Table 2
IOEB-TS-trap drift summary.

	B96-200m	S97-120m
Total drift distance (km)	1809.9	2723.6
Average IPL	0.14	0.27
Ave. displace/d (m)	702	2023
Ave. dift/d (m)	5068	7629
Tethered to: depth of TS-trap	Ice floe-IOEB 200 m	Ice floe-IOEB 120 m
Time segments	21	21
Unit period (days)	17	17
Accumulated days	357	357
First open date	04/27/1996	10/08/1997
Last close date	04/19/1997	09/30/1998
1st open location	79.1°N 132.2°E	75.2°N 142.2°E
Last close location	76.7°N 131.8°E	80.0°N 155.9°E

It is important to recognize the difference between a drifting time-series and bottom fixed time-series trap methods. Both intercept and collect exported settling particles at designated depth and for durations at one anchor station. In the case of the former the anchor position changes by time. We regarded each period as an independent mooring with 17 days of the open/close duration at a location that represented by the mid-day of a period. However just because an export event was not detected in a drifting trap data set, it does not mean that the event did not take place at a location(s) before or after the trap passed through it (them). This problem pervades the data from drifting platforms including SHEBA-CCGS *Des Groseilliers* ice camp (Sections 2.3 and 6.5.4–6.5.5).

2.3. 1997–1998 parallel drift of SHEBA-CCGS Des Groseilliers and S97-IOEB

The SHEBA research program was designed to investigate the processes that determine the surface energy budget and the sea-ice mass balance in the Arctic. SHEBA's main ice camp was the 98-m Canadian Coast Guard Ice Breaker *Des Groselliers*, which drifted in the cryopelagic Beaufort Sea and Chukchi Rise area close to and as approximately coincident with the drift of IOEB S97. Large sets of ocean, ice, and atmospheric data were collected from *Des Groselliers* beginning in mid October 1997 (Perovich et al., 1999; Uttal et al., 2002). Deployed about 20 nmi southeast of *Des Groselliers*, the S97-120m TS-trap first opened on October 8, 1997. Both *Des Groselliers* and IOEB S97 collected data for a year while keeping in remarkably close proximity, maintaining an average separation of about 27 nmi as they drifted from 76°N, 146°W to 75.5°N, 159°W. Although IOEB S97's drift lagged that of Des Groselliers by 5–6 days, their drift routes crossed three times. After the last crossing event, the ice took both northward, and their separation increased to >100 nmi.

2.4. Bottom-tethered TS-trap deployment in the abyssal Canada Basin, 2004

A TS-trap (CD04-3067m) was deployed on a bottom-tethered ocean profiler mooring at 75.2°N, 150.0°E in August 2004, before the September ice-minimum period, at 3067 m in collaboration with the Joint Western Arctic Climate Study (JWACS) and Beaufort Gyre Observing System (BGOS, www.whoi.edu/beaufortgyre; Proshutinsky et al., 2009). An MMP (McLane Moored Profiler) flawlessly shuttled 322 times (once a day) between 61 to 2003 m in total of 625 km along the BGOS mooring to gather various hydrographic data including CTD and current vectors while CD04-3067 m was operating. http://www.whoi.edu/beaufortgyre/pdfs/BGFE_MMP_Processing_2004-final_5-31-05.pdf. Web relaese: Krishfield et al. (2004). This mooring was set on one of the deepest flats in the Canada Abyssal Plain, at the base of the Mackenzie Fan (e.g., Macdonald et al., 2002), where there are no obstructing bottom topographies within 50 km in all directions applying newly developed deployment procedures (Ostrom et al., 2004; Kemp et al., 2005). However, there are imposing submarine topographies to the west and to the south. They are: (1) the very tall Northwind escarpment to the west (its foothills begin about 120–150 km from the mooring station) and (2) the Beaufort margin to the south, arguably the most precipitous continental slope in the Arctic Ocean. The closest distance from the CD04-3067m mooring to the shelf edge near Point Barrow was about 330 km (Figs. 2 and 3).

3. Laboratory analysis

3.1. Total dry mass flux and biogeochemical elemental compositions

Laboratory methods used to estimate total (dry) mass flux (TMF) and fluxes of biogeochemical elements from the samples collected during the opening periods of three TS-traps were essentially the same as those published in US-JGOFS reports (e.g. Honjo et al., 2000; Collier et al., 2000; reviewed in Honjo et al. (2008)). After sieving of particles collected during a sampling period, the particles that passed through the 1-mm mesh nylon sieve (<1 mm particles hereafter) were split into 10 equal aliquots using a McLane™ WSD-10 wet-sample divider; this method exhibited a statistical splitting error of 3.4% during processing deep Arabian Sea and equatorial trap samples based on three 1/10th aliquots that were filtered onto a pre-weighted polycarbonate filter with nominal pore size of 4.5 μm, rinsed with Milli-Q water and dried overnight at 60 °C. No >1-mm fraction was collected from TS-trap CD04-3067m. The TMF from each period was calculated from one 1/10th aliquot representing each of 21 periods, and a combination of four 1/10th aliquots from each period was used for detailed chemical and radiochemical analysis for TS-traps S97-120m and CD04-3067m samples.

Modified processing procedures were used for B96-200m samples because of the extremely small size of samples collected by this TS-trap. Eleven B96-200m time-series samples were too small to yield reliable TMF measurements; thus, we did not wet-divide samples but rather weighed all the material after drying to obtain TMF for each period. We combined the dried sample material from Periods 1 to 5 and Periods 8 to 21. Then, we determined the fluxes of five elements for five periods and calculated elemental fluxes for four periods where more reliable TMF values were available. We also used average TMF and average elemental fluxes from Periods 1 to 3 of S97-120m, which yielded very small particle masses.

We used 1–5 mg of dried sample in each of the following chemical analyses: Particulate inorganic carbon (PIC) was determined using a UIC™ coulometer with acidification module and 2 ml of 1 M phosphoric acid. PIC determinations on Specpure™ $CaCO_3$ reference material indicated 97% recovery, and a precision with based on replicate samples of 3.8% RSD (relative standard deviation). Total C and N concentrations were determined with the Perkin-Elmer™ Elemental 2400 analyzer with 98% and 97% recoveries, respectively, using acetanilide reference material; replicate samples showed precision of 1.5% and 4.3% RSD, respectively. POC was determined by the difference between total carbon and PIC concentrations. Total Si and Al concentrations were determined by ICP-ES using a Jobin-Yvon-Horiba™ Ultima 2-ICP elemental spectrometer. Samples were liquefied with a modified high-temperature alkali-fusion method using Alfa-Aesar™ Spectroflux™ and 5% nitric acid. The sample accuracies of Si and Al concentrations as determined with USGS MAG1 reference material, were 95% and 92%, respectively, with precision from replicate samples of 5.2% and 2.8% RSD, respectively. Si_{bio} was determined by the difference between total Si and lithogenic Si concentrations. The lithogenic Si content was estimated by multiplying the Al concentration by the Si/Al ratio (3.42) in average Earth Crustal Material. Total lithogenic material concentration was calculated by multiplying the Al concentration in the sample by 12.15, based on the Al concentration in crustal material of 8.23% (Taylor and McLennan, 1981).

The daily export fluxes F of each element are calculated from sampling-period length (17 days) and the 0.5 m^2 area of the TS-trap's aperture. Five key export fluxes are expressed in this paper: FC_{org}, FN_{org}, FC_{inorg}, FSi_{bio} and FAl, in mole units expressed either per year (mmol[C, N, Si, Al] $m^{-2}\,yr^{-1}$) or per day (in μmol[C, N, Si, Al] $m^{-2}\,d^{-1}$).

3.2. Carbon isotope composition

The ^{13}C ($\delta^{13}C$) and radiocarbon ($\Delta^{14}C$) content of the POC collected for each period, or for bundled periods for S97-120m and CD04-3967m TS-traps, were measured by the National Ocean Sciences Accelerator Mass Spectrometry Facility at the Woods Hole Oceanographic Institution. Three to five 1/10th aliquots were freeze-dried and treated with concentrated HCl to remove PIC, and then further processed following standard procedures for carbon isotopes (McNichol et al., 1994). Initial results of carbon isotope values were published in Hwang et al. (2008).

4. Annual flux of biogenic and lithogenic particles in the Beaufort Gyre

4.1. Annual flux of particles collected by sea-ice tethered TS-traps in the upper ocean

Surprisingly, the annual TMF estimated from the particles intercepted in the cryopelagic eastern Canada Basin by TS-trap B96-200m over a year's drift was only 0.4 g $m^{-2}\,yr^{-1}$ (approximately 1 mg $m^{-2}\,d^{-1}$; Table 1). This is the smallest annual TMF so far reported from the world ocean's epipelagic depths. The entire drift of IOEB B96 was under genuinely cryopelagic ocean conditions; the ocean it traversed was covered with arguably the thickest multi-year sea ice in the Arctic Ocean (e.g., Bourke and Garrett, 1987; Rothrock et al., 1999).

S97-IOEB (and SHEBA Ice Camp) drifted across the cryopelagic ocean in the beginning, to the south of the B96 track, where there was a similar, but thinner, ice cover. We divided drift track of S97-120m into three phases (Figs. 2-4-2). It traveled roughly along 75°N latitude from early October 1997 until late February 1998 (S97-120m-Phase-1, Periods 1–8; Fig. 3), spending approximately 38% (883 km) of its drift distance in ice-covered seas. S97-IOEB next entered the Chukchi Rise area and traveled there till mid August 1998, approximately tracing the shallowest topography of the Rise to the north (1045 km, 45% of its total drift distance; Phase-2, Periods 9–18, spring to summer). S97 then crossed the northern Canada abyssal basin before drifting to the Mendeleyev abyssal plain and completing its journey on September 30, 1998 (Phase-3, Periods 19–21, autumn; Fig. 3).

The average daily TMF during S97-120m-Phase 1 was 2.0 mg $m^{-2}\,d^{-1}$ (0.7 g $m^{-2}\,yr^{-1}$). The annual flux was larger than but comparable to the annual TMF of B96-200m (0.4 g $m^{-2}\,yr^{-1}$). The TMF increased 10 times during Phase 2, reaching 20.5 mg $m^{-2}\,d^{-1}$ (7.5 g $m^{-2}\,yr^{-1}$). Phase 2 accounted for approximately 64% of annual TMF and 77% of annual FC_{org}; Phase 3 FC_{org} remained relatively large, but smaller than that of Phase 2. The large TMF, 10 mg $m^{-2}\,d^{-1}$ (15%), during three periods in late summer-early autumn was attributed to the export of blooming pteropods' shells contributing a large amount of FC_{inorg}.

The annual FC_{org} for B96-200m was 7.0, comparable to that for S97-120m-Phase 1, which was 10.2 mmol C $m^{-2}\,yr^{-1}$. S97-120m FC_{inorg} was 0.5 mmol C $m^{-2}\,yr^{-1}$, much smaller than that for B96-200m (2.0 mmol C $m^{-2}\,yr^{-1}$), perhaps because Phase 1 occurred essentially in winter and did not include ice-edge conditions; thus, there was no export of pteropod shells. The annual FSi_{bio} for B96-200m and S97-120m-Phase 1 were comparable, 0.3 and 0.5 mmol Si $m^{-2}\,yr^{-1}$, respectively. It is noteworthy that annual lithogenic particle flux for B96-120m as represented by Al flux of <0.1 mmol Al $m^{-2}\,yr^{-1}$ was extremely small (see Section 2.2). The daily FAl during S97-120m-Phase 1 ranged from 0.7 to 2.5 mmol Al $m^{-2}\,d^{-1}$ (0.6 mmol Al $m^{-2}\,yr^{-1}$). The FAl during S97-120m-Phase 1 was also small, 0.6 mmol Al $m^{-2}\,yr^{-1}$.

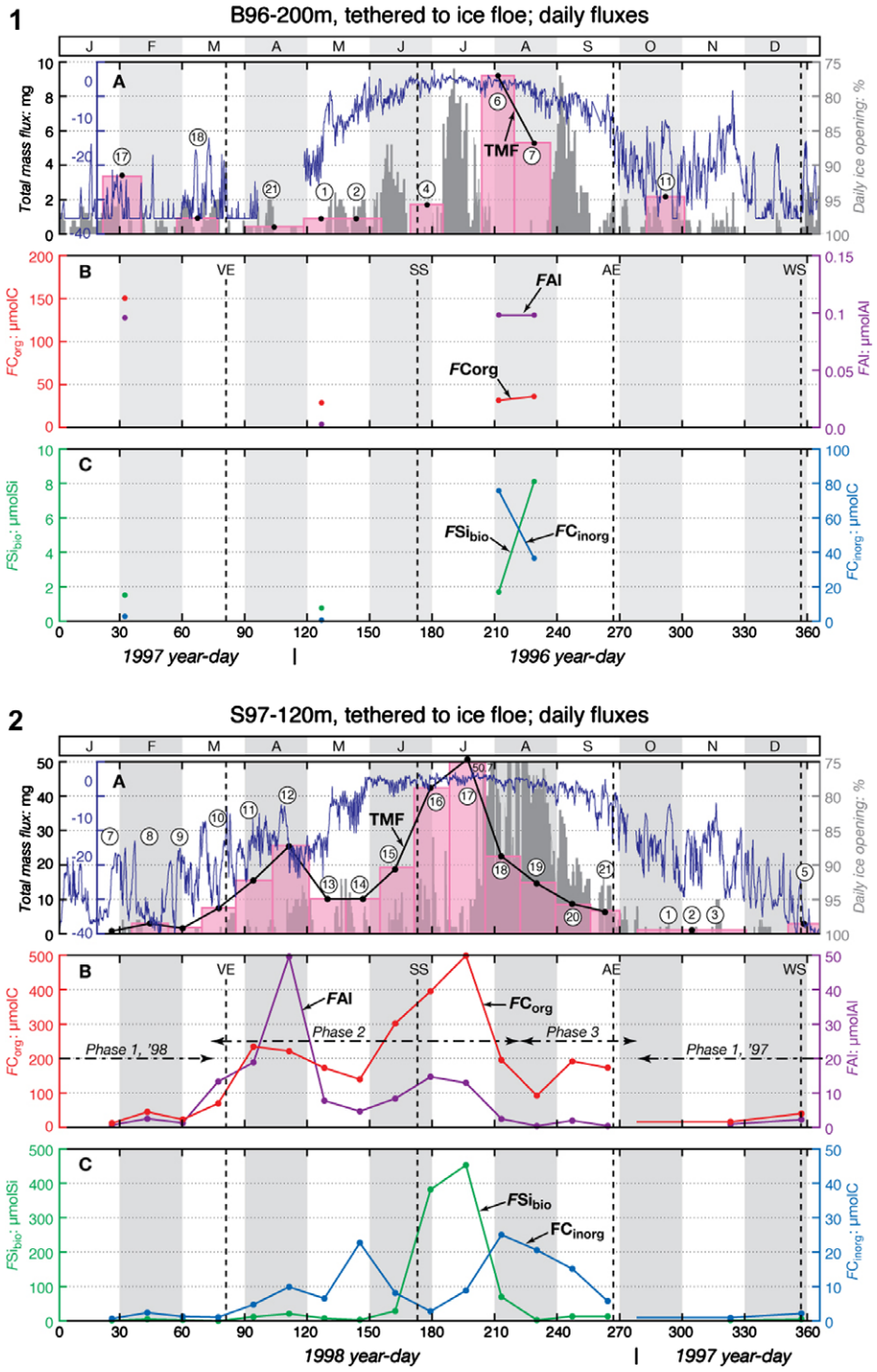

Fig. 4. Fig. 4-1 to 4-6 displays time-series export fluxes of the total mass flux and the export fluxes of four biogeochemical element types. The yearlong TS-trap deployments began at arbitrary points in a year and thus extended into the next year in most cases, making it difficult to compare the timing of critical events such as flux maxima or minima. The figure shows 21 periods arranged in a year that begins January 1 and ends December 31; months are indicated at the top of each figure. At the bottom of the figures, year-days and the year of the experiment are displayed corresponding to the monthly calendar at the top. At bottom, a short vertical line separating experiment years indicates the date that the 21st sampling cup was closed. Panel A: the pink shaded step diagram shows time-series total dry mass flux (TMF in mg m^{-2} d^{-1}); the black plot line connects the midpoint of each of the data periods where export flux was successfully acquired. The scale at right indicates daily ice opening in % of the 25 km^2 satellite-image footprint over drifting IOEB or mooring locations, synchronized with each TS-trap schedule throughout the deployment term; this indicator is absent in Fig. 4-5 and 4-6. The blue lines in Fig. 4-1A and 4-2A plot air temperature recorded by IOEB S97 at 1.5 m above the ice surface (Krishfield et al., 1999). Panels B and C: comparison displays of annual time-series export fluxes of POC (FC_{org}), PIC (FC_{inorg}), biogenic Si (FSi_{bio}), and lithogenic Al (FAl) in µmol m^{-2} d^{-1} (Fig. 4-1 to 4-4 and 4-6) or mmol m^{-2} d^{-1} (Fig. 4-5). VE, SS, AE, and WS on Panel B indicate vernal equinox, summer solstice, autumn equinox, and winter solstice. In Fig. 4-3, Panel D shows the annual current vector measured at 2000 m along the CD-04 mooring (Proshutinski and Krishfield, unpublished), Panel E depicts time-series of $\Delta^{14}C$ and $\delta^{13}C$ disequilibrium indices (Hwang et al., 2008; Hwang and Eglinton, 2007, unpublished). Fig. 4-4-1 and 4-4-2 shows export flux data collected by two sediment traps located at depths of 150 m and 1550 m on a Lomonosov Ridge mooring. Data from Fahl and Nöthig (2007) and O'Brien et al. (2006) was recompiled into a line diagram for Fig. 4-4 to 4-6 after conversion to mole-flux units. (For interpretation of the references to color in this figure legend, the reader is referred to the web version of this article.)

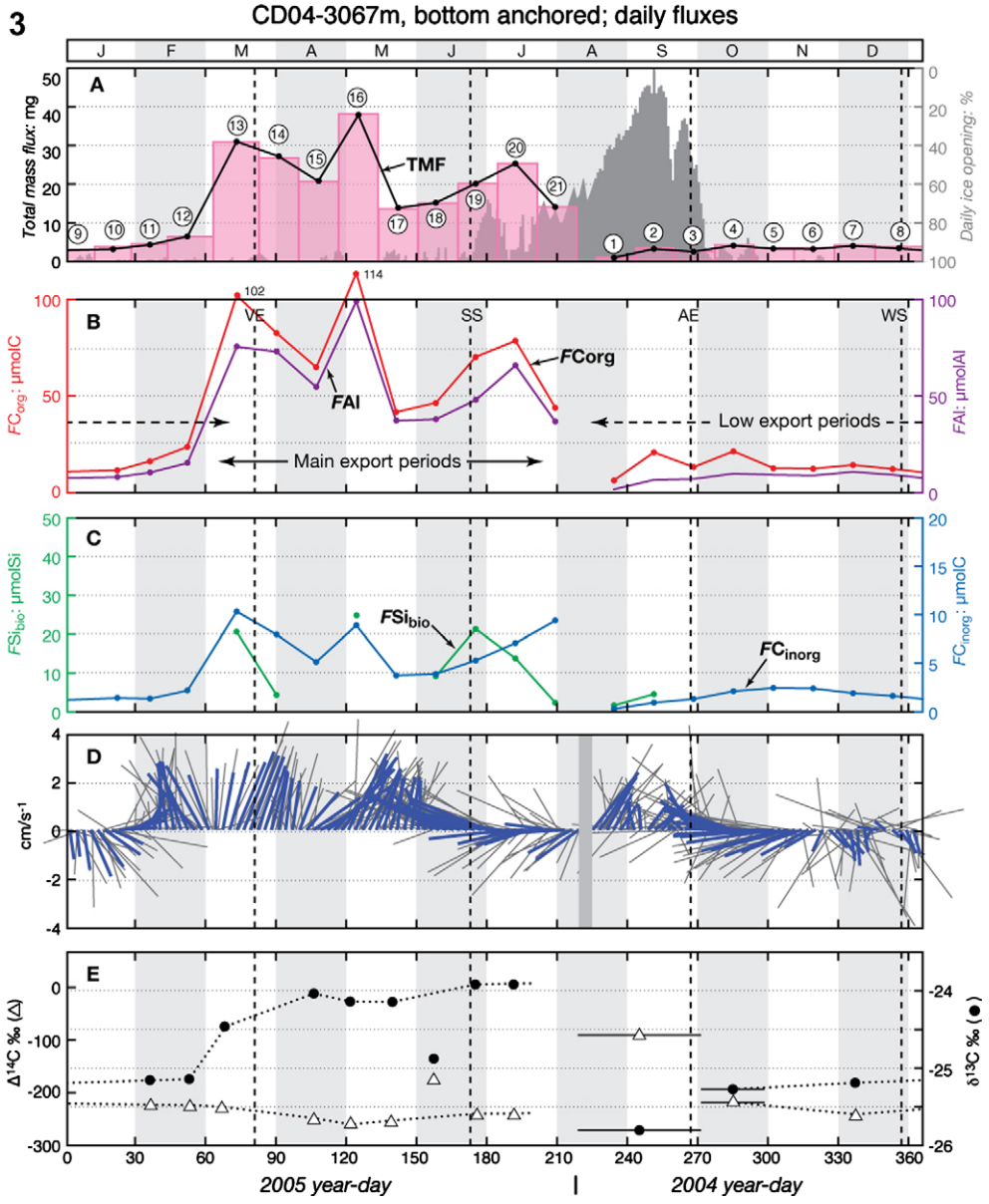

Fig. 4 (*continued*)

4.2. Annual flux of export particles over the Chukchi Rise (S97-120m-Phase 2)

The FC_{org} for S97-120m-Phase 2 was 225 mmol C m^{-2} yr^{-1} compared to only 7–10 mmol C m^{-2} yr^{-1} for S97-120m-Phase 1 and B96-200m. During Phase 2, while the TS-trap was located above the Chukchi Rise, annual FSi_{bio} was as much as 97 mmol Al m^{-2} yr^{-1}, while it was 1.0 mmol Al m^{-2} yr^{-1} during Phase 1. The FC_{inorg} for S97-120m-Phase 2 was relatively small compared to FSi_{bio} of 9.1 mmol C m^{-2} yr^{-1} (in the <1 mm fraction). The *F*Al during Phase 2 was 13.4 mmol Al m^{-2} yr^{-1}, much larger than the flux observed for B96-200m and S97-120m-Phase 1 (0.6 mmol Al m^{-2} yr^{-1}).

4.3. Annual particle export to the deep interior Canada Basin collected by a moored TS-trap

The annual TMF, 4.3 mg m^{-2} yr^{-1}, estimated from the samples collected by TS-trap CD04 set at 3067 m, about 800 m above the abyssal basin floor (3824 m), was an order of magnitude larger than that of the export flux measured in overlying upper pelagic waters by both B96-200 m and S97-120 m-Phase 1, 0.4 and 0.75 mg m^{-2} yr^{-1}, respectively (Section 3.1). This large annual TMF difference between the deep interior layer export flux and the upper ocean was primarily attributed to a very large annual export of lithogenic particles (as represented by Al flux of 10.9 mmol Al m^{-2} yr^{-1}) to the deep layer, where the lithogenic particle content of CD04-3067m comprised as much as 85 wt% of the annual TMF.

Annual FC_{org} was also significantly larger for CD04-3067m: 14.2, compared to 7.0 and 10.2 mmol C m^{-2} yr^{-1} in B96-200m and S97-120m-Phase 1, respectively. The annually averaged C/N ratio was 14.6 (s = 4.3), larger than in the sample collected by S97-120m-Phase 1 (C/N = 7.3). The annual export flux of other biogenic elements, FC_{inorg} and FSi_{bio}, for CD04-3067m was very small, similar to that for the IOEB-tethered TS-trap samples: only 1.4 mmol C m^{-2} yr^{-1} (B96-200m) and 1.8 mmol Si m^{-2} yr^{-1} (S97-120m). However, they were much smaller than S97-120m-Phase 2 samples.

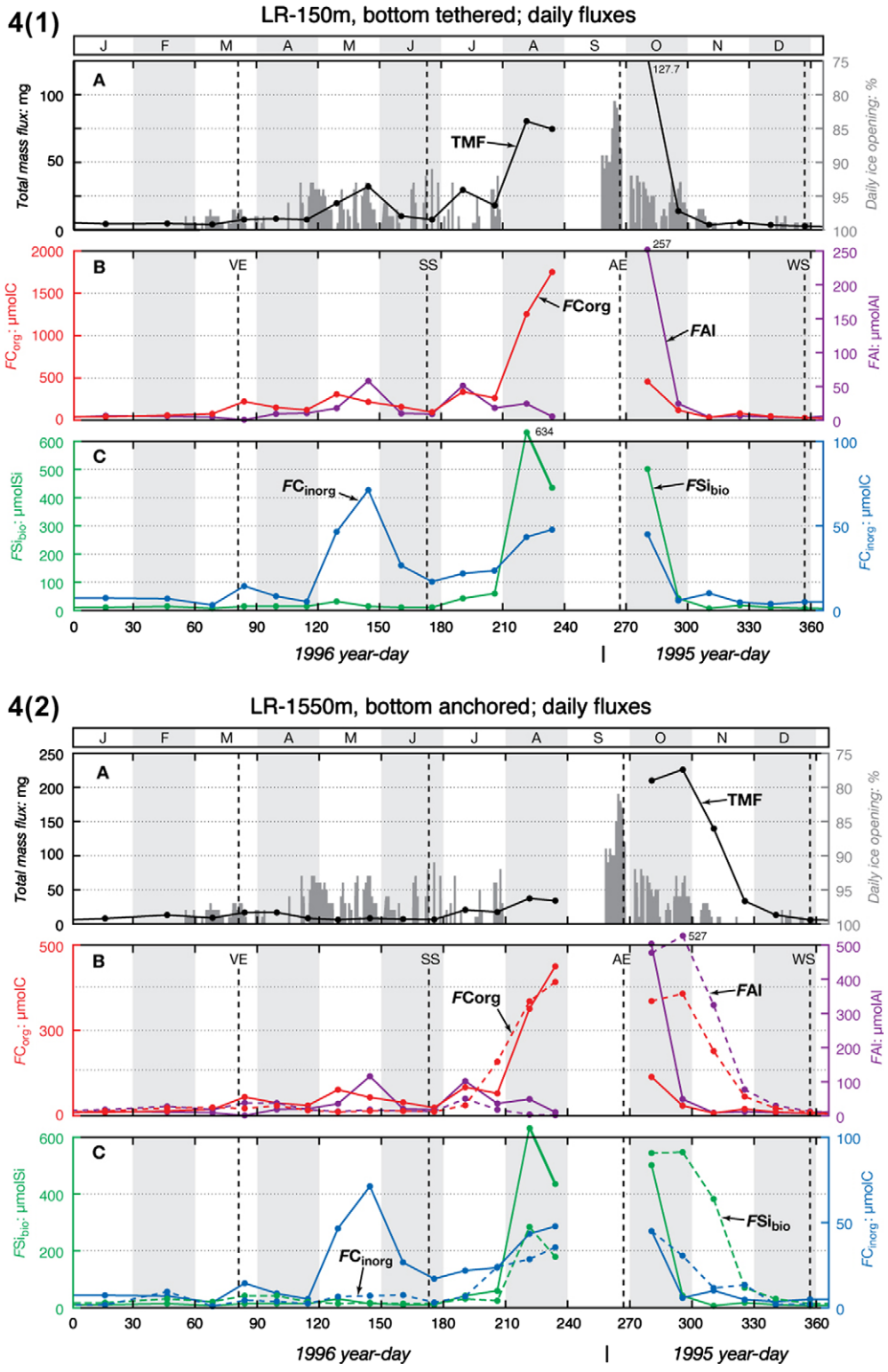

Fig. 4 (*continued*)

5. Seasonal progression of particle export in the Canada Basin

5.1. Seasonal particle export in the cryopelagic eastern Canada Basin as assessed from samples collected by TS-traps B96-200-m and S97-120m-Phase

TS-trap B96-200m shows an inconspicuous FC_{org} maximum during late July to late August, with an export of 32–36 µmol C m^{-2} d^{-1} at 200 m. We observed uncharacteristically large FC_{org}, 150 µmol C m^{-2} d^{-1}, during Period 17 in late January to early February. Associated with some PIC and biogenic opal particles, a relatively large yellowish aggregate of approximately 3.1 mg (dry weight) was recorded with a high C/N ratio of 14. This single aggregate contributed 36% and 25% of annual FC_{org} and FN_{org} (maximum estimates), respectively. We assume this object is a post-preservation re-aggregate comprised of a transparent exo-

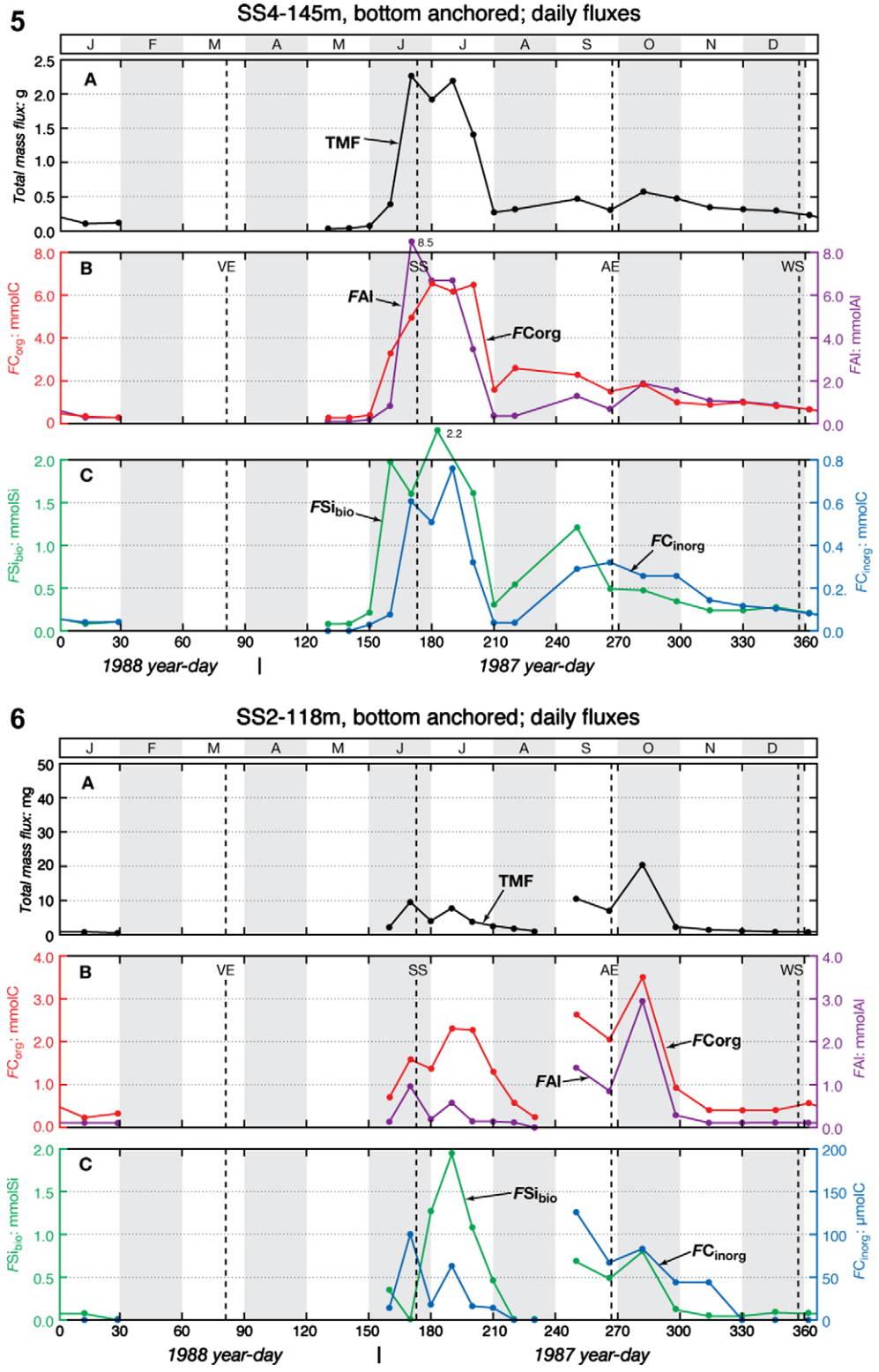

Fig. 4 (*continued*)

polymetric substance (EPS) often found in nutrient-limited ice algae that is characterized by high C/N (>20); Engel and Passow, 2001; Engel et al., 2002). The C/N of the aggregate collected during Period 17, from late January to early February, was 17. (The C/N should have been much higher; the ratio was artificially reduced by the averaging process.) The FC_{org} maxima, 76 and 36 µmol C m^{-2} d^{-1}, that occurred during Periods 6 and 7, respectively, were the major contributors to the maximum TMF (Fig. 4-1A). This PIC flux comprised small planktonic foraminifer tests and small pteropod shells.

As mentioned in the previous section, the TMF during S97-120m-Periods-1–8 (Phase 1) was quite small during the drift over the pelagic Beaufort Sea from late January to early March (Table 3, lower panel, and Fig. 4-2A). Particle export to 120 m increased abruptly when S97-120m reached the Chukchi Plateau shortly before the vernal equinox. The first TMF maximum, 25.4 mg m^{-2} d^{-1},

Table 3
Elemental fluxes at each period: B96-200m and S97-120m.

TS #[a]	Cal.#[b]	Open/close	96 YD[c]	97 YD	ac.d.[d]	Lat.	Long.	TDM/(mg m^{-2} d^{-1})		Litho.
								>1 mm	<1 mm	
B96-200m										
1	7	04/27/1996	118		17	79.10	−132.20	0.6	1.0	0.02
2	8	05/14/1996	135		34	79.08	−131.46	0.3	1.3	
3	9	05/31/1996	152		51	79.39	−131.22			
4	10	06/17/1996	169		68	79.17	−131.57	0.6	1.0	
5	11	07/04/1996	186		85	79.32	−129.45			
6	12	07/21/1996	203		102	79.07	−128.53	0.5	8.7	0.03
7	13	08/07/1996	220		119	79.14	−126.68	0.0	5.1	0.04
8	14	08/24/1996	237		136	79.10	−126.79			
9	15	09/10/1996	254		153	78.78	−128.40			
10	16	09/27/1996	271		170	78.58	−130.98			
11	17	10/14/1996	288		187	78.37	−131.78	1.3	0.8	
12	18	10/31/1996	305		204	78.40	−133.63			
13	19	11/17/1996	322		221	78.20	−132.33			
14	20	12/04/1996	339		238	78.36	−131.52			
15	21	12/21/1996	356		255	78.11	−134.29			
16	1	01/07/1997	373	8	272	77.42	−133.07			
17	2	01/24/1997	390	25	289	77.09	−132.74	0.0	3.1	0.02
18	3	02/10/1997	407	42	306	77.03	−132.17			
19	4	02/27/1997	424	59	323	76.94	−132.11	0.0	0.8	
20	5	03/16/1997	441	76	340	76.74	−131.86			
21	6	04/02/1997	458	93	357	76.75	−131.85	0.0	0.2	
S97-120m										
Phase 1										
1[e]	17	10/08/1997	281		17	75.16	−142.19			
2[e]	18	10/25/1997	298		34	75.24	−141.93			
3[e]	19	11/11/1997	315		51	75.90	−144.64		1.05	0.29
4[f]	20	11/28/1997	332		68	75.96	−145.19			
5[f]	21	12/15/1997	349		85	75.44	−148.17	0.20	2.67	0.72
6	1	01/01/1998	366	1	102	75.07	−147.70			
7	2	01/18/1998	383	18	119	74.68	−149.06		0.79	0.21
8	3	02/04/1998	400	35	136	75.09	−155.17	0.04	2.99	0.81
Phase 2										
9	4	02/21/1998	417	52	153	75.01	−156.94	0.10	1.53	0.41
10	5	03/10/1998	438	69	170	75.53	−158.29		5.84	4.34
11	6	03/27/1998	451	86	187	76.09	−162.00	0.95	14.55	6.18
12	7	04/13/1998	468	103	204	76.22	−163.38	0.82	24.63	16.26
13	8	04/30/1998	485	120	221	76.06	−164.10	1.20	8.87	2.53
14	9	05/17/1998	502	137	238	76.43	−163.55	1.32	8.81	1.52
15	10	06/03/1998	519	154	255	76.95	−165.35	4.87	13.89	2.73
16	11	06/20/1998	536	171	272	77.59	−164.10	1.40	40.97	4.80
17	12	07/07/1998	558	188	289	78.17	−163.58	2.49	48.24	4.23
18	13	07/24/1998	570	205	306	78.52	−161.89	4.72	17.84	0.80
Phase 3										
19	14	08/10/1998	587	222	323	78.69	−154.77	0.94	13.69	0.13
20	15	08/27/1998	604	239	340	79.55	−155.13	1.15	7.53	0.64
21	16	09/13/1998	621	256	357	79.96	−155.87	1.08	5.26	0.13

occurred during Period 12 in mid-to-late April. The mass flux decreased to about 10 mg m^{-2} d^{-1}, forming a small minimum, during Periods 13 and 14 (most of May) while IOEB S97 proceeded to the northwest. The TMF then increased rapidly for three periods (51 days), reaching the annual maximum flux for this drift, 50.7 mg m^{-2} d^{-1}, in mid-July. This June–July maximum supplied about 65% of the annual particle flux. The TMF decreased rapidly when IOEB S97 entered Phase 3 during Periods 19–21. The TMF was 6.3 mg m^{-2} d^{-1} at the completion of IOEB S97's drift in the southern Mendeleyev Abyssal Plain.

The average FC_{org} during S97-120m Phase 1 was small. It averaged 7 μmol C m^{-2} d^{-1} during October and November 1997. The FC_{org} fluctuated during Periods 7–9 while IOEB S97 crossed the Northwind Ridge. In early Phase 2 of Period 10, the FC_{org} increased to 69 μmol C m^{-2} d^{-1} and continued to increase thereafter. FC_{org} was elevated during Periods 11–13 (235–173 μmol C m^{-2} d^{-1}). The FC_{org} reach a maximum during Periods 16 and 17, measuring 395 and 499 μmol C m^{-2} d^{-1}, respectively, while the IOEB drifted over the shallowest ridge topography, 279 m and 385 m deep, respectively. The FC_{org} decreased to 92 μmol C m^{-2} d^{-1} during Period 18 when the IOEB was traveling over the steep escarpment on its return to the northern Canada Abyssal Plain (Fig. 3). During Phase 3, while IOEB S97 moved north in ice-edge conditions during August and September 1998, the FC_{org} was much reduced compared to Phase 2, but the export remained larger than during Phase 1 at 92–192 μmol C m^{-2} d^{-1}.

The FSi_{bio} was extremely small throughout Phase 1 and the first two periods of Phase 2 (Fig. 4-2C). It increased slightly, to 11.3–20.5 μmol Si m^{-2} d^{-1} during Periods 11–13. Spectacular exports of diatom opal occurred when IOEB S97 reached the summit of the Chukchi Cap during Periods 16 and 17 (July 7–24), for which 381 and 452 μmol Si m^{-2} d^{-1} were measured, respectively (Fig. 4-2C). During these periods, FSi_{bio} was temporally coupled with FC_{org}, although the maxima for the latter began one period earlier. The FC_{inorg} was also very small, 0.6–2.4 μmol C m^{-2} d^{-1}, during Phase 1.

The lithogenic particle flux (clay) represented by *F*Al was very small during the Phase 1 and Phase 3 drift of the S97-120m TS-trap (Fig. 4-2B). *F*Al during these phases were only between 0.4 (Period

Table 3
(*continued*)

Mole elementary flux (μm E m^{-2} d^{-1})					Mole elementary ratio						Elemental flux concentration (%)					
C_{org}	N_{org}	C_{inorg}	Si_{bio}	Al	Co/N	Co/Ci	Si_{bio}/Ci	Si_{bio}/Co	Co/Si_{bio}	Co/Al	TDM <1 mm	Co	N	Ci	Si_{bio}	Al
28.7	4.6	0.5	0.8	0.0	6.2	59.1	1.6	0.0	37.7	592	100	34.5	6.4	0.13	2.1	0.13
31.5	4.2	75.6	1.7	0.1	7.4	0.4	0.0	0.1	18.7	323	100	4.4	0.7	0.03	0.5	0.03
36.0	5.2	36.4	8.1	0.1	6.9	1.0	0.2	0.2	4.4	299	100	8.4	1.4	0.06	4.4	0.06
150.4	10.4	2.6	1.5	0.1	14.4	57.1	0.6	0.0	100.1	2354	100	57.4	4.6	0.05	1.3	0.05
15.7	2.3	0.8	1.6	0.9	7	19	2	0	10	18	100	17.9	3.0	1.0	4.3	2.2
39.8	5.8	2.1	4.0	2.2	7	19	2	0	10	18	100	17.9	3.0	1.0	4.3	2.2
11.7	1.7	0.6	1.2	0.7	7	19	2	0	10	18	100	17.9	3.0	1.0	4.3	2.2
44.5	6.5	2.4	4.5	2.5	7	19	2	0	10	18	100	17.9	3.0	1.0	4.3	2.2
22.8	3.3	1.2	2.3	1.3	7	19	2	0	10	18	100	17.9	3.0	1.0	4.3	2.2
69.0	10.7	1.0	0.0	13.2	6	68				5	100	14.2	2.6	0.2	0.0	6.1
234.5	45.6	4.7	11.3	18.9	5	50	2	0	21	12	100	19.3	4.4	0.4	2.2	3.5
221.4	34.2	9.9	20.5	49.6	6	22	2	0	11	4	100	10.8	1.9	0.5	2.3	5.4
172.5	31.6	6.5	6.8	7.7	5	27	1	0	25	22	100	23.3	5.0	0.9	2.2	2.4
139.1	25.8	22.6	2.3	4.6	5	6	0	0	61	30	100	19.0	4.1	3.1	0.7	1.4
301.6	50.9	8.1	28.4	8.3	6	37	4	0	11	36	100	26.1	5.1	0.7	5.7	1.6
395.1	56.2	2.7	381.1	14.6	7	145	140	1	1	27	100	11.6	1.9	0.1	26.1	1.0
498.9	48.2	8.8	452.0	12.9	10	56	51	1	1	39	100	12.4	1.4	0.2	26.3	0.7
195.7	18.1	25.0	69.7	2.4	11	8	3	0	3	80	100	13.2	1.4	1.7	11.0	0.4
91.7	7.5	20.5	1.9	0.4	12	4	0	0	48	240	100	8.0	0.8	1.8	0.4	0.1
191.9	12.2	15.1	12.7	2.0	16	13	1	0	15	98	100	30.6	2.3	2.4	4.7	0.7
172.8	6.3	5.7	12.6	0.4	28	30	2	0	14	440	100	39.4	1.7	1.3	6.8	0.2

[a] Time-series period #.
[b] Period # in calendar days.
[c] YD = # day of year.
[d] ac.d = # days accumulated.
[e] Combined for analysis. Average value on 3.
[f] Average value on 5.

19) and 2.5 μmol Al m^{-2} d^{-1} (Period 8) (Fig. 4-2B). The *F*Al increased while IOEB S97 was approaching the Chukchi Plateau and the extension of the Chukchi Shelf edge. This increase began during Period 10 (13 μmol C m^{-2} d^{-1}), and a strikingly large *F*Al maximum, reaching to as 49.6 μmol Al m^{-2} d^{-1}, was observed during Period 12 (March 10 to March 27). This large *F*Al continued while IOEB S97 moved along the Chukchi Cap, particularly during Periods 16 (14.6 μmol C m^{-2} d^{-1}) and 17 (12.9 μmol C m^{-2} d^{-1}) when other biogenic particle export, FC_{org} and FSi_{bio} also intensified.

5.2. Seasonal particle export flux cycles in the interior of the Canada Abyssal Plain

The annual sequence of export fluxes observed at the interior of the Canada Abyssal Plain in data from the seafloor-tethered TS-trap CD04-3067m was quite different from that observed in data from the two TS-traps drifting in the cryopelagic surface ocean. CD04-3067m data exhibited two contrasting export modes, one high and one low, for TMF and other elements. The high export cycle, which we will call the "main export period" (Table 4), began abruptly in March when the TMF surged from 6.5 mg m^{-2} d^{-1} in Period 12, to 31 mg m^{-2} d^{-1} in Period 13. This main export period continued for about 170 days, until Period 21 when the flux decreased to 14 mg m^{-2} d^{-1} (Fig. 4-3A). The average TMF during the main export period was 22.9 with a considerable standard deviation (SDV) of 8.3 mg m^{-2} d^{-1} (36%). Approximately 77% of the annual TMF occurred during this time. During the "low export period" (Table 4), the average TMF was only 2.6 mg m^{-2} d^{-1} with a smaller SDV of 1.3 mg m^{-2} d^{-1} (50%).

Table 4
CD04-3067m.

TS #[a]	Cal.#[b]	Open/close date	04YD[c]	05 YD	ac.d.[d]	TDM	Litho	Mole elementary flux (μm E m^{-2} d^{-1})				
						<1 mm	mg m^{-2} d^{-1}	C_{org}	N_{org}	C_{inorg}	Si_{bio}	Al
Low export period start												
1	13	08/13/2004	226		17	1.0	0.5	6.3	0.5	0.3	1.6	1.6
2	14	08/29/2004	243		34	3.3	2.2	20.8	1.5	0.9	4.5	6.6
3	15	09/15/2004	260		51	2.6	2.3	13.2	0.5	1.3		7.0
4	16	10/02/2004	277		68	4.1	3.2	21.4	0.9	2.1		9.8
5	17	10/19/2004	294		85	3.3	3.0	12.7	1.0	2.4		9.1
6	18	11/05/2004	311		102	3.2	2.9	12.3	1.0	2.4		8.8
7	19	11/21/2004	328		119	4.1	3.5	14.3	1.0	1.9		10.7
8	20	12/08/2004	345		136	3.5	3.0	12.2	0.8	1.6		9.2
9	21	12/25/2004	362		153	2.7	2.3	9.9	0.6	1.2	1.3	7.0
10	1	01/11/2005	379	14	170	3.2	2.6	11.5	0.7	1.4		8.0
11	2	01/28/2005	396	31	187	4.4	3.4	16.2	0.8	1.3	2.1	10.4
12	3	02/13/2005	413	48	204	6.5	5.0	23.7	1.1	2.2		15.2
Main export period start												
13	4	03/02/2005	430	65	221	31.0	24.7	101.8	10.0	10.3	20.6	75.4
14	5	03/19/2005	447	82	238	27.2	23.9	82.5	7.2	7.9	4.3	72.8
15	6	04/05/2005	464	99	255	20.9	17.9	64.8	5.7	5.1		54.5
16	7	04/22/2005	481	116	272	37.9	32.4	114.1	9.8	8.9	25.2	98.8
17	8	05/08/2005	498	133	289	13.9	12.2	41.7	3.5	3.7		37.1
18	9	05/25/2005	515	150	306	15.2	12.4	46.4	3.8	3.9	9.1	37.9
19	10	06/11/2005	532	167	323	20.2	15.7	70.1	6.0	5.3	21.3	47.8
20	11	06/28/2005	549	184	340	25.3	21.5	78.5	7.8	7.1	13.8	65.7
21	12	07/15/2005	566	201	357	14.1	12.0	43.9	4.2	9.4	2.3	36.6
Main export period over												

The temporal sequences of *F*Al, FC_{org}, and TMF were similar. The mole fluxes of Al and POC also paralleled one another through the year. The contrast between the main and low export cycles was more pronounced for *F*Al and FC_{org} than for other elements. The FC_{org} numbers were always large, averaging 30% with an SDV of 17.5%, regardless of high or low export cycles. During Period 16 (April 22–May 8), FC_{org} and *F*Al reached annual maxima of 114 μmol C m^{-2} yr^{-1} and 99 mmol Al m^{-2} yr^{-1}, respectively (Fig. 4-3B). The variability of FSi_{bio} and FC_{inorg} was similar to that of FC_{org} and *F*Al, with one exception, during Periods 20 and 21 when FC_{inorg} significantly increased in a trend that was opposite to the other elements (Fig. 4-3C).

The sea ice above the CD-04 mooring site began to dissipate rapidly in early August of 2005 (Fig. 4-3A). In early October of the same year, the ice abruptly closed in again, and the CD-04 mooring site was covered by nearly solid-sea ice for more than 10 months (Fig. 4-3A). Surprisingly, this August to October ice-opening event had no impact on the export of biogenic and lithogenic particles at the abyssal interior depth of 3067 m under the low export domain (Table 4). The export of *F*Al, FSi_{bio}, and FC_{inorg} were extremely low and constant from late August 2004 to February 2005 (Fig. 4-3B and C). The FC_{org} showed some increase in September and October (Fig. 4-3B).

6. Discussion

6.1. Minuscule particle fluxes in the upper 200 m of the cryopelagic ocean

The annual FC_{org} was 7.0 mmol C m^{-2} yr^{-1} at 200 m (B96-200m) in the central Canada Basin and 10.2 mmol C m^{-2} yr^{-1}at 120 m (S97-120m-Phase 1, converted from daily averages). Pioneering deployments of ice-tethered TS-traps took place at two shelf stations in the northern Canadian archipelago facing the Beaufort Sea (Stations AH and ER, Fig. 1; abbreviations assigned by us) (Hargrave et al., 1989, 1994). Here, the sea ice is believed to be the thickest and oldest in the High Arctic Ocean (i.e., Bourke and Garrett, 1987; Fig. 1), and the biogenic particle flux was extremely small, similar to the export measured by B96-200: The FC_{org} was 18 mmol C m^{-2} yr^{-1} at station AH and 15-8 at station ER farther offshore. The FSi_{bio} at station ER was 0.3–0.6 mmol Si m^{-2} d^{-1}. In contrast, the FC_{org} and FSi_{bio} from the Mackenzie shelf/slope and Amundsen Gulf (O'Brien et al., 2006; Forest et al., 2007, 2008; Sampei et al., 2009) were larger by orders of magnitude (Table 1).

These export fluxes are far smaller than any other published export fluxes recorded at 200–250 m in the pelagic world ocean (e.g., Manganini et al., 2007;. http://usjgofs.whoi.edu/mzweb/data/Honjo/sed_traps.html). For example, the annual FC_{org} from Ross Sea stations M6 (73°32′S, 176°53′E) and M7 (76°39′S, 178°1′W) in the Southern Ocean, were two orders of magnitude greater, 415 and 160 mmol C m^{-2} yr^{-1} at 200 and 206 m, respectively (Collier et al., 2000). Annual FC_{org} at the geographic center of the Sea of Okhotsk, also partially covered by sea ice, at 258 m was 260 mmol C m^{-2} yr^{-1} (Broerse et al., 1990; Honjo et al., 2008). In the mid latitude ocean, 4-year time-series measurements of annual FC_{org} at Station P (200 m), a well-documented boreal gyre station in the northern North Pacific, ranged from 280 to 814 mmol C m^{-2} yr^{-1} (Wong et al., 1994, 1999). Recent epipelagic-zone measurements of FC_{org} using neutrally-buoyant free-floating traps at stations ALOHA, north of Hawaii, and K2, east of the Krill Archipelago, ranged from 548 to 1700 mmol C m^{-2} yr^{-1} (estimates from Buesseler et al., 2000 and Buesseler et al., 2007, were converted to annual values by us), two to three orders of magnitude larger than FC_{org} recorded in the ice-covered pelagic Canada Basin.

6.1.1. Absence or dearth of ballast particles in the cryopelagic environment

The observations discussed above indicate that a unique characteristic of the cryopelagic Canada Basin is a serious deficiency of the ballast particles required to settle fine, lightweight POC to the deep ocean (Honjo, 1996; Armstrong et al., 2001; Francois et al., 2002; Honjo et al., 2008). The coccoliths that play a major role in removing POC from upper layers elsewhere were not found in either B96-200m or S97-120m TS-trap samples. Diatomaceous frustules, which work in concert with (or substitute for) coccoliths in the "silica ocean biological pump" (Honjo et al., 2008), were also extremely scarce in the ice-tethered TS-traps. The annual FSi_{bio} observed by BS96-200 and S97-120-Phase

Table 4
(*continued*)

Mole elementary ratio						Elemental flux concentration (%)				
Co/N	Co/Ci	Si_{bio}/Q	Si_{bio}/Co	Co/Si_{bio}	Co/AI	Co	N	Ci	Si_{bio}	Al
13.5	22.5	5.6	0.3	4.0	3.9	7.6	0.7	0.3	4.5	4.4
13.5	22.5	4.8	0.2	4.6	3.1	7.6	0.7	0.3	3.8	5.4
24.1	10.2				1.9	6.2	0.3	0.6		7.4
24.1	10.2				2.2	6.2	0.3	0.6		6.4
12.7	5.2				1.4	4.6	0.4	0.9		7.4
12.7	5.2				1.4	4.6	0.4	0.9		7.3
14.9	7.5				1.3	4.2	0.3	0.6		7.1
14.9	7.5				1.3	4.2	0.3	0.6		7.1
15.8	8.2	1.0	0.1	7.9	1.4	4.3	0.3	0.5	1.3	6.9
15.8	8.2				1.4	4.3	0.3	0.5		6.8
20.8	12.2	1.6	0.1	7.7	1.6	4.5	0.3	0.4	1.4	6.4
22.2	10.9				1.6	4.4	0.2	0.4		6.3
10.2	9.9	2.0	0.2	5.0	1.4	3.9	0.5	0.4	1.9	6.6
11.5	10.4	0.5	0.1	19.2	1.1	3.6	0.4	0.4	0.4	7.2
11.4	12.7				1.2	3.7	0.4	0.3		7.1
11.7	12.8	2.8	0.2	4.5	1.2	3.6	0.4	0.3	1.9	7.0
12.0	11.2				1.1	3.6	0.4	0.3		7.2
12.2	11.9	2.3	0.2	5.1	1.2	3.7	0.4	0.3	1.7	6.7
11.6	13.3	4.0	0.3	3.3	1.5	4.2	0.4	0.3	3.0	6.4
10.1	11.1	1.9	0.2	5.7	1.2	3.7	0.4	0.3	1.5	7.0
10.4	4.7	0.2	0.1	19.0	1.2	3.7	0.4	0.8	0.5	7.0

[a] Time-series period #.
[b] Period # in calendar days.
[c] YD = # day of year.
[d] ac.d = # days accumulated.

1 was only 0.3 and 2.4 mmol Si m^{-2} yr^{-1}, respectively (Table 3). The annual average mole ratios of POC in the opal Si (mole C_{org}/Si_{bio}) found in B96-200m and S97-120m-Phase 1 samples were approximately 23.3 and 10.2, respectively, indicating an unusual deficiency of opal to ballast POC. In the lower epipelagic export fluxes of other oceans, these ratios are much smaller, between 1 and 4 at most. (Uniquely high ratios, 7.8 and 9.1, were reported only in traps deployed at 250 m, below the chemocline, in the Black Sea (Hay et al., 1990)). Pteropod shells contributed to the relatively large FC_{inorg} during the two summer periods of the B96-200m drift (Fig. 4-1C). However, unlike coccoliths, they may not contribute significantly to POC removal as ballasting, in part because they sink too rapidly, (thousands of meters per day), (Honjo et al., 2008).

In the case of lithogenic aerosol particles, if there is a large amount supplied to the productive ocean it can fuel the biological pump as ballasting, such as observed in the upwelling tropical Atlantic off western Africa where the export of lithogenic particles reaches 14–26 g m^{-2} yr^{-1} (Fischer et al., 2003). The export flux of lithogenic particles at 100–200 m in the cryopelagic Canada Basin ranges 0.7–1.5 g m^{-2} yr^{-1} (Hargrave et al., 1989, 1994; Table 1 of this work). The estimated rate of sedimentation to the Arctic Ocean area is also as small as 0.01–0.6 g m^{-2} yr^{-1} and the average aerosol lithogenic matter over the Beaufort Sea is particularly small (Shevchenko and Lisitzin, 2004). We suspect that such a small supply of lithogenic aerosol particles would have only a minimum effect on the biological pump.

The global average ternary ratio in the interior of the rest of the world ocean among FC_{org}, FC_{inorg}, and FSi_{bio} is approximately 1:1:1 (Honjo et al., 2008). The ternary ratios for B96-200m and S97-120m-Phase 1 are strongly skewed toward POC, 75:22:3 and 87:4:9, respectively. The higher percentage of PIC flux in B96-200m reflects a capricious export of pteropod shells in early August (Fig. 4-1C). The ternary percent ratio was 72:5:23 in the yearlong samples collected at the Lomanosov Ridge station (TS-trap LR-150m; Fahl and Nöthig, 2007). It was strongly skewed toward FC_{org} but also reflected export of large diatom frustules (32 mmol Si m^{-2} yr^{-1}) during the summer export maximum (Fahl and Nöthig, 2007). From a global point of view, the Central Arctic Ocean can therefore be considered an extreme "Organic Carbon Domain" compared to the "Biogenic Silicon" and "Bioinorganic Carbon" domains that were defined based on the ternary ratios of biogenic export fluxes (Honjo et al., 2008).

Collectively, Arctic rivers supply 10% of global runoff to the Arctic Ocean (Aagaard and Carmack, 1989). Arctic rivers entrain large quantities of terrigenous POC and detrital minerals in their suspended loads (Darby et al., 1989), and these inputs are further augmented by that derived from coastal erosion (Stein and Macdonald, 2004). The Mackenzie River is the largest in terms of sediment discharge to the Arctic Ocean (Rachold et al., 2004) and dominates sediment delivery to the eastern Beaufort shelf and Canada Basin (Grantz et al., 1996). Available estimates indicate that about 50% of the 127 Mt of sediment delivered annually by the Mackenzie River is captured in the delta, 40% stays on the shelf, and 10% escapes to the slope or interior (Macdonald et al., 1998). Arctic rivers generally exhibit strong seasonal cycles with most freshwater and sediment delivery occurring as intense, short discharges during the spring freshet (Whitehouse et al., 1989; Macdonald et al., 1998; Carson et al., 1998).

Freshet (late May/early June) occurs before near-shore breakup, discharging large quantities of fluvial sediments under and onto the ice (Macdonald et al., 1998; Reimnitz, 2002). Some of the material settling beneath the land-fast ice will be re-suspended and transported during the open-water season in response to winds and currents. Fall storms, especially during freeze-up, also result in incorporation of re-suspended sediment into frazil ice (Reimnitz and Barnes, 1987). Sediment-laden or "dirty" ice (concentrations up to 1600 g/m^3) formed via this and other processes (Pfirman et al., 1990; Reimnitz et al., 1990, 1993a, 1994) has been observed in the eastern Chukchi and Beaufort Sea (Barnes et al., 1982; Eicken et al., 2005). During break-up, turbid ice from rafting and scouring is entrained in the clockwise motion of the Beaufort Gyre (Gor-

dienko and Laktionov, 1969; Colony and Thorndike, 1985; Rigor, 1992). The Transpolar Drift ice also contains a large amount of particles contributed by Russian rivers. Subsequent ice melting and release of the sediment load results in net export of terrigenous and marine material from the shelf (Pfirman et al., 1993, 1995). In this manner, lithogenic particles can be transported thousands of kilometers from their source prior to release and ultimate deposition (Reimnitz et al., 1993a,b; Macdonald et al., 1998; Eicken et al., 2005).

A major portion of the *F*Al intercepted by a 150-m-deep Lomonosov TS-trap (20.6 μmol C m^{-2} yr^{-1} during the winter, spring, and late autumn) may have been supplied by dirty ice in the Transpolar Drift. In contrast, the source of the 351 μmol C m^{-2} d^{-1} surge of *F*Al during the summer is attributed to the Laptev freshet as described by Fahl and Nöthig, 2007. Current-driven sediment resuspension and transport represents another potential cause of higher *F*Al, particularly during periods of extensive sea-ice cover (Lalande et al., 2009b). The low *F*Al in B96 may be because the eastern Canada Basin, particularly in the area where this IOEB drifted, is distant from potential sources of dirty ice, and also because the thawing rate of the multi-year ice in this area is slow. However, these processes should be further investigated.

Why is the FC_{org} in S97-120m-Phase 1 (equivalent to 10.2 mmol C m^{-2} yr^{-1}) significantly larger than that of B96-200m (7.0 mmol C m^{-2} yr^{-1}) although these samples were collected by identical ice-tethered TS-traps in sequential years? There are a number of possible explanations, including a difference in POC productivity between these 2 years or a difference in the PP between these two areas in the Canada Basin. Another explanation could be that the lower annual FC_{org} at 200 m compared with 120 m is due to the vertical progression of POC remineralization and degradation. We will continue to seek an answer to this question.

6.1.2. Relationship between primary production and FC_{org} in the upper cryopelagic ocean

According to a recent review by Sakshaug (2004), total PP in the Beaufort Sea ranges from 2.5 to 5.8 molC m^{-2} yr^{-1}, and new production from 0.6 to 1.5 molC m^{-2} yr^{-1} (it is not clear whether this includes the mid to northern Canada Basin, the cryopelagic ocean that extends to the Alpha Ridge and beyond). With total primary production of >1 mol m^{-2} yr^{-1} and new production of <0.1 mol m^{-2} yr^{-1}, Sakshaug (2004) describes the Nansen Basin, which lies at the same latitude as the mid to northern Canada Basin, as the most barren ocean area in the High Arctic. The traditional general estimate for PP in the ice-covered pelagic High Arctic is roughly 2 molC m^{-2} yr^{-1} (e.g., Macdonald and Carmack, 1991; Gosselin et al., 1997). There is a surface cap of oligotrophic water in the Chukchi-Beaufort Gyre called the Polar Mixed Layer (PML); it is composed of outflow from the Mackenzie and other Arctic rivers mixed with sea-ice melt water. Following Sakshaug (2004, p. 70 in Stein and Macdonald, 2004), we estimate the annual PP in the euphotic PML of the cryopelagic Canada Basin is 0.5–2.5 mol m^{-2} yr^{-1}. A ^{13}C incubation-based estimate of PP at a station near the Phase 1 drift route on a day in August 1993 was 90–97 mg $m^{-2}dy^{-1}$ with 6–8 h of incubation (Cota et al., 1996), that is, 2.7–3.0 molC m^{-2} yr^{-1}, which likely represents a maximum annual estimate in this area.

This estimated PP is quite small compared to primary production in most other world-ocean provinces. However, other examples of extremely small PP oceans are found in the Antarctic (Section 7) and the tropical Pacific, such as the Equatorial Warm Water region. The annual PP at many cryopelagic Antarctic Zone TS-trap stations was about 2.6 molC m^{-2} yr^{-1}, including estimates from Bransfield Strait (Wefer and Fischer, 1991; Fischer et al., 2000), the pelagic Ross Sea (Collier et al., 2000), and Prydz Bay (Pilskaln et al., 2004). (Unless otherwise noted, PP values given for non-Arctic locations in this section were estimated using the ocean-color-based model of Behrenfeld and Falkowski, 1997). The FC_{org} at these Southern Ocean stations ranges from 28 to 48 mmol C m^{-2} yr^{-1} (about a third to a half of the global average flux) despite PP similar to that in the cryopelagic Canada Basin.

It is noteworthy that such unexpectedly large FC_{org} at these locations was associated with large FSi_{bio} of 67–397 mmol Si m^{-2} yr^{-1} and relatively small FC_{inorg} of 10–28 mmol C m^{-2} yr^{-1} as foraminiferal tests and pteropod shells. Both particle exports served as ballast to remove POC from the epipelagic Antarctic Zone in the Southern Ross Sea (Collier et al., 2000; Honjo et al., 2000). Surface water nutrient concentration is extremely low in the Equatorial Western Pacific Warm Pool province (WARM in Longhurst et al., 1995) (e.g., King, 1954; Vinogradov et al., 1997; Kawahata et al., 2002; Kobayashi and Takahashi, 2002), and ocean-color-based PP is as small as <5 molC m^{-2} yr^{-1}. FC_{org} at the deep interior of these provinces is 25–35 mmol C m^{-2} yr^{-1}. This modest FC_{org} is associated with FC_{inorg} and FSi_{bio} of 26–39 mmol C m^{-2} yr^{-1} and 14–11 mmol Si m^{-2} yr^{-1}, respectively (Kempe and Knaack, 1996; Kawahata et al., 2000).

The comparisons discussed above indicate that in an ocean with extremely low levels of PP, such as the cryopelagic Canada Basin, epipelagic POC can potentially be effectively removed to the interior by biomineral particles. Examples would be the Antarctic Zone or the Pacific WARM zone, where diatom frustules and coccoliths are available, respectively (e.g., Kobayashi and Takahashi, 2002; Kawahata et al., 2002). Thus, a plausible explanation for extremely small FC_{org} at 200 m and 120 m in the cryopelagic Canada Basin could be that the inefficiency of the biological pump stems from a lack of ballast biominerals and/or fine lithogenic particles. The only non-Arctic area suspected to have an inefficient biological pump is the PP-depleted Station WS-1 in the northern Weddell Sea (62.4°S 34.8°E) where the PP was estimated at 1.3 molC m^{-2} yr^{-1}. The FC_{org} at the interior was only 1 mmol C m^{-2} yr^{-1}, associated with >0.1 mmol C m^{-2} yr^{-1} of FC_{inorg} and 5 mmol Si m^{-2} yr^{-1} (Wefer and Fischer, 1991). Further investigation is required to determine whether this explanation is correct.

6.1.3. Fate of autochthonous POC in the upper layers of the cryopelagic Canada Basin

However small the amount, autochthonous POC must be removed from the surface epipelagic ocean within a seasonal cycle of the primary productivity in order to maintain both a steady chemical state and the annual carbon cycle. But if the biological pump is virtually inoperative, how and to where is this annual primary production removed from cryopelagic upper ocean layers? What biota and type of ecosystem are responsible for the primary and secondary production that sequester a minimum of, or no, biomineral substances in the cryopelagic environment? Flagellate blooms are either grazed and metabolized to $\sum CO_2$ or decomposed to fuel the microbial loop (Wassmann, 2004). The diel migration of both micro- and meso-zooplankton is a crucial process in the biological pump (Boyd and Trull, 2007; Honjo et al., 2008); thus, the zooplankton ecosystem throughout the cryopelagic ocean must be further understood (Ashjian et al., 2003). Bacterial plankton comprises a surprisingly large proportion of autochthonous POC in the High Arctic (Wheeler et al., 1996, 1997; Gosselin et al., 1997; Rich et al., 1997), contributing to remineralization and degradation of POC to DOC or to $\sum CO_2$. Although the details of the process are not defined, a considerable portion of POC is decomposed to "marine DOC" or "semi-labile DOC" that is known to be present in the Arctic Ocean at higher concentrations than in other oceans of the world (e.g., Hansel and Carlson, 2001). Gosselin et al. (1997) estimated that 20–40% of total pelagic phytoplankton and PP by

ice-dwelling algae in the central Arctic Ocean was released as DOC. Thus, the majority of the POC could be remineralized in the Arctic surface layer and the upper halocline by the biota, including microbes. Another question concerns how the quasi-steady state of alkalinity can be maintained without pumping significant carbonate minerals such as those found in coccolith shells. We can only assume that this autochthonous carbon is eventually ventilated or is exported to the North Atlantic mostly via the Transpolar Drift (Fig. 1).

6.2. Export of particles to the deep interior of the Canada Basin

As described in Section 3, the average daily TMF in the CD04-3067m TS-trap moored on the Canada Abyssal Plain was 11.8 mg m^{-2} d^{-1} (Section 4, Table 4, Fig. 4-3A). This was much larger than the corresponding fluxes in the S97-120m-Phase 1 TS-trap (1.9 mg m^{-2} d^{-1} in winter; Table 3) as it drifted approximately above the earlier location of the CD04-3067m TS-trap (Figs. 2 and 3). Particles exported to CD04-3067m were characterized by extraordinarily high lithogenic contents, as much as 85%, while it was 26% for S97-120m-Phase 1. The daily *F*Al for CD04-3067m was almost 20 times larger than that for S97-120m-Phase 1 (Fig. 4-1B and 2B). The FC_{org} for CD04-3067m (39.0 μmol C m^{-2} d^{-1}) was also significantly greater than for S97-120m-Phase 1 (28.0 μmol C m^{-2} d^{-1}).

The annual FC_{inorg} at CD04-3067m was extremely small, 1.4 μmol C m^{-2} yr^{-1}, and constituted only 0.5% of the TMF, approximately 1% of the global average flux for interior-ocean depths. The annual C_{org}/C_{inorg} ratio was as large as 11, while the global average for this ratio in the ocean interior is close to 1 at the equivalent bathypelagic depth of other world oceans (Honjo et al., 2008).

6.2.1. Comparison of $\Delta^{14}C$ and $\delta^{13}C$ values in epipelagic and abyssal TS-traps

The annual $\Delta^{14}C$ in the POC of CD04-3067m ranged from −97‰ to −257‰, averaging −217‰. This indicates that the POC delivered to 3067m contains a high proportion of reworked (allochthonous) carbon, resulting in an average age of about 1900 years (an apparent age calculated by Hwang et al. (2008)) while the average surface water DIC $\Delta^{14}C$ value of High Arctic ocean water is +25‰ (Jones et al., 1994). In contrast, $\Delta^{14}C$ for POC collected during S97-120m-Phase 1 as the TS-trap drifted at 120-m depth above CD04-3067m from November 11 to January 18, 1997, ranged from +6‰ to −78‰ while $\Delta^{14}C$ indices in the CD04-3067m TS-trap were consistently low, varying between −219‰ and −227‰ (Table 5 and Fig. 4-3E).

6.2.2. Statistical coherence in particle species over an annual cycle

An unusual characteristic of particulate matter exported to the abyssal Canada Basin TS-trap is the extraordinarily tight regression among the fluxes of four elements, *F*Al, FC_{inorg}, FSi_{bio}, and FN_{org}, throughout the 21 collecting periods, each of which records 17 days of export fluxes. As shown in Table 6, the linear regression coefficients (r^2) between FC_{org} and the other elements were *F*Al, 0.98; FC_{inorg}, 0.94; and FSi_{bio}, 0.93 (two outlying data points were excluded). The r^2 between FC_{org} and FN_{org} was as high as 0.99 in all 21 samples. There was no clear difference in the regression between the "main" and the "low" export seasons (discussed later, see Table 4 and Fig. 4-3B). The average C/N ratio in TS-trap CD04-3067m samples based on the seven periods, numbers 14–20, was 11.5, with an extraordinarily small STD of 5.7%. Such tight regression among the export fluxes of elements has not been observed at any other ocean stations studied thus far. The average C_{org}/C_{inorg} and C_{org}/Al among all periods of CD04-3067m samples was 10.5 and 1.1, again with small STDs (10.4% and 11.1%, respectively). In contrast, the STDs in the ratio of FC_{org} and FC_{inorg} to FSi_{bio} (C_{org}/Si_{bio} and C_{inorg}/FSi_{bio}) were quite large, as much as 88.5% and 54.7%, respectively. These simple statistics suggest that POC and lithogenic particles were transported together to TS-trap CD04-3067m, whereas diatom frustules are of more mixed origin (see the next section).

6.2.3. Effect of an ice-opening event on export of particles to the abyss

The sea ice retreated to the north during August to mid September in the Beaufort Sea, and the ice edge passed over TS-trap CD04-3067m in early August. Less than 20% of the sea surface was occupied by scattered ice floes for 10 days in mid September. During September 12–13, 2004, no sea ice was observed for a 24-h period within the 25-km satellite-observing parcel around the mooring location (Fig. 4-3A). An almost identical ice retreat pattern was observed during the summer of 2005 at this station. If euphotic productivity and the ecosystem were functioning as a biological pump, autochthonous POC export should be recorded in TS-trap CD04-3067m during October 2004 assuming a common settling speed of ocean particles of a few hundred meters per day. Importantly, this major ice opening did not have a significant impact on the export of biogenic and lithogenic particles, indicating that fresh autochthonous PP was not transported vertically by a biological pump.

Except for two periods when POC increased only slightly (Fig. 4-3B), TMF was small when TS-trap CD04-3067 was in the "low export period" (Table 4, Fig. 4-3B). However, $\Delta^{14}C$ values during this extensive ice-opening period increased to −97‰ from the general background value of −220‰ to −257‰ (Fig. 4-3E). This shows that a relatively small increase in the fraction of autochthonous POC influences the overall POC ^{14}C age. During this major opening period of about 50 days, $\delta^{13}C$ also deviated from generally more enriched values (∼−24‰), reaching as low as −25.8‰ (Table 5, Fig. 4-3E).

We observed that a relatively short ice opening (lasting up to several weeks) did not result in export of POC and other biogenic particles. As Fig. 4-2A shows, TS-trap S97-120m intercepted the largest amount of FC_{org} and FSi_{bio} in the Chukchi Cap area during late June and July 1998, indicating that an active biological pump was at work while the ocean surface was largely covered by ice. Also, Fig. 4-1A indicates that sea ice around IOEB B96 was tightly closed between late July and most of August 1996, the only period of peak export observed that year. Interestingly, this high export period was flanked by 3-week periods of very little ice when there was almost no export of particles.

Removal of sea ice and snow from the Arctic Ocean will admit more light and enhance primary production as well as add more productive days to the Arctic Ocean in general. Mixing extends to deeper layers in an ice-free ocean. On the other hand, winter ice and low temperatures cause year-round stratification in some places and prevents vertical migration of zooplankton. Overall, the above observations suggest that even when the cryopelagic ocean experiences a few months of reduced ice or ice-free conditions, this does not trigger PP; that is, an ice opening may not necessarily result in bloom conditions (Melnikov et al., 2002), addition of ballast biominerals to the water column, or, further, migration of a zooplankton community to enhance pumping of POC (Honjo et al., 2008). This interpretation implies that the generation of a large ice-free region by future sea-ice retreat may not immediately "jump-start" the biological pump in the polar pelagic ocean. Sakshaug (2004) argues that re-colonization of the zooplankton community may take time after thawing of sea ice.

6.3. Lateral transport hypothesis

If we use the vertical biological pump model to explain the rapid removal of POC from the world ocean's epipelagic zone to the deep interior, no FC_{org} should remain in the deep waters of the Can-

Table 5
POC indices: radio carbon disequilibium and C–N.

TS#	Open–close (date)	FC_{org} (μmol C m^{-2} d^{-1})	$\Delta^{14}C$ (‰)	$\partial^{13}C$ (‰)	Co–N (ratio)
S97-120m					
Phase 1					
1[a]	10/08/1997				
2[a]	10/25/1997				
3[a]	11/11/1997	15.7	−35	−25.3	6.9
4[b]	11/28/1997				
5[b]	12/15/1997	39.8	−78	−25.9	6.4
6	01/01/1998				5.1
7	01/18/1998	11.7	6	−25.0	6.6
8	02/04/1998	44.5	−88	−25.0	5.5
Phase 2					
9	02/21/1998	22.8	−94	−23.6	5.4
10	03/10/1998	69.0	−104	−23.6	6.4
11	03/27/1998	234.5	−146	−27.7	5.1
12	04/13/1998	221.4	−154	−26.2	6.5
13	04/30/1998	172.5	−97	−26.0	5.5
14	05/17/1998	139.1	−72	−24.5	5.4
15	06/03/1998	301.6	−73	−27.0	5.9
16	06/20/1998	395.1	−32	−25.3	7.0
17	07/07/1998	498.9	−38	−26.7	10.3
18	07/24/1998	195.7	−13	−26.3	10.8
Phase 3					
19	08/10/1998	91.7	−8	−26.4	12.2
20	08/27/1998	191.9	17	−23.2	15.7
21	09/13/1998	172.8	18	−22.70	27.5
CD04-3067m					
Low export period start					
1	08/13/2004	6.3			
2	08/29/2004	20.8			
3	09/15/2004	13.2	−97	−25.8	13.5
4	10/02/2004	21.4			
5	10/19/2004	12.7	−219	−25.3	12.7
6	11/05/2004	12.3			12.7
7	11/21/2004	14.3			14.9
8	12/08/2004	12.2	−227	−25.2	14.9
9	12/25/2004	9.9			15.8
10	01/11/2005	11.5			15.8
11	01/28/2005	16.2	−219	−25.1	20.8
12	02/13/2005	23.7			22.2
Main export period start					
13	03/02/2005	101.8	−226	−24.4	10.2
14	03/19/2005	82.5			11.5
15	04/05/2005	64.8	−253		11.4
16	04/22/2005	114.1	−245	−24.0	11.7
17	05/08/2005	41.7	−257	−24.1	12.0
18	05/25/2005	46.4	−247	−24.1	12.2
19	06/11/2005	70.1	−156	−24.7	11.6
20	06/28/2005	78.5	−230	−23.9	10.1
21	07/15/2005	43.9	−230	−23.9	10.4
Main export period over					

[a] Combined for radiocarbon and N analysis. Average value on 3.
[b] Average value on 5.

Table 6
Regression indices with FC_{org}. Numbers in bold letters highlight regression indices larger than 0.900.

	Chukchi	Canda A. P.	Lomanosov Rdge		Fram Strt.	Mackenzie Shelf		Other examples			
	S97-120m	CD04-3067m	LR-150m	LR-1550m	FS-2400m	SS4-128m	SS2-119m	Ross Sea 7		Ross Sea B	Arabian Sea
	Phase 2 and 3							206 m	481 m	230 m	746 m
Source	This paper	This paper	Fahl and Nöthig (2007)		Unpublished	O'Brien et al. (2006)		Collier et al. (2000)		Dunbar et al. (1998)	Honjo et al. (1999)
FAl	0.074	**0.979**	0.012	**0.994**	**0.914**	0.707	0.664	0.511	0.287	NA	0.894
FN	0.689	**0.984**	NA	NA	0.243	NA	NA	**0.997**	**0.997**	0.727	**0.992**
FC_{inorg}	0.009	**0.943**	0.331	0.869	0.024	0.643	0.3	**0.916**	**0.925**	0.069	0.787
FSi_{bio}	0.726	**0.925**	0.681	**0.986**	**0.922**	0.861	0.453	0.51	0.132	0.772	0.571

ada Abyssal Plain because no, or only a negligible amount of, ballasting particles are produced in its uppermost water column (Sections 3 and 5.1). However, the FC_{org}, FSi_{bio}, and *FAl* at the 3067-m TS-trap were far larger than their counterparts at 120 m and 200 m. Moreover, the $\Delta^{14}C$ values of POC intercepted by the 3067-m TS-trap were very low (equivalent to 1900 ^{14}C years), while corresponding POC from 120 m and 200 m contained predominantly contemporary carbon. Finally, there is a strong statistical link among the exported particle species with FC_{org} at 3067 m (except for FSi_{bio}) while there is no such link in the parti-

cles intercepted at 120 m and 200 m (Table 6). These observations lead us to hypothesize that the oceanic particles in the 3067-m TS-trap were exported from a pre-aged reservoir of organic carbon derived from the surrounding margins.

Fahl and Nöthig (2007) also reported that sedimentation rates at the seafloor in the Central Arctic were higher than could be accounted for by pelagic fluxes (48 g m^{-2} yr^{-1} (Stein and Fahl, 2004) vs. 14.2 gm^{-2} yr^{-1} at the LR-1550m station). Indeed, increases in lithogenic particle fluxes with depth on shelves and other margin environments, and in deep ocean trenches, including some Arctic locations, has been reported by many authors (e.g., Honjo et al., 1982, 1988; Ittekkot, 1991; Nozaki and Oba, 1995; Hwang et al., 2009).

Christensen (2000) and Klages et al. (2004) argued that total O_2 consumption rates measured at a few Arctic benthic stations, including in the Central Arctic basin, were much larger, when converted to carbon release based on the Redfield ratio, than the flux predicted by sediment trap-based FC_{org} measured at shallow depths. This observation indirectly supports our hypothesis that POC delivered to the deep seafloor of a cryopelagic ocean such as the Canada Basin must be augmented by that derived from lateral transport. The latter is uncoupled from surface primary production in terms of both POC quality and quantity (Section 5.1).

Macdonald et al. (1993) estimated that satisfying the O_2 drawdown in the Canada Basin along the 1500 m contour would require 40–50 mmol C m^{-2} yr^{-1}. The annual FC_{org} we measured at twice this depth (TS-trap CD04-3067m, Fig. 4-3B) was 14 mmol C m^{-2} yr^{-1} (Section 3, Table 4). The largest estimate of POC export based on the annual maximum FC_{org} observed during the height of the "main export period" (late April to early May 2005) (Table 4, Fig. 4-3B) was 42 mmol C m^{-2} yr^{-1}. The same estimate from the average of the main export periods was 27 mmol C m^{-2} yr^{-1}. The minimum estimate based on the August 2004 flux was just 0.12 mmol C m^{-2} yr^{-1}.

Recently, Stein and Macdonald (2004) obtained Holocene seafloor burial rates for total sediment (TS) and organic carbon (C_{org}) from six Arctic marginal seas based on a wider data set. They estimated modern TS and OC input to the Beaufort Sea as 123 and 1.51×10^{12} g yr^{-1}, respectively (Stein and Macdonald, 2004, pp. 317, 319). The area of the Beaufort Sea is estimated at 178×10^9 m^2; thus, the TS and CO burial rates are approximately 70 and 5.5 g m^{-2} yr^{-1}. These rates are larger by an order of magnitude than the export flux of particles intercepted at about 800 m above the seafloor by TS-trap CD04-3067m during its year-long deployment in 2004/2005. The TMF and FC_{org}, which were comparable to TS and OC, were 4.3 g m^{-2} yr^{-1} and 0.17 g m^{-2} yr^{-1}, respectively. While there is insufficient evidence to explain this discrepancy, one hypothesis is that the major lateral supply of the re-suspended sediment derives from the Mackenzie shelf (Lalande et al., 2009b), and that flows along the seafloor within the benthic nepheloid layer (BNL). Thus, the TS-trap at 800 m above the seafloor may have intercepted only a small portion of the lateral supply.

The BNL, along with water cascading over the shelf (e.g., Ivanov et al., 2004), is often used to provide an explanation for the distribution of sedimentary particles (e.g., Thomsen and van Weering, 1998; McCave et al., 2001). Although implication of the BNL in explaining Mackenzie plume data is still hypothetical, our results suggest that the vertical flux of particles in the middle of the basin, such as at station CD04, exceeds the capacity of the intermediate nepheloid layer (INL). Confirmation of these observations and hypotheses requires additional measurement of particle fluxes throughout the deep cryopelagic Arctic basins.

The FC_{org} measured at station LR-1550m on the Lomanosov Ridge (Fig. 4-4-2B) was 70 mmol C m^{-2} yr^{-1} (Table 1; Fahl and Nöthig, 2007). The TS-trap-based annual FC_{org} and the basinwide O_2 drawdown estimate by Macdonald et al. (1993) indicate that trap-based and oxygen-demand-based flux are comparable. Continued investigations of the relationship between oxygen demand and benthic fluxes (e.g., Smith et al., 2006) in cryopelagic benthic settings are clearly required. Most importantly, however, is a specific but critical question we must answer soon: Does allochthonous, aged, and highly refractory POC serve as the metabolic energy source that drives the deep ocean benthic ecosystem in the Arctic Ocean?

6.3.1. Comparison of the "main" and "small" particle export phases observed at CD04-3067m

One of the keys to understanding the provenance and supply of particles to the Canada Basin deep interior is determining the causes of the two phases of particle export flux evident in CD04-3067m time-series data. As Table 4 and Fig. 4-3B depict, the "main" export phase begins in early March (2004), is fully developed by late March (Period 14), and diminishes during mid-July (Period 21). During the 5 months (nine periods) of the main export phase, three distinct maxima were observed. Average TMF during the main phase was 22.9 mg m^{-2} d^{-1} (STD: 8.3 mg m^{-2} d^{-1}) whereas the average TMF during the remaining 7 months comprising the "small" export phase was 3.5 mg m^{-2} d^{-1} (STD: 1.3 mg m^{-2} d^{-1}).

An initial expectation would be that the "main" export phase resulted from seasonal (summer) enhancement of the biological pump at CD04-3067 m. However, as noted in Section 6.1, vertical supply of settling particles from overlying surface waters throughout the season, as inferred from the extremely small TMF intercepted by TS-traps B96-200m and S97-120m-Phase 1, indicates no significant biotic control on export fluxes at abyssal layers. In addition, development of the main export phase is decoupled from the solar cycle at northern latitudes, with the first major surge of TMF beginning as early as late February. The maximum TMF, although brief, occurred in late April and early May, then decreased significantly in summer (June and July) when solar forcing nears its maximum. Moreover, as discussed previously, FAl and FC_{org} were tightly coupled throughout the main export period. Overall, there seems to be no evidence for enhanced export during specific seasons of the year. Therefore, the "main" and "small" particle export phases observed in TS-trap CD04-3967m samples appear to be driven by physical forcing phenomena.

6.3.2. Provenance of Canada Basin abyssal POC

Although the low $\Delta^{14}C$ values and high abundance of lithogenic particles provide clear evidence for margin-derived POC supply, the source(s) or the processes of lateral particle delivery to the abyssal layers of the central Canada Basin are harder to constrain. Previous studies indicate that sediments along the Beaufort Sea margin contain substantial quantities of terrestrially-derived organic matter (e.g., Belicka et al., 2004; Yunker et al., 2005), but whether this material is exported to the abyssal basin is uncertain. Although further studies are necessary to resolve this puzzle, we have explored whether available $\delta^{13}C$ data can be used to constrain POC source(s) (Table 5). Reported $\delta^{13}C$ values range from −27‰ in the Mackenzie and Colville River estuaries (Fig. 2) to −24‰ further offshore in the area of the Alaskan Beaufort Sea shelf break, indicating a zonal distribution pattern that parallels the coastline (Naidu et al., 2000, 2004; Macdonald et al., 2004a,b). However, the origin of this zonal distribution of $\delta^{13}C$ along the Beaufort coast has not yet been explained. O'Brien et al. (2006) suggest that enhanced supply of freshly produced marine POC, resulting from a spatial and/or temporal decoupling of primary productivity and zooplankton grazing, may give rise to higher $\delta^{13}C$ values (perhaps >−23.5‰). They also show that the $\delta^{13}C$ in POC exported at the edge of the Mackenzie River shelf changed quickly from −29‰ to −26‰ in less than 2 months. However, Goñi et al. (2005) point out that interpretation of $\delta^{13}C$ data is complicated because there are other sources of POC than that derived from terrestrial vegeta-

tion and marine productivity. In particular, the erosion of sedimentary rocks in river drainage basins may represent a significant source of POC with intermediate $\delta^{13}C$ values, and algal productivity within the rivers could be a source of ^{13}C-depleted POC (Goñi et al., 2005; Drenzek et al., 2007).

Fig. 5 shows the range of published C/N ratios and $\delta^{13}C$ values in surface sediments from various locations on the Mackenzie and Alaskan shelves (Macdonald et al., 2004a,b) with an overlay of our C/N vs. $\delta^{13}C$ data from CD04-3067m and S97-120m. As for $\delta^{13}C$ in sediment samples, there is considerable uncertainty surrounding the interpretation of C/N ratios in terms of POC provenance due to diagenetic effects and potential contributions from inorganic nitrogen tightly associated with fine-grained lithogenic particles (e.g., Müller, 1977). Accepting these caveats, it is interesting to explore the relationship between these geochemical parameters. The coordinates of the $\delta^{13}C$ vs. C/N ratio during the main export periods of CD04-3067 (⊕ symbols, Fig. 5) are concentrated around [−24:12]. This suggests that the POC and lithogenic particles originated from a single reservoir or area. On the other hand, samples from the small export period (+ symbols, Fig. 5) exhibit a wide range of C/N values while $\delta^{13}C$ values fall within a narrow range (−25‰ to −26‰) (these C/N vs. $\delta^{13}C$ values are similar to those of surface sediments from the Mackenzie and Alaska shelves and slopes (500–2500 m, p. 183; Stein and Macdonald, 2004).

During the main export phase, the annual deep current variability measured 1067 m above TS-trap CD04-3067m was meridional (offshore vector) at <5 cm s^{-1}. The pattern of TMF variability somewhat resembles the current vectors, but the peak periods of particle export are delayed for 2–3 weeks from the beginning of the northerly current flow, and the maxima and minima of TMF similarly lag those in current velocity (Fig. 4-3A, D). During the 7 months that the particle export was significantly depleted, the current at 2000 m was more longitudinal and generally weaker, with greater STD in the velocity. This observation suggests there may be a remote relationship between the export fluxes and the advection of deep water in the Canada Abyssal Plain (Hwang et al., 2008).

Fahl and Nöthig (2007) and Stein (1996) used abundances of lipid biomarkers (terrestrial plant wax *n*-alkanes; Eglinton and Hamilton, 1963, 1967) and diatom taxon analysis (Zernova et al., 2000) to determine that a major source of particles intercepted during the summer-fall maximum at the Lomonosov Ridge TS-trap station and accumulating in surface sediments on the Laptev shelf is derived from the Lena River. Although we have not yet applied lipid tracers in our study, we found no similar relationship between the cycle of Mackenzie River discharge and sedimentation farther offshore. In the following section, we compare our abyssal TS-trap data with well-documented sediment studies from the Beaufort coast and shelves (e.g., Macdonald et al., 1998, 2004a,b; O'Brien et al., 2006). However, we have not been able to reach a definitive, quantitative conclusion regarding the source and mode of supply of sediment intercepted by CD04-3067m.

6.3.3. Mackenzie plume sediment flux: A possible particle source for the deep interior

During 1987 and 1988, the Institute of Ocean Sciences (IOS), Sidney, Canada, deployed an extensive array of TS-traps along

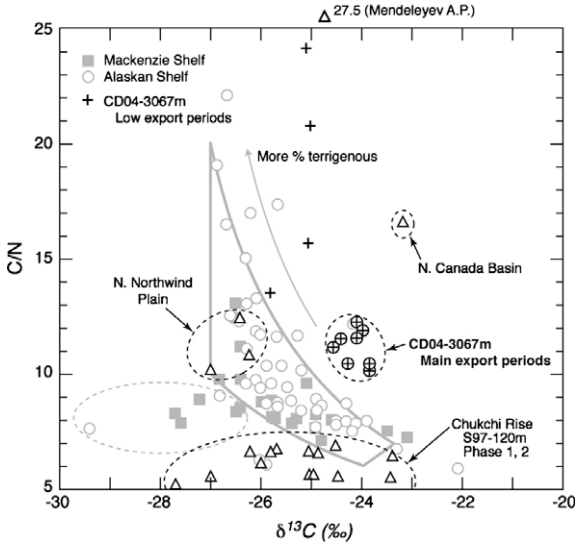

Fig. 5. Background (gray lines and type): A plot displaying the relationship between $\delta^{13}C$ and C/N from the Alaskan shelf (closed squares) and the Mackenzie shelf (open circles) drawn from Macdonald et al. (2004a,b, p. 184, Fig. 7.7.7a). Authors' data (Table 5) in black lines/type: During the Phase 2 drift of S97-120m, the $\delta^{13}C$‰ exhibits a wider range while the C/N ratios are more consistent (open triangles). During the Phase 3 drift, the C/N ratio was very high, between 12.2 and 27.5 (Table 5, Fig. 7-4). The C/N vs. $\delta^{13}C$ ratio in CD04-3067m samples are quite characteristic: there is a wide range of C/N vs. $\delta^{13}C$ ratios during the "small export periods" (+ symbols) due to the large variability of the C/N ratio. On the other hand, the C/N vs. $\delta^{13}C$ ratios during the "main export periods" (cross marks) are concentrated around 11.5 vs. 24 (⊕ symbols).

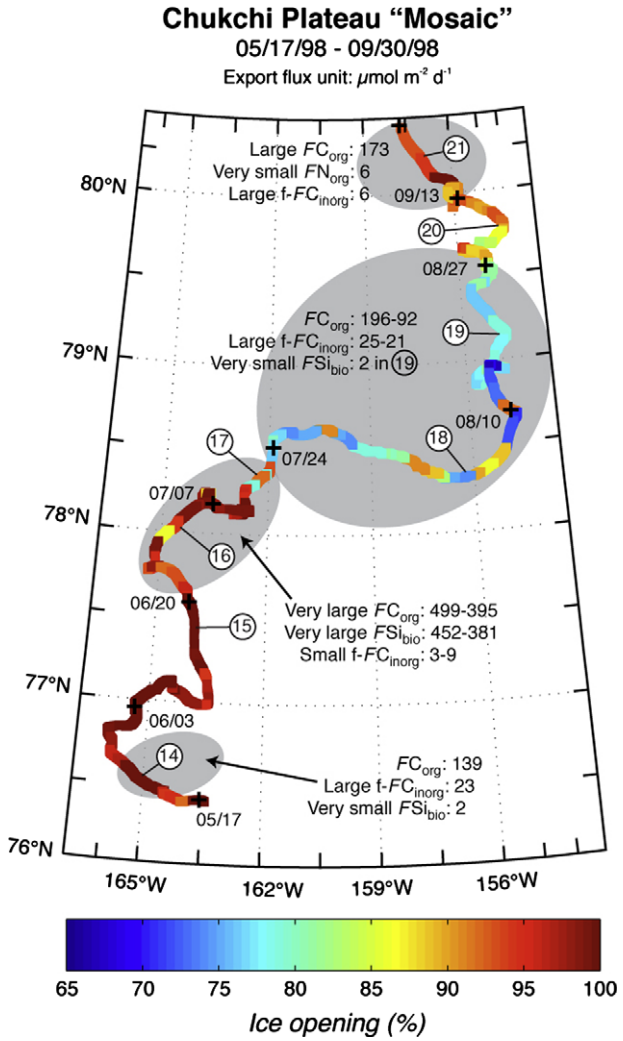

Fig. 6. Hemipelagic Chukchi Plateau: a mosaic or kaleidoscopic ocean. The export flux unit is μmol C m^{-2} d^{-1}. The combination of elements and the quantity of particle export fluxes at 120-m depth changed frequently and extensively while IOEB S97 proceeded northward over the Chukchi Plateau from May 17 to September 30, 1998, drifting in ice edge, polynya, and other ice-ocean interaction conditions. Also see Table 3 and Fig. 7-1, 7-5, and 7-6.

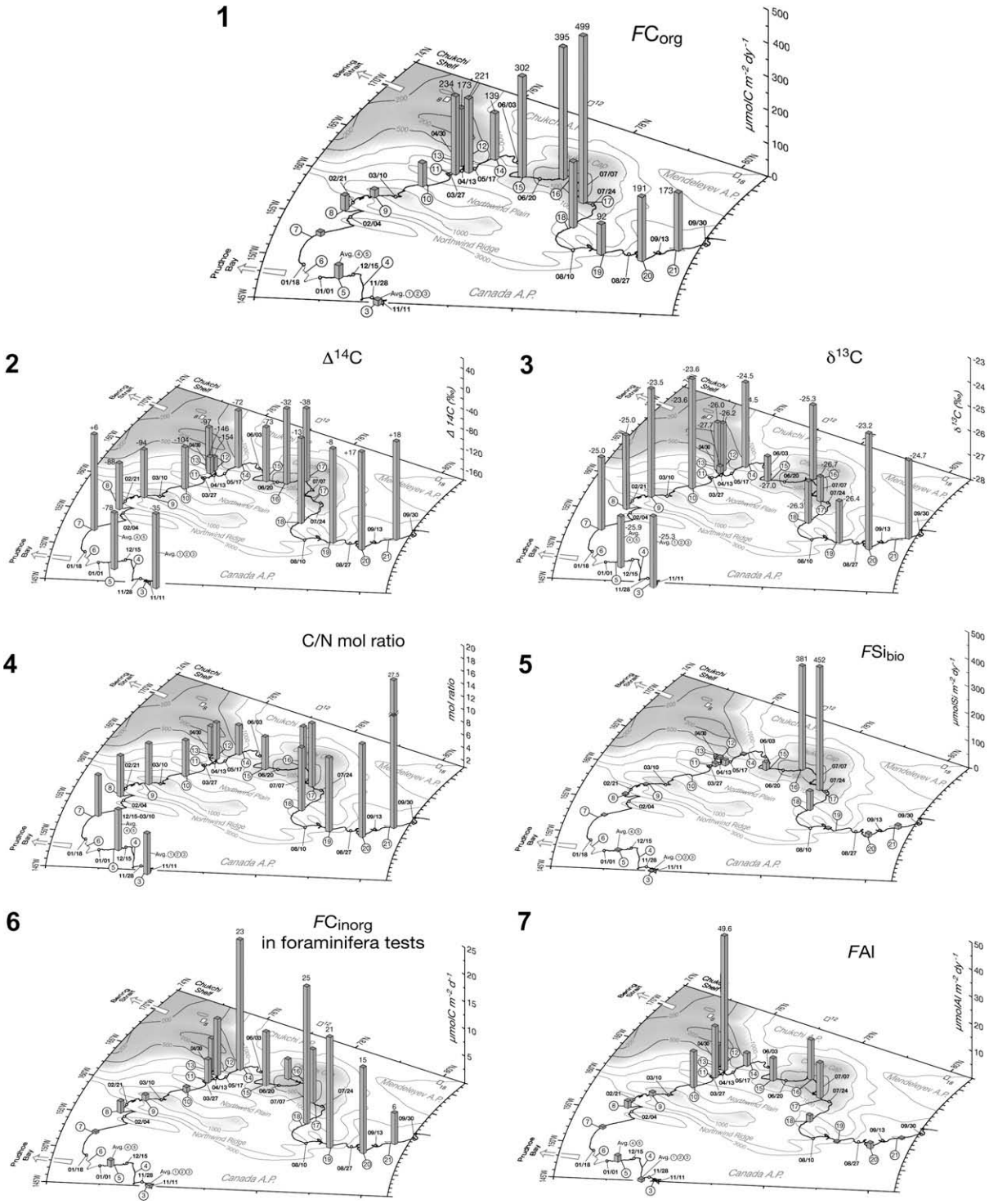

Fig. 7. Background: Index map of Chukchi Rise with topographic detail and open-close schedules of TS-trap S97-120m. Periods 1–3 are not shown in Fig. 7 (refer to Figs. 2 and 3). The topography is plotted in a conformal oblique-stereographic, North Pole-centered mode using the National Geophysical Data Center's open file (2006). The IBCAO-based 3-D illustration of the Bering Strait and Chukchi Submarine Highland is available in Stein and Macdonald (2004, Fig. 7.1.5, p. 175). Two open squares roughly along 170°W indicate the locations of detailed-nutrient-analysis stations from the 1994 Arctic Ocean Section Program (Wheeler et al., 1997). Numerical towers show export fluxes of FC_{org} (Fig. 7-1), FSi_{bio} (Fig. 7-5), FC_{inorg} in approximate foraminifera $CaCO_3$ (Fig. 7-6) in μmol m^{-2} d^{-1}; $\Delta^{14}C$ (Fig. 7-2) and $\delta^{13}C$ (Fig. 7-3) in –‰ and mole ratio of N_{org} in C_{org} (C/N ratio) (Fig. 7-4).

the Canadian Beaufort Sea shelf edge at 118–145 m depth (O'Brien et al., 2006; Figs. 1 and 2). Fig. 4-5 shows IOS export flux data from two representative TS-traps deployed at the head of the Mackenzie plume (SS4-145m in Fig. 2) and east of the Mackenzie estuary in Amundsen Bay (SS2-118m in Fig. 2). With the exception of TMF, we normalized the IOS annual fluxes by converting the data to mole-units in order to compare their data with ours (Table 1; Fig. 4-5 and 4-6). Total mass flux at the IOS stations ranged from 139 g m^{-2} yr^{-1} under the Mackenzie plume at 145 m depth to 23 g m^{-2} yr^{-1} in the Amundsen Gulf at 118 m deep. These fluxes were three orders of magnitude greater than the export to the 120- and 200-m TS-traps drifting 500–1000 km offshore from

these shelf-edge stations. Caution must, of course, be exercised in comparing particle fluxes measured in an energetic coastal environment to those measured in a very low-energy abyssal zone.

As represented by the Al flux in O'Brien et al. (2006), lithogenic particle export constituted 31–71% of the annual TMF in the Mackenzie plume and Amundsen Bay. Lithogenic particle flux also dominated (85% of TMF) at CD04-3067m. It is interesting that the annual molar flux ratio C_{org}/Al observed in the Mackenzie plume and at the nearby Beaufort shelf edge was 1.2–2.4. The C_{org}/Al ratios in the deep interior at CD04-3067, LR-1550, and FS-2400 were in the same range, 1.3, 2.4, and 0.8, respectively. However, the C_{org}/Al ratios in the two shallow Canada Basin pelagic traps were much larger due to an extremely small *F*Al (trace amounts) compared to CD04-3067m (>870). At LR-150, this ratio was 11.3, much higher than in the corresponding deep TS-trap. The C_{org}/Al at LR-1550 was 2.4 (Table 1). As depicted in Table 6, the regression between the fluxes of biogenic opal and POC export particles from TS-trap SS4-145m in the Mackenzie plume was 0.86. Also, the POC flux was weakly linked with the lithogenic flux at station SS4-145m. However, none of the particle species showed significant regression with POC flux at the Amundsen Gulf station, demonstrating the major difference in the composition of export particles.

As Fig. 4-5 shows, the annual progression of TMF in the Mackenzie plume (SS4-145m) can be expressed as a "single square-wave pulse" This pulse begins abruptly in mid June, and continues for a short period until export drops equally abruptly in late July (observed in 1987). The initiation of this pulse corresponds to the peak water discharge from the Mackenzie River during the spring freshet (Water Survey of Canada, Sydor (1988)). The export is very small to nonexistent during the rest of the year (O'Brien et al., 2006). The pattern of particle delivery to the Amundsen Gulf shelf-edge station at the mouth of the gulf (SS2-118m; Fig. 4-6) showed a similar, although more muted, pulse. It is interesting that seasonal coastal erosion signatures (e.g., Macdonald et al., 1998; Grigoriev et al., 2004) along the Beaufort Sea coast are not apparent in time-series sequences of TMF in IOS coastal TS-trap records.

Assuming the mode of sediment supply to the shelf edge observed in 1987–1988 by O'Brien et al. (2006) and the similar 2003–2004 observation by Forest et al. (2007), are generally applicable, then we might expect a temporal link to the main and small export period phases for the TMF at CD04-3067m (Table 4; Fig. 4-3). O'Brien et al. (2006) estimated the sediment flux in the plume that extends to the Canada Abyssal Plain at 0.61 Mt yr^{-1} in 1987–1988. The seasonal arrival of this sediment load at the head of the main Mackenzie River plume each year could have a major impact on the sediment distribution scheme on the Beaufort continental slope and further in the deep Canada Basin (Macdonald et al., 2004a,b). The temporal phasing of particle fluxes to the Mackenzie shelf and sedimentation to the abyssal floor therefore do not appear to be directly linked.

Lalande et al. (2009b) recently described results from a sediment trap deployment at 200 m on the Mackenzie shelf during 2005–2006 (Mooring CA04; water depth, 307 m). The annual mass flux (67 g m^{-2} yr^{-1}) was similar to that reported by O'Brien et al. (2006) and over three orders of magnitude higher than observed in the deep basin (0.004 g m^{-2} yr^{-1}; CD04-3067m). However, both total mass flux and POC flux exhibited similar temporal phasing to that observed at CD04-3067m, albeit slightly offset. Specifically, peak flux occurred for CA04 between February and May, whereas for CD04-3067m the "main" export phase was between March in July. Importantly, both exhibit the highest fluxes during the period of extensive sea-ice cover. Lalande et al. (2009b) attribute the increased fluxes during this period to sediment resuspension caused by intensified northeast currents associated with acceleration of the Beaufort Shelfbreak jet, and invoke these recurrent episodic

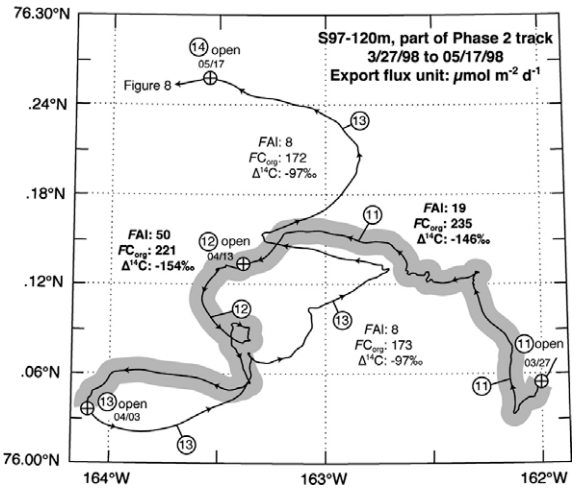

Fig. 8. Detailed drift track of IOEB S97 carrying TS-trap S97-120m during Periods 11–14 when significantly high concentrations of an allochthonous end member of FC_{org}, high FSi_{bio}, and *F*Al were observed.

events as a means for mobilizing shelf sediments and transferring it to the slope. In this way, there may be a temporal offset between sediment delivery from the Mackenzie River to the shelf, and its subsequent export and lateral (nepheloid layer) transport to the abyssal floor.

Period slumping of sediment could also be responsible for decoupling of sediment supply to the margins with its accumulation in the deep basin. Fine grain lithogenic detritus with high organic matter content was collected by a TS-trap located on the deep Norwegian Sea floor at the mouth of Storfjord, south of Spitsbergen, during January and February 1984. This pulse of detritus appears to be the result of gravitational sliding of sediment that was deposited the previous summer (Honjo et al., 1988; Honjo, 1990). Although no observations have been report except for this Storfjord case, this lateral transport may be an annual event that moves a large amount of labile carbon laterally to the deep ocean floor. Overall, further studies are necessary to determine both the source and mode of supply of particulate matter that is injected laterally to abyssal depths of the Canada Basin.

6.3.4. The biological pump in the southeast corner of the Beaufort Sea

In the summer of 2004, a bottom tethered TS-trap (CD-20) in Franklin Bay, western Amundsen Gulf (FB; Fig. 1), intercepted large biogenic particles, including coccolith and diatom frustules, compared to other traps in the Canada Basin (Forest et al., 2008; Sampei et al., 2009). Importantly, this observation suggests the existence of a genuine biological pump in the far southeast corner of the Beaufort Sea. The FC_{org} (marine POC) intercepted by TS-trap CD-20 at about 200 m (Forest et al., 2008) was approximately 40 mg m^{-2} d^{-1}. This marine POC export rate is comparable to that of the uppermost mesopelagic layer in productive lower-latitude oceans, such as the FC_{org} at the 200-m-deep Station P (Wong et al., 1999). Of approximately 40 mg C m^{-2} d^{-1}, about 63% of the FC_{org} was contributed by micro- and meso-zooplankton fecal pellets exported during July–August 2004 (from Fig. 8, Forest et al., 2008), about 5 mg m^{-2} d^{-1} of coccolithophores, and 15 mg m^{-2} d^{-1} of diatoms. This observation strongly indicates an active and typical "silica ocean" biological pump, similar to the other near-pole oceans and marginal seas (Honjo et al., 2008), was operating during summer 2004 in Franklin Bay.

At present, the nutrient-rich Bering-Yukon water (Anadyr Current) spreads beneath the euphotic zone under the PML and flows eastward in response to the Coriolis force (Aagaard and Carmack,

1989). We speculate that shoaling of the Anadyr Current caused by underwater topography in the southeast corner of the Beaufort Sea may result in mixing of Bering-Yukon water with the PML, but so far we have no evidence to support such a scenario (see Section 9, Future Implications, 2).

6.4. The biological pump in southernmost Lomonosov Ridge waters

A pair of TS-traps was deployed at 150 m and 1550 m (LR-150m and LR-1550m) along a deep ocean mooring on the southern Lomonosov Ridge close to the Laptev Sea margin (81.1°N, 138.9°E, 1712 m deep) from September 1995 to August 1996 (Fahl and Nöthig, 2007; Fig. 1). In order to compare the results of this highly successful experiment to our Canada Basin experiments and IOS's observations from the Mackenzie plume (O'Brien et al., 2006; Fig. 4-5, 4-6), we converted published export data from the Lomonosov Ridge station described in Fahl and Nöthig (2007) to molar flux values and re-plotted them in Fig. 4-4-1 and 4-4-2.

As described by Fahl and Nöthig (2007), the majority of the annual FC_{org} was received by the LR-150m TS-trap during the two August 1996 collection periods (totaling 31 days) and one October 1995 collecting period (15 days) for a total of 46 days (Fig. 4-4-2; the 150-m elemental fluxes [solid lines] are overlaid on the 1550-m fluxes [broken lines] in Fig. 4-4-2B and C). The maximum export of TMF and all export particle categories in October 1995 at LR-1550m was delayed for a 15-day period (Fahl and Nöthig, 2007) from the maximum at LR-150m, except for the FC_{inorg} (Fig. 4-4-1C). This delay of export is one of the signs that a biological pump is operating normally and that it was exporting carbon to the deep oceanic interior during this period.

At 150 m, the annual FC_{org} was 98.2 mmol C m^{-2} yr^{-1}, 10–14 times greater than that collected by the ice-tethered TS-traps that drifted over the Canada Basin at similar depths (B96-200m and S97-120m-Phase 1). The annual FC_{org} at 150 m was associated with relatively large FSi_{bio} and FAl, 32 mmol Si m^{-2} d^{-1} and 8.7 mmol Al m^{-2} d^{-1}, respectively. Vertically settling FSi_{bio} and FAl-ballasted POC were intercepted by the 150-m TS trap. The timing of this export bloom detected at the 150-m TS-trap was slightly delayed from the maximum Lena River freshet, which supplied nutrients and particles (particularly clay and diatom frustules) to the Laptev Shelf and to the LR-TS-trap site (Fahl and Nöthig, 2007). These observations also clearly indicate that a biological pump is fully functioning at the Lomonosov Ridge station from the surface to 150 m during the summer season, utilizing as ballast autochthonous and allochthonous diatom frustules and lithogenic particles supplied by Siberian river freshets and from sediment resuspension from the shelf.

Except for this significant vertical summer export event when the biological pump functioned in genuine manner like in a lower latitude pelagic ocean, perhaps using abundant diatom frustules (Zernova et al., 2000) as the main ballast, FC_{org} and fluxes of ballast particles were small, similar to those observed in the B96-200m and S97-120m-Phase 1 TS-trap records, indicating an ineffective biological pump (Section 6.1) similar to our observation in the Canada Basin cryopelagic experiment. Thus, during this period, the PP over the LR-150m TS-trap is remineralized or degraded to DOC, an thus "recycled *in situ*" (Fahl and Nöthig, 2007). Recent estimates of total PP and new production in the Laptev Sea were 2.1–3.0 and 0.5–1.3 mmol C m^{-2} yr^{-1}, respectively (similar to the Canada Basin PP; Sakshaug, 2004). A more efficient biological pump transported 60% of the annual primary production carbon to 150 m during the two summer months of 1995 and 1996, implying that 40% of PP was remineralized or degraded to marine DOC (Hansell et al., 2004) in waters shallower than 150 m. In contrast, approximately 95% of POC may be remineralized in the upper 150 m at the Lomonosov Ridge during the rest of the year.

Despite the apparently similar cryopelagic ocean environments in the Laptev Sea and the Canada Basin, the biological pump therefore appears to function well at Lomonosov Ridge, albeit only during a narrowly limited season, whereas it is virtually nonexistent in the Canada Basin. This contrast exists despite the fact that the Mackenzie River discharges a much larger volume of sediment (ballast) than the Lena River. One factor may be the shorter distance from the Laptev shelf break to the LR-150m and LR-1550m TS-trap stations compared to that between the Mackenzie and Colville shelf break (S97-120m-Phase 1 track). The Lena River drains onto a much broader shelf than the Mackenzie or Colville rivers; thus, the shelf break is much closer to the LR-150m/LR-1550m site than it is to the CD04-3067m site. However, Macdonald et al. (2002) indicate that the Mackenzie River water is capable of reaching the Canada Basin; indeed Mackenzie River water accompanied the SHEBA drift right from the start. The turbid Mackenzie plume was clearly imaged by satellite in July 1998 (Macdonald et al., 1999; O'Brien et al., 2006).

We calculated the linear regression indices (r^2) for available biogeochemical properties (FAl, FC_{inorg}, and FSi_{bio}) against FC_{org} in Fahl and Nöthig (2007) for each period of the LR-150m and LR-1550m TS-traps throughout their year of deployment (Table 6). With the exception of FSi_{bio} and FC_{org} (r^2 = 0.681), the relationship between particle classes exported to LR-150m were insignificant. Of particular note was the very low r^2 value (0.012) for FAl vs. FC_{org} in TS-trap 150 m. In contrast, all the elements exported to TS-trap LR-1550m were tightly coupled statistically: The FC_{org} exhibited strong relationships (r^2 = 0.99) with both FAl and FSi_{bio} (Table 6). The regression between FC_{inorg} and FC_{org} was slightly smaller compared to the above elements, but it was significant (0.87). These observations indicate that the particles exported to TS-trap LR-1550m underwent mechanical homogenization comparable to the process we observed at CD04-3067m.

From September 2005 to August 2007, a decade after above mentioned mooring experiment at LR station (Fahl and Nöthig, 2007), a seafloor-tethered mooring with two TS-traps at 175 m and 850 m was deployed on the continental slope in the Laptev Sea (Station M3, 79°55 N 142°21E, water depth 1350 m, Lalande et al., 2009a,b). M3 station was located at approximately 90 nautical miles SSE of LR station. The POC flux at M3 station was 4.1 g C m^{-2} yr^{-1} at both 175 m and 850 m during September 2005 to August 2006. During the next year, September 2006 to August 2007, the POC flux at 175 m and 850 m were considerably larger; 9.0 and 6.5 g C m^{-2} yr^{-1}, respectively (Lalande et al., 2009b). Lalande et al. (2009b) explained this increase of POC flux as a consequence of extensive opening of sea-ice cover during the second year that enhanced chlorophyll concentrations over the wide areas of the Laptev Sea in the summer of 2007.

The annual POC flux at LR station in September 1995 to August 1996 was 1.5 g C m^{-2} yr^{-1}at 150 m and 1.05 g C m^{-2} yr^{-1} at 1550 m. The reason why POC export flux was significantly higher for both depths at M3 station in September 2005 to August 2006 than at LR station 10 years prior is an intriguing question given their close proximity to one another. This difference may be a reflection of sea ice extent, which was much greater in 1996 than 2006 (Lalande et al., 2009b). However, this difference may also be due to local topography and the locations M3 and LR stations in reference to the transport path of Lena River sediment; M3 station is located on the steep slope directly under the Laptev shelf break whereas LR station is located on the western flank of Lomonosov Ridge outside of direct influence from possible Lena sediment plumes.

The pattern of the seasonal variability of the POC flux at M3 station was similar to the one observed at LR station, namely the occurrence of a single, intense pulse in summer (Fig. 4-4-1 and 2) supplied the majority of the annual export of POC. The maxi-

mum flux at M3 station at 175 m was about 280 mg C m^{-2} d^{-1} (2007) while it was 21 mg C m^{-2} d^{-1} at LR-150m. The POC flux during the background periods at M3 station is comparable with LR-150m non-peak flux; <400 μmol C m^{-2} d^{-1} (<5 mg C m^{-2} d^{-1}; surmising from Fig. 2, Lalande et al., 2009a). However, the timing when such peaks occurs is offset between LR and M3 stations: The 1995 POC flux data shows the peak was ended in the late October. The peak of POC flux at M3 station began in June, reach the maximum in mid-July and ends in August during both years. Clearly, further study is warranted to understand the causes of the intra- and inter-annual variability in POC flux in the Laptev Sea.

6.5. Particle flux and sediment transport to the Chukchi Rise

6.5.1. Submarine topography and the IOEB drift route over the Chukchi Rise

The Chukchi Rise (Figs. 1–3) is a large submarine highland comparable to the Svalbard Complex in geographic scale. It leads to the southern edge of the Chukchi Sea, where a vast continental shelf forms a path to the Bering Strait, and where the water chemistry is often influenced by Yukon River outflow. Published nomenclature used to describe the topographic features of the Chukchi Sea area is somewhat inconsistent. Referring to GEBCO-5-17, the National Geographic Society's Tharp and Heezen map, Pry and Fleming (1986) and Stein and Macdonald (2004), we used the following definitions: The eastern and northern perimeters of the Chukchi Rise abut the flat Canada Abyssal Basin. The Northwind Escarpment is an extremely steep, continuous escarpment rising as high as 2.5 km from the basin floor. The Northwind Ridge hems this escarpment (Fig. 3). The Northwind Plain in the western half of the Chukchi Sea is incised by numerous gorges, many over 1 km deep (Stein and Macdonald, 2004, p. 174; IBCAO-based map). The minimum depth of the Northwind Plain is several hundred meters. The Chukchi Plateau, forming the eastern half of the highland, is the shallowest area on the Chukchi Rise. The highest portion of the Chukchi Rise, the Chukchi Cap, lies on the northwest corner of the rise and has a minimum depth of a few hundred meters. This topography consists of domes that are roughly aligned along 173°.

Remarkably, the nature and amplitude of export, and the biological pump modes/rates changed frequently and quickly in response to local sea ice conditions, seasonal procession, bottom topography, and other Arctic Ocean environmental conditions. We believe this highly dynamic variability of the POC biological pump is unique in the world ocean. This quick and frequent change of the quantity, quality, and rates of settling particle fluxes was captured by S97-120m while drifting 136 days over the Chukchi Rise, and is summarized in Fig. 6.

6.5.2. Variability of FC_{org}, $\Delta^{14}C$, and $\delta^{13}C$

The variability of $\Delta^{14}C$ in the S97-120m TS-trap depended principally on topographic and seasonal variability. As Fig. 7-2 illustrates, while IOEB S97 was drifting in the pelagic, cryospheric Canada Basin, the $\Delta^{14}C$ value for POC exported to 120 m was −60‰ (Period 2) to +8‰ (Period 7), indicating autochthonous POC with a minor component of aged carbon. As IOEB S97 approached the Chukchi Plateau, the POC became older (i.e., more ^{14}C-depleted), with $\Delta^{14}C$ values of −80‰ to −100‰.

Around Periods 11 and 13, $\Delta^{14}C$ values decreased further to −154‰ (Period 12; Table 5), the minimum value recorded during the drift of TS-trap S97-120m. During Period 12, the *F*Al suddenly surged to 50 μmol Al m^{-2} d^{-1} (Fig. 7-7). In fact, 85% of the annual *F*Al was captured by TS-trap S97-120m during this single period. The TS-trap did not touch the bottom sediment as it remained >400 m abs during this time. Also, a large export of POC, 221 μmol C m^{-2} d^{-1}, was recorded during this period.

$\Delta^{14}C$ values increased consistently toward the north from −97‰ in Period 14 to +17/18‰ in Periods 20/21 in the northern Canada Abyssal Plain (Fig. 7-2). The $\Delta^{14}C$ value was −32‰ during Period 16 when IOEB S97 arrived approximately over the summit of the Chukchi Cap with a clearance of only160 m above the seafloor. As we elaborate in the next section, the largest FC_{org} at the top of the Chukchi Cap was associated with a very large FSi_{bio}; the C_{org}/Si_{bio} ratio was close to 1 (Table 3). During these periods, we attribute the majority of FC_{org} to photosynthetic carbon derived from a diatom bloom.

The influences of topography and seasonality on the distribution of $\delta^{13}C$ are less clear than on $\Delta^{14}C$ values (Fig. 7-3), which may be due to multiple sources with less distinct stable carbon isotopic signatures. For example, the $\delta^{13}C$ of POC from the upper Yukon River (Guo and Macdonald, 2006) is comparable to that of POC exported over the Chukchi Rise POC. The $\delta^{13}C$ was between −25‰ and −26‰ during S97-120m-Phase 1. The average $\delta^{13}C$ during the winter periods at CD04-3067m beneath S97-120m's drift route during Periods 5 and 7 is −25.5‰, matching the Phase 1 value. Interestingly, the $\delta^{13}C$ was −26.3‰ during Period 11, which occurred near the Chukchi shelf edge. Similarly, low POC $\delta^{13}C$ values were found at the land-sea boundary near the Colville and Mackenzie rivers' estuary-front areas (Naidu et al., 2000; Macdonald et al., 2004a,b).

Mole C/N ratios during the Phase 1 drift averaged 7, within the range of the pelagic Redfield ratio. During Periods 11–14 (Table 3; Fig. 7-4), the C/N ratio lowered to 5, the lowest C/N ratio for the entire S97-120m TS-trap deployment. As mentioned before, the $\Delta^{14}C$ was the lowest around these periods. The C/N ratio steadily increased while TS-trap S97-120m was drifting northward over the Chukchi Cap. After exiting the northern end of the Chukchi Rise and crossing onto the Canada Abyssal Plain, the C/N ratio increased rapidly and reached a maximum of 27.5 during the drift over the northern Canada Abyssal Plain (Fig. 7-4). We are not presently able to explain this extraordinary increase in the C/N ratio except possibly as a change in the plankton community.

The $\delta^{13}C$, $\Delta^{14}C$, and C/N data obtained for the S97-120 TS-trap samples, particularly those intercepted while the trap drifted over the deep basin, provides some insight into the origin of particles exported from surface waters. It is interesting to note that when $\Delta^{14}C$ values were high and C/N values were low – indicating the export of predominantly fresh, autochthonous carbon – corresponding $\delta^{13}C$ values were quite low (−24‰ to −26‰). This implies that the phytoplankton-derived POC is ^{13}C-depleted, consistent with prior observations for high latitude oceans (e.g., Goericke and Fry, 1994). These low $\delta^{13}C$ values also suggest that export of POC from sea ice diatom productivity is minor as these organisms produce biomass that is enriched in ^{13}C (e.g., Belt et al., 2008).

6.5.3. Export of biogenic silicon and $CaCO_3$-PIC at the Chukchi Plateau

Both the FSi_{bio} and FC_{inorg} were very small during the Phase 1 drift of TS-trap S97-120m. 1.2–4.5 μmol Si m^{-2} d^{-1} (Fig. 7-5 and 7-6), corresponding to less than 1% of the global average of biogenic silicon export in the upper ocean. The FSi_{bio} was also small, 1.9–12.6 μmol Si m^{-2} d^{-1}, in the northern Canada Abyssal Plain during the last phase of IOEB S97's drift from August to October, but it surged to 395 and 452 μmol Si m^{-2} d^{-1} during Periods 16 and 17, respectively, as IOEB S97 crossed the top of the Chukchi Cap (Fig. 7-5). These fluxes are even larger than annual averages of daily export fluxes in many lower latitude pelagic sites observed at 500–200 m depth. However, it should be noted that the Chukchi Cap FSi_{bio} bloom is strongly restricted both in time and space; thus, the high export flux should have only minor impact on biogeochemical cycles in this area.

SiO_3-rich Bering Sea water mixed with Yukon River water is supplied directly to the Chukchi Plateau across the wide, fertile

Chukchi shelf (Macdonald et al., 2002). The Joint US/Canadian 1994 Arctic Ocean Section transect (e.g., Wheeler et al., 1997), which ran approximately 120 km west of the S97-120m drift route during Periods 13–17 (water sampling stations are indicated in the background of Fig. 7), provide insights into the nutrient regime in this region. Nearby Arctic Ocean Section Stations 8–11 maintained very high SiO_3 concentrations, 43–45 μmol L^{-1}, compared to the rest of the sections from the Mendeleyev Abyssal Plain to the Nansen Basin across the Pole, where the SiO_3 concentration averaged <10 μmol L^{-1} (Stations 20–35; Carmack et al., 1997). It is puzzling that the very large FSi_{bio} in TS-trap S97-120m occurred only in limited areas along the summit of the Chukchi Cap in July. The FSi_{bio} was considerably smaller, only about 3% of maximum flux, at the Canada Abyssal Plain, near the Mendeleyev Abyssal Plain.

The <1 mm fraction of FC_{inorg} (planktonic foraminifera) was quite small during the S97-120m-Phase 1 drift (Section 5.2). Also, the FC_{inorg} was small, 0.8–2.37 μmol C m^{-2} d^{-1}, during the periods when the TS-trap traversed the Northwind Plain from March to mid May 1998 but increased significantly during Periods 9, 13 and 14. The <1 mm fraction of FC_{inorg} was very large during Period 14, 23 μmol C m^{-2} d^{-1}, except when FSi_{bio} surged in relatively small areas at the top of the Chukchi Cap (Fig. 7-5 and 7-6). With the exception of Period 18, the FC_{inorg} was relatively small and vice versa during such FSi_{bio} "surges". It therefore appears that, in general, the zooplankton (pteropod and planktonic foraminifera) and diatom blooms do not coincide.

6.5.4. Transport of lithogenic particles on the Chukchi Plateau

We suspect clay particles can remain in suspension and be transported offshore to the pelagic Canada Basin from many regions and depths of the Beaufort coast, shelf edge, and slope. Such lithogenic particles were intercepted along the drift track of TS-trap S97-120m. Because of the near absence of the biological pump in the cryopelagic ocean, small particles such as clay are not grazed by filter feeders within the sparse zooplankton communities; thus, particles may remain in suspension over longer time scales than is typical under normal ocean conditions. This interpretation would help explain the virtual absence of lithogenic particles in TS-trap B96-200m (Tables 1 and 2; Fig. 4-1): coastal erosion along the nearby ocean/land boundary, the west coast of Queen Elizabeth Island, is limited by lack of river discharge and, particularly, more robust fast ice protection than is found on the Beaufort Sea coasts where there are major fluvial sediment sources and there is severe beach erosion.

The possible modes of offshore transport of particles of biogenic and lithogenic origin requires more investigation. Mathis et al. (2007) and Kadko et al. (2008) observed that Chukchi eddies could transport a "parcel of coastal sea" offshore while the coastal water retained its original ecosystem and POC attributes. Interestingly, IOEB S97 exhibited hovering and circling motions, both cyclonic and anti-cyclonic, that were up to several n-miles in diameter during Periods 11, 12, and 13 (Fig. 8); the 98-m-long CCGS *Des Groseilliers*, drifting in parallel with IOEB S97, made a tight loop of similar scale and direction about 25 n-miles west of the IOEB (Fig. 9). The ship and the IOEB executed at least three pairs of tight loops over

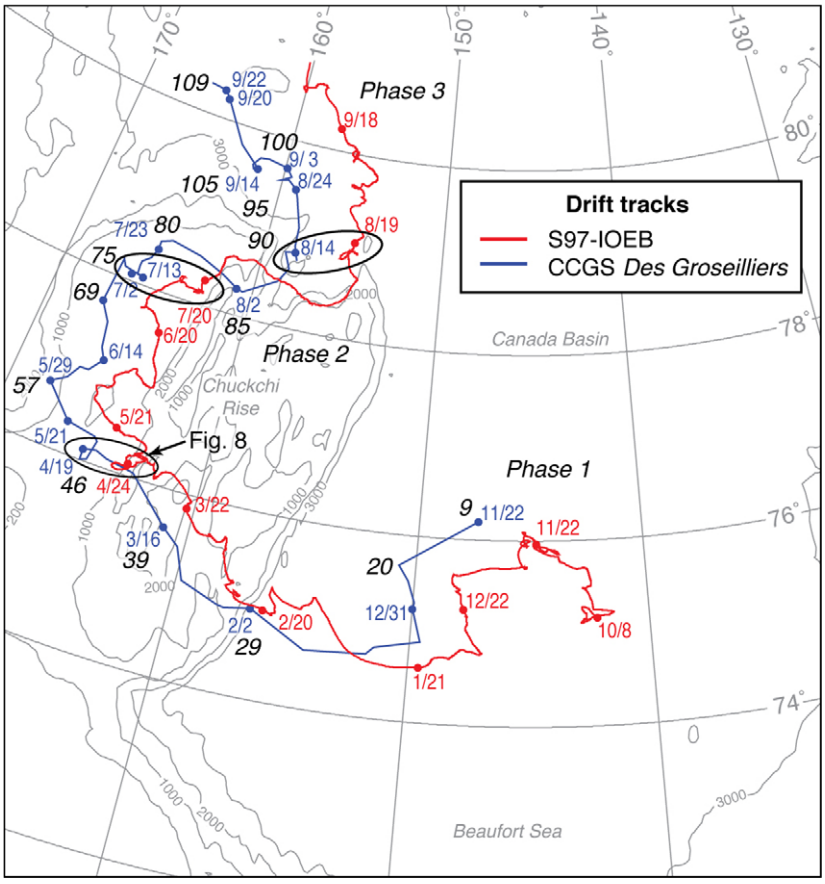

Fig. 9. Parallel 1997–1998 drift tracks of IOEB S97 and the SHEBA (Surface Heat Budget of the Arctic Ocean) Ice Camp on board the Canadian Coast Guard Ice Breaker *Des Groseilliers*. A TS-trap was moored to the S97-IOEB at 120m, and the buoy also carried many ice/atmosphere and underwater sensors. S97-IOEB (red line) was deployed in the mid Beaufort Sea on October 8, 1997, and the ice camp (blue line) drift began in mid October. After drifting in close proximity for about 10 months, their tracks diverged in early August 1998, although both headed generally northwest. Numbers in black letters along the blue line indicate ice camp water-cast stations for nutrient concentration profiles to 200 m (Figs. 10-1 and 10-2). Three ovals bridging the red and blue lines indicate locations where both the IOEB and the icebreaker executed synchronous spins, with the IOEB spin lagging that of the ice camp by about 5 days. An enlarged drifting track of S97-IOEB in the area marked as "Fig. 8" is illustrated in Fig. 8. (For interpretation of the references to color in this figure legend, the reader is referred to the web version of this article.)

the Chukchi Rise (Fig. 9), indicating the pronounced influence of eddies in this region.

During Periods 11 and 12, TS–trap S97-120m recorded a conspicuously large export of lithogenic particles (fine clay) (*F*Al was 19 and 50 μmol Al m^{-2} d^{-1}, respectively), associated with sudden surges of FSi_{bio} (11 and 21 mmol Si m^{-2} d^{-1}). The FC_{org} also surged to 235 and 221 mmol C m^{-2} yr^{-1} with low C/N ratios of 5 and 6, while FC_{inorg} was quite small. Interestingly, corresponding $\Delta^{14}C$ values were strongly depleted, −146‰ and −154‰, respectively (Fig. 7-2; Table 5), indicating the POC intercepted in the Chukchi shelf/slope waters (approximately 750–800 m deep) contains reworked (aged) carbon. The diatom frustules intercepted during these periods also included an allochthonous end member. The cause of this temporally and spatially localized supply of allochthonous particulate material emanating from the shelf break is not clear. It may be due to slumping or a coastal eddy, as described above. However, it remains uncertain if an eddy is capable of transporting substantial sediment loads over a significant distance.

The above observations over the Chukchi Plateau suggest that: (1) The large export of POC during Periods 16 and 17 was assisted by ample ballast particles of diatom frustules, and occurred while the zooplankton community was developing, perhaps under ice-edge conditions; (2) In the newly formed polynya, such as encountered during Periods 18 and 19, the export of foraminifera-FC_{inorg}, pteropod shells, and copepod molts was high, implying a thriving zooplankton community. Under these conditions, FC_{org} was moderately high but variable (reflecting the export of POC in the molts), and FSi_{bio} was conspicuously low. We interpret this observation to be a consequence of intensified zooplankton grazing on phytoplankton that initially results in export of POC and Si_{bio} particles (Period 18) but that rapidly exhausts the food supply shortly thereafter (Period 19). This suggests that the phasing of blooms of primary and secondary producers is often temporally offset (e.g., Smith and Schnack-Schiel, 1990) in the Chukchi hemipelagic environment.

6.5.5. Ocean stratification, nutrient concentration, and zooplankton standing crop compared to the Chukchi Rise biological pump

The SHEBA-CCGS *Des Groseilliers* drift camp (hereafter, SHEBA ice camp) provided detailed hydrographic and nutrient profiles (SHEBA nutrient profiles, hereafter) to 200 m (50–60 m at some stations) for 76 stations throughout the drift from November 22, 1997, to September 25, 1998, (Cota and Pomeroy, 2003; Section 2.3; http://www.eol.ucar.edu/projects/sheba/). Comparing particles collected by IOEB S97 with SHEBA nutrient profiles (Figs. 3 and 10-1 and 10-2), we found that PO_3, NO_3, and SiO_3 are strongly depleted in the PML occupying the surface 50–70 m (e.g., Macdonald et al., 2002; Sakshaug, 2004). During Phase 1, the nutrient concentration in layers deeper than about 100 m (i.e., corresponding to the halocline layer; Macdonald et al., 2004a,b) was much higher than in the PML water, reflecting contributions from Pacific water along with Yukon outflow (e.g., Codispoti and Lowman, 1973; Ekwurzel et al., 2001; Guo and Macdonald, 2006). Swift et al. (1997) observed concentrations of SiO_3 >90 μmol C L^{-1} in Chukchi slope water at about 100 m along the shelf front. SHEBA nutrient profiles also indicate that the Chukchi Rise is covered by oligotrophic water (<19 mmol Si L^{-1}) to approximately 120 m deep. A thin tongue of nutrient-rich Pacific water (>40 mmol Si L^{-1}) lies

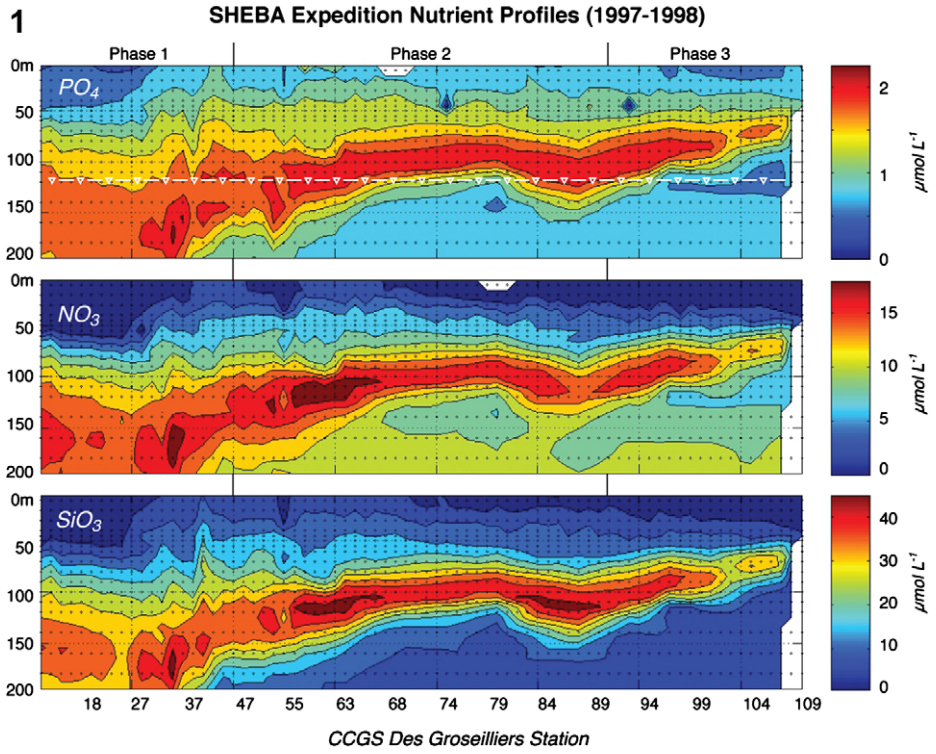

Fig. 10. Surface to 200 m (Fig. 10-1) and to 5–55 m (Fig. 10-2) profiles of the concentration of PO_4, NO_3, and SiO_3 based on the daily nutrient profile (76 castings) from CCGS *Des Groseilliers* began on November 22, 1997 and completed on September 25, 1998. The original profile numbers are shown below the SiO_3 panels. The top panel of Fig. 10-2 shows a Sigma-*t* profile. The hydrographic and nutrient data in Fig. 10-1 and 2 are based on Cota and Pomeroy (2003, http://www.eol.ucar.edu/projects/sheba/). We used equal spacing MatLab software. (1) These SHEBA ice camp nutrient profiles reflect a robust Pacific halocline with a well defined nutrient maximum between 100 and 150 m. Some disorder in the layering of nutrient concentrations in the halocline at the Phase 1/Phase 2 boundary could be caused by eddy activities. The nutrient maximum on the top of the Pacific Halocline appears to taper off around 80°N in this profile. A horizontal line of white triangles across the uppermost panel indicates the S97-120m TS-trap drift depth. (2) Nutrient profiles of the euphotic layer and the nutrient-depleted PML. The 0.1% light level depth in this area is 37 ± 13 m on average (Section 6.5.5). NO_3 and SiO_3 profiles and FC_{org} and FSi_{bio} values are all indicated in μmol C m^{-2} d^{-1}. The white broken vertical lines designate the approximate midpoints of the 14 (out of a total of 21) drift periods; some periods overlap considerably.

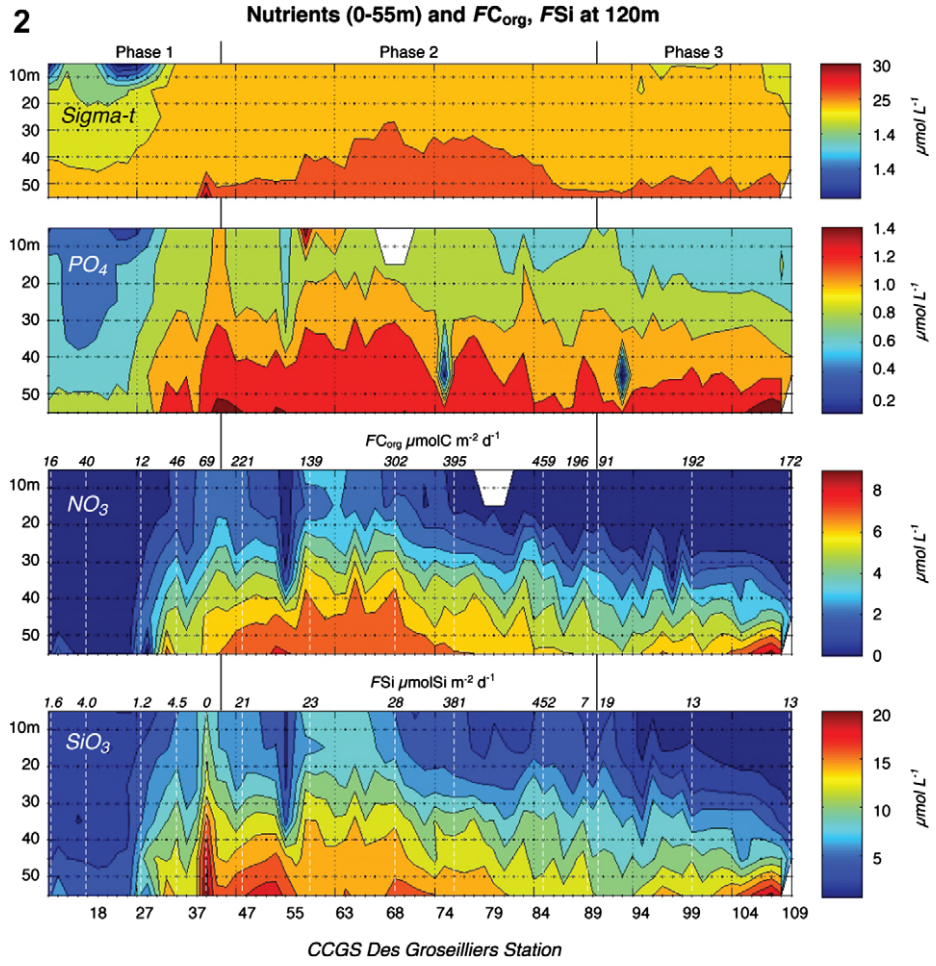

Fig. 10 (*continued*)

beneath the PML, maintaining its characteristic configuration at the northern end of the Chukchi Rise, 80° to 81°N (Fig. 10-1). Importantly, the autotrophic plankton community is not able to utilize these nutrients since the tongue develops below polar ocean euphotic depths; Cota et al. (1996) found that the 0.1% light level in this area is 37 ± 13 m on average and ranges from 25 to 61 m on the southern Chukchi Rise. The biological pump operating on the Chukchi Rise uses the nutrients contained in the oligotrophic PML, thus leaving the rich but deep reservoir halocline nutrients intact.

We compared the pattern of particle export from TS-trap S97-120m (Fig. 4-2) and SHEBA nutrient profiles in the upper 60 m (Fig. 10-2). However, no clear relationship emerged between nutrient concentrations and export rates of POC or other biogenic components. PLM nutrients were highly depleted during the late autumn and winter (Phase 1 of S97-120m; Fig. 10-2). The export fluxes at 120 m were extremely small during this phase. Between SHEBA stations 37–68, the upper PML NO_3 and SiO_2 nutrient concentration was elevated in two cases. However, the export flux increased insignificantly except during Period 12, when the flux was augmented by allochthonous POC. Although existing data are insufficient to draw any conclusions, it appears that enriched parcels of water can be transported quickly by passing eddies (Section 6.1.3; Fig. 9) as reported by Kadko et al. (2008). While the SHEBA ice camp drifted over the Chukchi Cap, the concentration of PML NO_3 and SiO_3 varied frequently with time and space (vertical bands of maxima/minima in Fig. 10-2). The export flux maximum of biogenic silicate particles and POC (e.g., Periods 16 and 17) may be related to this pattern of depletion and re-supply. The nutrient cycle was less distinct when the SHEBA ice camp re-entered the cryopelagic, oligotrophic PML (Phase 3). POC export remained large, but the export of biogenic silicate particles was significantly reduced during Phase 3.

Although much further investigation is required to establish this relationship, we anticipate that zooplankton biomass will correlate with particle export flux. Indeed, seasonal variability of the proportion of zooplankton biomass collected from the upper 100 m compared to total zooplankton biomass in the water column obtained along the SHEBA drift appears similar in regard to time variability (Ashjian et al., 2003; Fig. 4, p. 1242). Further effort must be made to clarify the role of the ice-algae community in the biological pump before the production of sea ice is radically reduced (i.e., Melnikov et al., 2002).

7. Comparison of the Canada Basin with the Antarctic Zone (Ross Sea) and Bering Sea biological pumps

The deep Ross Sea Gyre and the Indian Ocean Sector of the Antarctic Zone (AZ) can be considered the Antarctic counterpart of the cryopelagic Canada Basin and the Central Arctic Ocean. PP estimates from the ocean-color model (Behrenfeld and Falkowski, 1997) at the Weddell Sea Gyre station (designated U. Bremen WS-65; Wefer and Fischer, 1991) were 2.3 molC m^{-2} yr^{-1}. Estimated primary production using the same model for both the Ross Sea Gyre station (MS-5 at 66.10°S, 169.40°W: Honjo et al., 2000) and the Prydz Bay station (62.0°S, 73.0°W; Pilskaln et al., 2004) was 2.5 molC m^{-2} yr^{-1}. Using ^{14}C uptake experiments, Nelson

et al. (2002) estimated primary production in the Ross Sea Gyre at 3.7 molC m^{-2} yr^{-1}. These levels are at the upper end of recent estimates of PP in the cryopelagic Central Arctic Ocean (e.g., Sakshaug, 2004) but generally of the same order of magnitude.

Quite remarkably, the interior annual FC_{org} at these Antarctic Zone stations (Tréguer and Jaques, 1992) was 43–84 mmol C m^{-2} yr^{-1} when normalized to the flux at 2000 m, about 50–70% of the global average. The annual FSi_{bio} at these stations was 269–397 mmol Si m^{-2} yr^{-1}, two to three times the global average (Honjo et al., 2008). However, the annual FC_{inorg} was small at both stations, 7–28 mmol C m^{-2} yr^{-1}. It is hypothesized that the low FC_{inorg} at pelagic Antarctic Zone stations such as MS-5 and Prydz Bay results from stratification caused by a persistent winter water layer. This "dicothermal" layer creates a boundary that inhibits development of a zooplankton community, including planktonic foraminifera and pteropods (Honjo et al., 2000; Honjo, 2004). These observations indicate that the biological pump fully functions in these Antarctic Zone areas, and is driven by diatom frustules as principal ballast particles that efficiently remove POC (Francois et al., 2002), despite very limited PP.

In contrast, the annual FC_{org} of 14.2 mmol C m^{-2} yr^{-1} intercepted by CD04-3067m in the central Canada Basin is 33–17% of the equivalent flux to the deep Antarctic Zone. Likewise, FC_{inorg} of 1.8 mmol C m^{-2} yr^{-1} is only 0.3–0.6% of the Antarctic flux, and FSi_{bio} of 1.2 mmol Si m^{-2} yr^{-1} corresponds to 0.3–0.5% of the Antarctic flux. Moreover, the major portion of the POC intercepted at 3067 m in the Canada Basin was allochthonous; therefore, the actual export to this deep Arctic basin station can be considered near zero.

The cause for such a contrast in the export of biogenic particles may be the fundamental differences in nutrient supply and water stratification between the Antarctic Zone and Central Arctic seas. Upwelling caused by the vigorous Antarctic Divergence enriches the surface layers of the Antarctic Zone, making them among the most nutrient-replete of any world ocean surface waters (e.g., Jones et al., 1990). The concentrations of NO_3 and SiO_3 in Ross Sea in various seasons (1996/1997) at approximately 60 m depth were 10–31 μmol N kg^{-1} and 65–75 μmol Si kg^{-1}, respectively (Gordon et al., 2000). In contrast, these concentrations at 0–49 m depth were <2–3 μmol N kg^{-1} and <2–7 μmol Si kg^{-1} in the PML during the S97-IOEB drift (Fig. 10-2).

Differences in phytoplankton community structure may be another reason for the major discrepancy between these Arctic and Antarctic regimes. The Antarctic Zone supports an extraordinarily large primary production of diatoms, up to the limit of chemical equilibrium (1.3 molC m^{-2} yr^{-1} in the Ross Sea Gyre; Nelson et al., 2002). This huge production of diatom frustules must be removed from the surface layers to maintain a steady chemical state in the surface water. Frustules form large, rapidly settling aggregates that scavenge POC and serve as effective ballast material (Honjo, 2004) (in contrast to the eastern Equatorial Pacific where biogenic $CaCO_3$ particles such as coccoliths are the major ballast material (Honjo et al., 1995b)). Thus, the biological pump functions highly efficiently in the Antarctic Zone (Honjo et al., 2000; Francois et al., 2002), despite the absence of coccoliths, which comprise the major ballast particles in low-latitude oceans (e.g., Honjo et al., 2008). In contrast, the cryopelagic Arctic Ocean, including the Canada Basin, does not produce a well-developed diatom community because of SiO_3 depletion in the upper layers and perhaps other reasons. In addition, coccolith production appears to be nearly absent in the PML (e.g., Hargrave et al., 2002). The resulting absence of ballast materials severely hampers the biological pump in the cryopelagic Arctic Ocean. As a consequence, rather than being transported to deep waters, most of photo-synthetically derived POC in the Central Arctic must be remineralized or degraded *in situ* to marine DOC. As a result, the cryopelagic Arctic Ocean contributes minimally to the sequestration of atmospheric CO_2 in the form of POC whereas in the Southern Ocean, the vigorous biological pump, maintained by a very large supply of biomineral ballast particles, is effective at removing carbon from surface waters.

Bering Sea surface waters support extremely high total PP both in shelf and deep-basin waters (e.g. Springer et al., 1996), and a large proportion of it is new production C (e.g., Walsh and Dietele, 1994). For example, the "Green Belt" along Kamchatka yielded >25–75 molC m^{-2} yr^{-1} (Sapozhnikov et al., 1993). Both Springer et al. (1996) and Fukuchi et al. (1993) observed very large POC flux, from the same area, >67 molC m^{-2} yr^{-1}, and also >33 molC m^{-2} yr^{-1}, respectively. Primary production along the Aleutian Arc was 17–25 molC m^{-2} yr^{-1} (Schell and Saupe, 1989), and the FC_{org} at 2 km was around 300 mmol C m^{-2} yr^{-1} (Takahashi et al., 1997, 2000). The Green Belt produces an unusual amount of carbonate biominerals as abundant *Emiliania* coccolithophorids, although they are strongly patchy and seasonal, and abundant diatom frustules for ballast. The FC_{org} in the deep (3783 m) northwestern Bering Abyssal Basin was 248 mmol C m^{-2} yr^{-1}, twice as large as the global FC_{org} at the 2-km isobath (Honjo et al., 2008). The primary production in surface waters of the deep basin is 21 molC m^{-2} yr^{-1}, half of which is new production (Maita et al., 1999). The main cause of the extraordinarily high PP and export flux observed in the Bering Sea is the abundant supply of nutrients from the upwelling Global Thermohaline Circulation pattern as it meets the Bering Sea's imposing shallow topography. The high supply of nutrients in the Ross Sea is also linked to the upwelling Global Thermohaline Circulation. (The Arctic Basin is, at this time, the ocean that is most severely segregated from the Global Thermohaline Circulation beside the Black Sea.) It is intriguing that a very large patch of *Emiliania* occurred on the eastern Bering shelf area (Overland et al., 1999). Such patches are now often reported in the Kamchatka coast. Are such *Emiliania* blooms (i.e., Holligan et al., 1983, in the North Atlantic Ocean) in the Bering Sea only a recent occurrence or are they a persistent phenomenon?

8. Conclusions

The mass flux of ocean particles (TMF) beneath the cryopelagic Canada Basin was as small as 0.6 g m^{-2} yr^{-1} at 120 m and 0.4 g m^{-2} yr^{-1} at 200 m measured by TS-traps tethered to instrumented buoys (IOEBs) drifting with the sea ice. The POC export flux collected in these two TS-traps was 7.0–10.0 mmol C m^{-2} yr^{-1}, two to three orders of magnitude smaller than the POC fluxes recorded at equivalent depths from lower-latitude oceans, the Southern Ocean, and the Sea of Okhotsk. In contrast, the upper estimates of annual primary production in the Canada Basin (0.5–2.5 molC m^{-2} yr^{-1}) are comparable to the annual primary production in some low-latitude pelagic oceans. One of the major reasons for the low primary productivity in the Beaufort Gyre is the broad cap of oligotrophic Polar Mixed Layer waters. However, this nutrient deficiency and strong stratification does not explain the lack of a biological pump in the cryopelagic ocean. The POC export fluxes in other low-primary production areas, including the Antarctic Zone, are at least two orders of magnitude larger than the POC export fluxes we observed in the cryopelagic Canada Basin. This extremely low POC export flux was also associated with extremely small biomineral particle export (e.g., diatom frustules, coccoliths and lithogenic particles) and a poorly developed zooplankton ecosystem in the water column, as indicated by the lack of fecal pellet export. We hypothesize that the biological pump does not function effectively in the Arctic cryospheric ocean because of a lack of ballast particles required to export the POC to the deep layers. Thus, we suspect the majority of primary production POC in the Canada Basin does not reach the deep oceanic interior as it does in all other

areas of the world ocean that have been studied. We also hypothesize that most of the primary production is instead remineralized by the ecosystems and degraded to marine DOC that is ultimately removed from the Arctic Basin by advective processes to maintain the carbon cycle in a steady state. However, the recent finding of a strong biological pump with abundant coccoliths and diatom frustules and apparently full-fledged micro-, meso-zooplankton ecosystem in the southeast corner of the Beaufort Sea (Franklin Bay) (Forest et al., 2008; Sampei et al., 2009) hints at a dynamic environmental evolution of the High Arctic. The cause of this apparently isolated biological pump-dominated area remains uncertain. We hypothesize that the bloom was supported by the shoaling of nutrient-rich Anadyr Current water that was transported along the southern coast of the Beaufort Sea.

The annual mass flux of particles collected by a seafloor-anchored TS-trap in the deep interior of the Canada Basin at 3067 m (757 m above the seafloor) in 2004–2005 was 4.3 g m^{-2} yr^{-1}, an order of magnitude larger than the flux measured at 120 m and 200 m by the ice-tethered TS-traps drifting over the same geographic domain from 1996 to 1997. The POC export flux at this depth was 14.2 mmol C m^{-2} yr^{-1}, also substantially larger than the export flux at 120 m and 200 m. This observation indicated that the origin of the POC exported to the interior was fundamentally different from the POC and particles exported to 120 m and 200 m under the cryopelagic ocean. In particular, for the 3067-m TS-trap samples: (1) $\Delta^{14}C$ values of the POC (annual average, −217‰) indicated that it contained a large proportion of an aged, allochthonous component. (2) The particles consisted of 85-wt% of clay-size lithogenic particles (compared to a minor lithogenic flux in the samples intercepted by the 120 and 200 m TS-traps). (3) There was an extremely high correlation coefficient (r^2 = 0.978) throughout the year between *F*Al and FC_{org}, which did not exist for the shallow TS-trap samples. Together, these observations indicate that particles intercepted in the deep interior of the Canada Basin were highly homogenized, and likely transported via physical processes from a distal source. We observed two distinct modes of particle export to the 3067-m trap that are decoupled from either the seasonal procession or biological forcing, and are most plausibly explained via gravitational-hydrodynamic processes: The majority of particles exported during

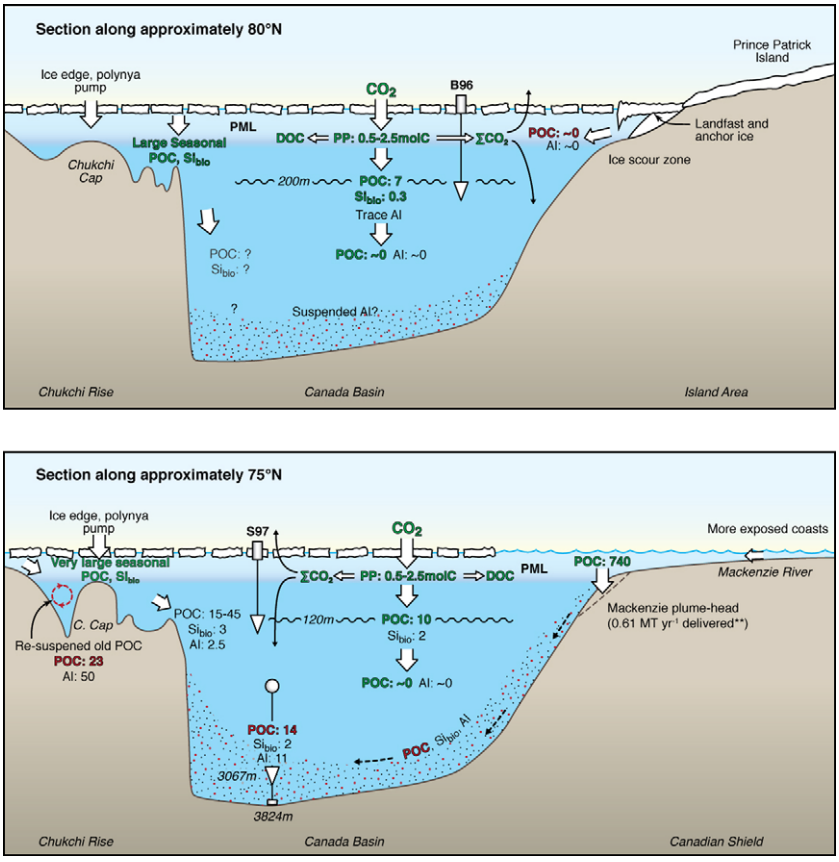

Fig. 11. Schematic diagrams of the estimated annual export flux of POC, particulate biogenic Si, and lithogenic Al (in mmol m^{-2} yr^{-1}, except primary production C is shown in molC m^{-2} yr^{-1}) to the interior of the cryopelagic Canada Basin and Chukchi Submarine Highland). Note that these are not model values but display the authors' data and other published observational data. Upper panel: An east-west section of the cryopelagic Beaufort Sea along approximately 78–80°N in the Canada Basin beginning at Prince Patrick Island (in the Canadian Arctic Archipelago), which supplies only minimal biogenic or lithogenic particles to the cryopelagic Canada Basin. The primary production (PP) is Sakshaug's (2004, p. 70) estimate/compilation from the Central Arctic Ocean in molC m^{-2} yr^{-1}. Lower panel: An east-west section of the cryopelagic Beaufort Sea along approximately 74–76°N. The POC flux and the bulk sediment delivery at the head of the Mackenzie Plume in 1987 and 1988 are cited from O'Brien et al. (2006), p. 65). In both panels, autochthonous fluxes are in green, allochthonous fluxes are in red, and Al fluxes are in black type. PML indicates the Polar Mixed Layer (Macdonald et al., 2004a,b) Fig. 9 (Figure and caption do not match, so not reviewed). Schematic diagram of the estimated annual export flux of POC, particulate biogenic Si, and lithogenic Al (in mmol m^{-2} yr^{-1}, except primary production C is shown in molC m^{-2} yr^{-1}) to the interior of the cryopelagic Canada Basin and Chukchi Submarine Highland as measured by three TS-traps. Note that these are not model values but display the authors' data and other published observational data. Upper panel: Approximate east-west section of the Canada Basin beginning at Prince Patrick Island (in the Canadian Arctic island sea), which supplies only minimal biogenic or lithogenic particles to the cryopelagic Canada Basin. The primary production (PP) is Sakshaug's recent estimate/compilation from the Central Arctic Ocean in molC m^{-2} yr^{-1} (Sakshaug, 2004, p. 70). In both panels, autochthonous fluxes are in green, allochthonous fluxes are in red, and elements of unknown origin and Al fluxes are is in black type. PML indicates the Polar Mixed Layer (Macdonald et al., 2004a,b). Lower panel: Approximate east-west section of the Beaufort Sea and Canada Basin through the Canada Abyssal Plain. Both the POC flux collected by TS-traps and the bulk sediment delivery at the head of the Mackenzie Plume in 1987 and 1988 are from O'Brien et al. (2006, p. 65). (For interpretation of the references to color in this figure legend, the reader is referred to the web version of this article.)

the 4.5-month-long "main export period" in 2005 exhibited distinct $\delta^{13}C$ and C/N ratios compared to the "low export periods" which persisted for the rest of the annual deployment (summarized in Fig. 11).

These observations lead us to hypothesize that POC and oceanic particles were transported to the abyssal depths from the adjacent flanks of the Canada Basin. Sedimentary reservoirs on the margins contain POC and particles derived from river discharge, coastal erosion, and local marine primary production. Resuspension and lateral transport provides a source of lithogenic particles and aged POC to the adjacent basin. The POC biological pump therefore may operate in lateral or tangential vectors in response to gravity and hydrodynamic forcing. In way, POC supply to the abyssal Canada Basin occurs without regard for seasonal solar cycles or upper ocean ecosystem dynamics, and instead is moderated by processes that deliver POC and associated materials to the shelves, and that remobilize this material and transport it across margin and down-slope. This is fundamentally different from the world's other pelagic oceans (including the Southern Ocean) where POC is exported vertically to depth by a biological pump that is driven by a tight combination of gravitational and zooplankton community processes.

POC export and ocean particle sedimentation processes over the hemipelagic Chukchi Plateau differed markedly from those in the cryopelagic Canada Basin. The drift of TS-trap S97-120m across the Chukchi Plateau (Phase 2) provided intriguing insights into the export process for biogenic and lithogenic particles. Remarkably, the nature and amplitude of export changed frequently and quickly in response to the availability of nutrients in the shallow euphotic zone of the oligotrophic Polar Mixed Layer, which is further influenced by local sea ice conditions, seasonal procession, bottom topography, and other Arctic Ocean environmental conditions. The extremely nutrient-rich Bering Sea-Yukon River water that penetrates into the Canada Basin at about 100 m does not induce local primary production and removal of POC by a biological pump because it is inaccessible to phytoplankton communities.

9. Future implications: the biological pump in the context of future Arctic change

How will carbon cycling in the Arctic Ocean change in response to regional warming? At present it remains unclear how environmental regime shifts caused by Arctic warming will influence the efficiency of the Arctic biological pump. It seems likely that intensification of the biological pump may take place if certain critical conditions occur, however there is a severe lack of data needed to better understand the underlying processes. Swift emplacement of observational programs based on technology suited to sustained and comprehensive characterization of the Arctic Ocean and its marginal seas is crucial while high rates of change are underway. In particular, answers to the following questions are urgently needed:

(1) Could potential transformations in the Polar Mixed Layer (e.g., Macdonald et al., 2002) induce a change in the operation of the Arctic Ocean biological pump? The increasing difference in Atlantic and Pacific evaporation rates and other causes are likely to strengthen the Anadyr Current, which transports nutrient-rich Bering Sea water and Yukon River outflow to the Arctic Basin (e.g., Roach et al., 1995; Jones et al., 2003) and feeds nutrient-rich water into the Pacific halocline layer. At the same time, the river water and thawing of sea ice would supply more freshwater to the PML. What will be the interplay between these two factors under Arctic warming conditions and how might they change the biological pump? The PML, which is presently thicker than the euphotic zone in the Beaufort Gyre (Cota et al., 1996), renders nutrients in the Pacific halocline layer inaccessible to phytoplankton. The boundary between the PML and the halocline also obstructs the vertical migration of micro-zooplankton (this study, Section 6.1) and may arrest particle settling, exposing biogenic constituents to more extensive remineralization (Moran et al., 1997). Together, these conditions inhibit the operation of a vigorous Arctic Ocean biological pump as our research indicates. However, if the PML is significantly modified or eroded, then the biological pump may be activated. Physical and biogeochemical observations are needed to enhance our understanding of how the PML may evolve in the future and what the biogeochemical implications may be for the Arctic Ocean.

(2) Could changes in the ecosystems of the Arctic Ocean result in an increased capacity for sequestering atmospheric CO_2, similar to that of the North Pacific "Silica Ocean" (Honjo et al., 2008), including the Bering Sea? Operation of the biological pump in the world ocean requires a certain level of plankton diversity, especially ballast particles in the form of coccolith and/or diatom frustules with biogenic aggregating substances (EPS) as well as a vertically migrating zooplankton community (Honjo et al., 2008). The recent discovery of POC export accompanied by coccolithophorid, diatom, and micro-zooplankton fecal pellets in Franklin Bay (Forest et al., 2007, 2008; Sampei et al., 2009) raises the key question of whether this discovery is a harbinger of a developing biological pump in the Beaufort Sea, or whether there have long been unrecognized coccolithophorid blooms in Franklin Bay. Historical (paleoceanographic) investigations would help to determine whether such ecosystem changes are linked to other oceanographic variations such as a North Pacific/Bering Sea Regime Shift (e.g., Hare and Mantua, 2000). Genetic surveys of primary producers, especially coccolithophorids (e.g., Iglesias-Rodriguez et al., 2007), from the Bering Sea and the Beaufort Sea to Baffin Bay would shed light on the potential transformation of the Arctic biological pump.

(3) Where might the Arctic biological pump first experience change? The earliest indication of regime shift in the Arctic biological pump in the form of a coccolithophore and diatom bloom (often expressed as the mol ratio between C in the biogenic $CaCO_3$ and Si in biogenic SiO_2, Honjo et al., 2008, Tables 1, 3 and 4) may occur in slope and shelf waters of the eastern Beaufort Sea (O'Brien et al., 2006; Forest et al., 2008).

(4) What physical changes in the Arctic current system could bring such a major biogeochemical regime shift? At present, the nutrient-rich Bering-Yukon water spreads out beneath the PML and the euphotic zone after entering the Chukchi Sea, and this water flows eastward as the Anadyr Current in response to the Coriolis force (Aagaard and Carmack, 1989) known as the Pacific Layer (PL) Boundary Current (e.g., Jones, 2001; Macdonald et al., 2004a,b) (Fig. 1). Although speculative, shoaling of the boundary current caused by underwater topography may result in mixing of Bering-Yukon water with the PML, possibly in the southeastern Beaufort Sea on the Mackenzie shelf, in the Amundsen Gulf and the Banks Island area. Bering-Yukon water may potentially flow through the Canadian archipelago toward the North Atlantic (Codispoti and Owens, 1975; Jones and Coote, 1980; Jones et al., 2003). Data collected from 1997 to 1999 at the Northern Water Station (NOW, Fig. 1) in northernmost Baffin Bay showed large export fluxes of FC_{org} and FSi_{bio} (but no coccolithophorid export is reported so far) and abundant zooplankton fecal pellets (Hargrave, 2004;

Sampei et al., 2004; Lalande et al., 2009a). Sustained measurements of water flow in the eastern Beaufort Sea and Baffin Bay toward the North Atlantic are required to determine whether regime shift is indeed underway.

(5) What influence might changing terrestrial inputs exert on the Arctic Ocean carbon cycle? The Arctic rivers are expected to respond rapidly to global warming by exporting more run-off water, nutrients, and sediments to the Arctic Ocean. With the exposure of soils and peat, terrigenous POC may be transported to the deep basin slopes and floors by an invigorated "lateral biological pump (Section 6.3)." Mobilization of this pre-stabilized carbon in peat deposits and permafrost soils and its sequestration in the deep Arctic basins results in no net change in terms of the overall sink. As such, it does not help to offset the increase in atmospheric CO_2 from anthropogenic activity. However, our knowledge of this phenomenon is poor because of the limited observations of carbon export to deep waters of the Central Arctic basin. Time-series studies on the magnitude of POC supplied by vertical and lateral components of the biological pump, together with determination of the provenance of exported carbon, are required to further explore these influences.

Funding sources

The Office of Naval Research, Arlington, VA, USA, National Science Foundation, Arlington, VA, USA, Japan Marine Science and Technology Center, Yokosuka, Japan, Woods Hole Oceanographic Institution, Woods Hole, MA, USA, McLane Research Laboratories, Inc., East Falmouth, MA, USA.

Acknowledgements

We heartily thank R. Macdonald for his generosity in reviewing the first manuscript and offering many suggestions for improving the manuscript. We sincerely thank Editor C. Warner and numerous reviewers who also provided valuable suggestions. We are deeply indebted to long-term colleagues, including W.B. Tucker and D. Perovich of the US Cold Region Research and Engineering Laboratory (CRREL); A. Proshutinsky, A. Pleuddemann, R. Goldsmith of the Woods Hole Oceanographic Institution (WHOI); and R. Moritz and A. Heiberg of the Polar Science Center (PSC) at the University of Washington for many discussions, valuable advice, and field cooperation. Our thanks are due to many colleagues who collaborated to develop and deploy IOEBs in Canada Basin sea ice; they include W. Ostrom, L. Costello, and J. Lord (WHOI); W. Bosworth (CRREL); and K. Hatakeyama (Japan Agency for Marine-Earth Science and Technology, JAMSTEC). The IOEB-tethered TS-trap project could not have happened without the field support of the AREA Program, US Navy Space and Naval Warfare Command (SPARWAR), whose staff facilitated ice camps for IOEB TS-trap operations. The National Science Foundation's Surface Heat Budget of the Arctic Ocean Experiment (SHEBA) assisted launch of IOEB S97. We acknowledge the critical data collected during the side-by-side yearly drifting of CCGS *Des Groseilliers* during 1997/1998, particularly to G. Cota and L. Pomeroy who provided invaluable onboard data for this study. We would like to give special mention to the late D. Nasogaluak, Canadian Helicopters, Inc., who facilitated the Canada Basin IOEB program with enthusiasm and outstanding skill. Significant logistic support from the Beaufort Gyre Observation System (WHOI) and the collaboration of the Captain and the crews of Canadian Coast Guard Icebreaker *Louis S. St-Laurent* were vital to launching the CD04-3067m TS-trap mooring in a challenging marginal ice situation. We sincerely thank J. Cook, WHOI Graphic Arts Department, for superb and imaginative graphic design, V. Cullen, Red Pen Ink, Inc., for professional editing, and P. White for her able administrative assistance to this project. The primary sponsors of this research were the Office of Naval Research (ONR) (Code 322) and the Japan Marine Science and Technology Center. We acknowledge additional funding from US National Science Foundation grant # OCE-9986766 to S. Honjo and # ARC-0909377 to T. Eglinton, the Comer Science and Education Foundation, the Ocean Climate Change Institute of the Woods Hole Oceanographic Institution, and McLane Research Laboratories, Inc., East Falmouth, MA, USA.

References

Aagaard, K., Carmack, E.C., 1989. The role of sea ice and other fresh water in the Arctic circulation. Journal of Geophysical Research 94, 14485–14498.

ACIA (Arctic Climate Impact Assessment), 2004. Impacts of a Warming Arctic. Cambridge University Press. p. 1046.

Armstrong, R.A., Lee, C., Hedges, J.L., Honjo, S., Wakeham, S.G., 2001. A new mechanistic model for organic carbon fluxes in the ocean, based on the quantitative association of POC with ballast minerals. Deep-Sea Research II 49, 219–236.

Ashjian, C.J., Campbell, R.G., Welch, H.E., Butler, M., Van Keuren, D., 2003. Annual cycle in abundance, distribution, and size in relation to hydrography of important copepod species in the western Arctic Ocean. Deep-Sea Research I 50, 1235–1261.

Barnes, P.W., Reimnitz, E., Fox, D., 1982. Ice rafting of fine-grained sediment, a sorting and transport mechanism, Beaufort Sea, Alaska. Journal of Sedimentary Petrology 52, 493–502.

Behrenfeld, M.J., Falkowski, P.G., 1997. Photosynthetic rates derived from satellite-based chlorophyll concentration. Limnology and Oceanography 42, 1–20.

Belicka, L.L., Macdonald, R.W., Yunker, M.B., Harvey, H.R., 2004. The role of depositional regime on carbon transport and preservation in Arctic Ocean sediments. Marine Chemistry 86, 65–88.

Belt, S.T., Massé, G., Vare, L.L., Rowland, S.J., Poulin, M., Sicre, M.-A., Sampei, M., Fortier, L., 2008. Distinctive ^{13}C isotopic signature distinguishes a novel sea ice biomarker in Arctic sediments and sediment traps. Marine Chemistry 112, 158–167.

Boyd, P.W., Trull, T.W., 2007. Understanding the export of biogenic particles in oceanic waters: is there consensus? Progress in Oceanography 72, 176–312.

Bourke, R.H., Garrett, R.P., 1987. Sea ice thickness distribution in the Arctic Ocean. Cold Region Science Technology 13, 259–280.

Broerse, A.T.C., Ziveri, P., Honjo, S., 1990. Coccolithophore ($-CaCO_3$) flux in the Sea of Okhotsk: seasonality, settling and alteration processes. In: Coccolithophore Export Production in Selected Ocean Environments, Ph.D. Thesis, Vrije University, Amsterdam, The Netherlands, pp. 93–119.

Buesseler, K.O., Lamborg, C.H., Boyd, P.W., Lam, P.L., Trull, T.W., Bidigare, R.R., Bishop, J.K.B., Casciotti, K.L., Dehairs, F., Elskens, M., Honda, M., Karl, D.M., Siegel, D.A., Silver, M.W., Steinberg, D.K., Valdes, J., van Mooy, B., Wilson, S., 2007. Revisiting carbon flux through the ocean's "twilight zone". Science 316, 567–570.

Buesseler, K.O., Steinberg, D.K., Michaels, A.F., Johnson, R.J., Andrews, J.E., Valdes, J.R., Price, J.F., 2000. A comparison of the quantity and composition of material caught in a neutrally buoyant versus surface-tethered sediment trap. Deep-Sea Research I 47, 277–294.

Carmack, E.C., 1990. Large-scale physical oceanography of polar oceans. In: Smith, W. (Ed.), Polar Oceanography, Part A. Academic Press, San Diego, pp. 171–222.

Carmack, E.C., Aagaard, K., Swift, J.H., Macdonald, R.W., McLaughlin, F.A., Jones, E.P., Perkin, R.G., Smith, J.N., Ellis, K.M., Killius, L.S., 1997. Changes in temperature and tracer distribution within the Arctic Ocean: result from the 19994 Arctic Ocean section. Deep-Sea Research II 44, 1487–1502.

Carmack, E.C., Macdonald, R.W., Perkin, R.G., McLaughlin, F.A., Pearson, R.J., 1995. Evidence for warming of Atlantic Water in the Southern Canadian Basin of the Arctic Ocean: results from the Larsen-93 expedition. Geophysical Research Letters 22, 1061–1067.

Carson, M.A., Jasper, J.N., Conly, F.M., 1998. Magnitude and sources of sediment input to the Mackenzie Delta, Northwest Territories, 1974–1994. Arctic 51, 116–124.

Christensen, J.P., 2000. A relation between deep-sea benthic oxygen demand and oceanic primary productivity. Oceanological Acta 23, 65–82.

Codispoti, L.A., Lowman, D., 1973. A reactive silicate budget for the Arctic Ocean. Limnology and Oceanography 18, 448–456.

Codispoti, L.A., Owens, T.G., 1975. Nutrient transport through Lancaster Sound in relation to the Arctic Ocean's reactive silicate budget and the outflow of Bering Strait waters. Limnology and Oceanography 20, 115–119.

Collier, R., Dymond, D., Honjo, S., Manganini, S.J., Francois, R., Dunbar, R., 2000. The vertical flux of biogenic and lithogenic material in the Ross Sea: moored sediment trap observations 1996–1998. Deep-Sea Research II 47, 3491–3520.

Colony, R., Thorndike, A.S., 1985. Sea ice motion as a drunkard's walk. Journal of Geophysical Research 90, 965–974.

Comiso, J.C., Yang, J., Honjo, S., Krishfield, R.A., 2003. Detection of change in the Arctic using satellite and in situ data. Journal of Geophysical Research 108 (C12), 3384. doi:10.1029/2002JC001347.

Cota, G.F., Pomeroy, L.R., Harrison, W.G., Jones, E.P., Peters, F., Sheldon Jr., W.M., Weingartner, T.R., 1996. Nutrients, primary production and microbial heterotrophy in the southern Chukchi Sea: Arctic summer nutrient depletion and heterotrophy. Marine Ecology Progress Series 135, 242–258.

Cota, G.F., Pomeroy, L.R., 2003. Arctic Nutrient Data Base 1904–2000. <http://www.eol.ucar.edu/projects/sheba/>.

Darby, D.A., Naidu, A.S., Mowatt, T.C., Jones, G.A., 1989. Sediment composition and sedimentary processes in the Arctic Ocean. In: Herman, Y. (Ed.), The Arctic Seas: Climatology, Oceanography, Geology and Biology. Van Nostrand Reinhold, New York, pp. 657–720.

Drenzek, N.J., Montluçon, D.B., Yunker, M.B., Macdonald, R.W., Eglinton, T.I., 2007. Constraints on the origin of sedimentary organic carbon in the Beaufort Sea from coupled molecular ^{13}C and ^{14}C measurements. Marine Chemistry 103, 146–162.

Dunbar, R., Leventer, A.R., Mucciarone, D.A., 1998. Water column sediment fluxes in the Ross Sea, Antarctica: atmospheric and sea ice forcing. Journal of Geophysical Research 103, 741–759.

Eglinton, G., Hamilton, R.J., 1963. The distribution of alkenes. In: Swan, T. (Ed.), Chemical Plant Taxonomy. Academic Press, London, pp. 187–208.

Eglinton, G., Hamilton, R.J., 1967. Leaf epicuticular waxes. Science 156, 1322–1335.

Eicken, H., Gradinger, R., Gaylord, A., Mahoney, A., Rigor, I., Melling, H., 2005. Sediment transport by sea ice in the Chukchi and Beaufort Seas. Deep-Sea Research II 52, 3271–3302.

Ekwurzel, B., Schlosser, P., Mortlock, R.A., Fairbanks, R.G., 2001. River runoff, sea ice, and Pacific water distribution and mean residence times in the Arctic Ocean. Journal of Geophysical Research 106, 9075–9092.

Engel, A., Passow, U., 2001. Carbon and nitrogen content of transparent exopolymer particles (TEP) in relation to Alcian Blue adsorption. Marine Ecology Progress Series 219, 1–10.

Engel, A., Goldthwait, S., Passow, U., Alldredge, A.L., 2002. Temporal decoupling of carbon and nitrogen dynamics in mesocosm diatom bloom. Limnology and Oceanography 47, 753–761.

Fahl, K., Nöthig, E-M., 2007. Lithogenic and biogenic particle fluxes on the Lomonosov Ridge (Central Arctic Ocean) and their relevance for sediment accumulation: vertical vs. lateral transport. Deep-Sea Research I 54, 1256–1272.

Fischer, G., Ratmeyer, V., Wefer, G., 2000. Organic carbon fluxes in the Atlantic and the Southern Ocean: relationship to primary production compiled from satellite radiometer data. Deep-Sea Research II 47, 1961–1997.

Fischer, G., Wefer, G., Romero, O., Dittert, N., Ratmeyer, V., Donner, B., 2003. Transfer of particles into the deep Atlantic and the Global Ocean: control of nutrient supply and ballast production. In: Wefer, G., Mulitsa, G., Ratmeyer, V. (Eds.), The Southern Atlantic in the Late Quarterly: Reconstruction of Material Budget and Current System. Springer-Verlag, Berlin, Heidelberg, pp. 21–46.

Forest, A., Sampei, M., Hattori, H., Makabe, R., Sasaki, H., Fukuchi, M., Wassmann, P., Fortier, L., 2007. Particulate organic carbon fluxes on the slope of the Mackenzie Shelf (Beaufort Sea): physical and biological forcing of shelf-basin exchanges. Journal of Marine Systems 68, 39–54.

Forest, A., Sampei, M., Hattori, H., Makabe, R., Sasaki, H., Barber, D.G., Gratton, Y., Wassmann, P., Fortier, L., 2008. The annual cycle of particulate organic carbon export in Franklin Bay (Canadian Arctic): environmental control and food web implications. Journal of Geophysical Research 113, CO3SO5. doi:10.1029/2007JC004262.

Francois, R., Honjo, S., Krishfield, R., Manganini, S., 2002. Factors controlling the flux of organic carbon to the bathypelagic zone of the ocean. Global Biogeochemical Cycles 16, 1087.

Fukuchi, M., Sasaki, Hattori, H., Matsuda, O., Tanimura, A., Handa, N., McRoy, C.P., 1993. Temporal variability of particulate flux in the northern Bering Sea. Continental Shelf Research 13, 603–704.

Goericke, R., Fry, B., 1994. Variations of marine plankton (^{13}C with latitude, temperature, and dissolved CO_2 in the world ocean. Global Biogeochemical Cycles 8, 85–90.

Goñi, M.A., Yunker, M.B., Macdonald, R.W., Eglinton, T.I., 2005. The supply and preservation of ancient and modern components of organic carbon in the Canadian Beaufort shelf of the Arctic Ocean. Marine Chemistry 93, 53–73.

Gosselin, M., Levasseur, M., Wheeler, P.A., Horner, F., Booth, B.V., 1997. New measurements of phytoplankton and ice algal production in the Arctic Ocean. Deep-Sea Research II 44, 1623–1644.

Gordienko, P.A., Laktionov, A.F., 1969. Circulation and physics of the Arctic Basin waters. Annuals of the International Geophysical Year 46, 94–112.

Gordon, L.I., Codispoti, L.A., Jennings Jr., J.C., Millero, F.J., Morrison, J.M., Sweeney, C., 2000. Seasonal evolution of hydrographic properties in the Ross Sea, Antarctica, 1996-1997. Deep-Sea Research II 47, 3095–3117.

Grantz, A., Phillips, R.L., Mullen, M.W., Starratt, S.W., Jones, G.A., Naidu, A.S., Finney, B.P., 1996. Character, paleoenvironment, rate of accumulation, and evidence for seismic triggering of Holocene turbidites, Canada Abyssal Plain, Arctic Ocean. Marine Geology 133, 51–73.

Grigoriev, M.H., Rachold, V.R., Hubberten, H.-W., Schirmeister, L., 2004. Organic carbon input to the Arctic Seas through coastal erosion. In: Stein, R., Macdonald, R.W. (Eds.), The Organic Carbon Cycles in the Arctic Ocean. Springer, Berlin, Heidelberg, pp. 41–55.

Guo, L., Macdonald, R.W., 2006. Source and transport of terrigenous organic matter in the upper Yukon River: evidence from isotope ($\delta^{13}C$, $\Delta^{14}C$, and $\delta^{15}N$) composition of dissolved, colloidal and particulate phases. Global Biogeochemical Cycles 20, GB2011. doi:10.1029/2005GB002593.

Hansell, D.A., Carlson, C.A., 2001. Deep ocean gradients in the concentration of dissolved organic carbon. Nature 393, 263–266.

Hansell, D.A., Kadko, D., Bates, N.R., 2004. Degradation of terrigenous dissolved organic carbon in the western Arctic Ocean. Science 304, 858–861.

Hare, S.R., Mantua, N.J., 2000. Empirical evidence for North Pacific regime shifts in 1977 and 1989. Progress in Oceanography 47, 103–145.

Hargrave, B.T., 2004. North Water Polynya. In: Stein, R., Macdonald, R.W. (Eds.), The Organic Carbon Cycles in the Arctic Ocean. Springer, Berlin, Heidelberg, pp. 103–106.

Hargrave, B.T., von Bodungen, B., Conover, R.J., Fraser, A.J., Phillips, G., Vass, W.P., 1989. Seasonal changes in sedimentation of particulate mater and lipid content of zooplankton collected by sediment trap in the Arctic Ocean off Axel Heiberg Island. Polar Biology 9, 467–475.

Hargrave, B.T., von Bodungen, B., Stoffyn-Egli, P., Mudie, P.J., 1994. Seasonal variability in particle sedimentation under permanent ice cover in the Arctic Ocean. Continental Shelf Research 14, 279–293.

Hargrave, B.T., Walsh, I.D., Murray, D.C., 2002. Seasonal and spatial patterns in mass and organic matter sedimentation in the North Water. Deep-Sea Research II 49, 5227–5244.

Hay, B.J., Honjo, S., Kempe, S., Ittekkot, V., Degens, E., Konuk, T., Izdar, E., 1990. Interannual variability in particle flux in the southwestern Black Sea. Deep-Sea Research 37, 911–928.

Holligan, P.M., Viollier, M., Harbour, D.S., Camus, P., Campagne-Phillips, M., 1983. Satellite and ship studies of coccolithophore production along a continental shelf edge. Nature 304, 339–342.

Honjo, S., 1990. Particle fluxes and modern sedimentation in the polar oceans. In: Smith, W. (Ed.), Polar Oceanography, Part B. Academic Press, San Diego, pp. 684–739.

Honjo, S., 1996. Fluxes of particles to the interior of the open oceans. In: Ittekkot, V., Schafer, P., Honjo, S., Depetris, P.J. (Eds.), Particle Flux in the Ocean. J. Wiley & Sons, New York, pp. 91–154.

Honjo, S., 2004. Particle export and the biological pump in the Southern Ocean. Antarctic Science 16, 501–516.

Honjo, S., Takizawa, T., Krishfield, R.A., Kemp, J., Hatakeyama, K., 1995a. Drifting buoys make discoveries about interactive processes in the Arctic Ocean. EOS, Transactions, American Geophysical Union 76, 209–219.

Honjo, S., Dymond, J., Collier, R., Manganini, S.J., 1995b. Export production of particles to the interior of the equatorial Pacific Ocean during the 1992 EqPac experiment. Deep-Sea Research 42, 831–870.

Honjo, S., Francois, R., Manganini, S., Dymond, J., Collier, R., 2000. Particle fluxes to the interior of the Southern Ocean in the Western Pacific sector along 170°W. Deep-Sea Research II 47, 3521–3548.

Honjo, S., Manganini, S.J., Cole, J.J., 1982. Sedimentation of biogenic matter in the deep ocean. Deep-Sea Research 29, 609–625.

Honjo, S., Manganini, S.J., Krishfield, R.A., Francois, R., 2008. Particulate organic carbon fluxes to the ocean interior and factors controlling the biological pump: a synthesis of global sediment trap programs since 1983. Progress in Oceanography 76, 217–285.

Honjo, S., Manganini, S.J., Wefer, G., 1988. Annual particle flux and a winter outburst of sedimentation in the northern Norwegian Sea. Deep-Sea Research 35, 1223–1234.

Hwang, J., Eglinton, T., Krishfield, R.A., Manganini, S.J., Honjo, S., 2008. Lateral organic carbon supply to the deep Canada Basin. Geophysical Research Letters 35, L11607. doi:10.1029/2008GL034271.

Hwang, J., Manganini, S.J., Montlucon, D.B., Eglinton, T.I., 2009. Dynamics of particle export on the Northwest Atlantic margin. Deep-Sea Research I 56, 1792–1803.

Iglesias-Rodriguez, M.D., Halloran, P.R., Rickaby, R.E.M., Hall, I.R., Colmenero-Hidalgo, E., Gittins, J.R., Green, D.R.H., Tyrrell, T., Gibbs, S.J., von Dassow, P., Rehm, E., Armbrust, E.V., Boessenkool, K.P., 2007. Phytoplankton calcification in a high-CO_2 world. Science 320, 336–340.

Ittekkot, V., 1991. Particle flux studies in the Indian Ocean. EOS 72, 527–530.

Ivanov, V.V., Shapiro, G.I., Huthnance, J.M., Aleynik, D.L., Golovin, P.N., 2004. Cascade of dense water around the world ocean. Progress in Oceanography 90, 47–98.

Johannessen, O.M., Miles, M.W., Bjorgo, E., 1995. The Arctic's shrinking sea ice. Nature 376, 126–127.

Jones, E.P., 2001. Circulation in the Arctic Ocean. Polar Research 20, 139–146.

Jones, E.P., Coote, A.R., 1980. Nutrient distributions in the Canadian Aerchipelago: indicators of summer water-mass and flow characteristics. Canadian Journal of Fisheries, Aquatic Science 37, 589–599.

Jones, G.A., Gagnon, A.R., Schneider, R.J., Von Reden, K.F., McNichol, A.P., 1994. High precision AMS radiocarbon measurements of Central Arctic Ocean waters. Nuclear Instruments and Methods, Section B 92, 426–430.

Jones, E.P., Nelson, D.M., Treguer, P., 1990. Chemical oceanography. In: Smith, W. (Ed.), Polar Oceanography, Part B. Academic Press, San Diego, pp. 407–476.

Jones, E.P., Swift, J.H., Anderson, L.G., Lipozer, M., Civitarese, G., Falkner, K.K., Katner, G., McLaughlin, F., 2003. Tracing Pacific water in the North Atlantic. Journal of Geophysical Research 108 (C4), 3116. doi:10.1029/2001JC001141.

Kadko, D., Pickart, R.S., Mathis, J., 2008. Age characteristics of a shelf-break eddy in the western Arctic and implication for shelf-basin exchange. Journal of Geophysical Research 113, C0218. doi:10.1029/2009JC004429.

Kawahata, H., Nishimura, A., Gagan, M.K., 2002. Seasonal change of foraminiferal production in the western equatorial Pacific warm pool: evidence from sediment trap experiments. Deep-Sea Research II 40, 2783–2800.

Kawahata, H., Suzuki, A., Ohata, H., 2000. Export fluxes in the Western Pacific warm pool. Deep-Sea Research I 47, 2061–2091.

Kempe, S., Knaack, H., 1996. Vertical particle flux in the western Pacific below the north equatorial current and the equatorial counter current. In: Ittekkot, V., Schafer, P., Honjo, S., Depetris, P.J. (Eds.), Particle Flux in the Ocean. J. Wiley & Sons, New York, pp. 313–323.
Kemp, J., Newhall, K., Ostrom, W., Krishfield, R., Proshutinsky, A., 2005. The Beaufort Gyre Observation System 2004: Mooring Recovery and Deployment Operations in Pack Ice. Technical Report of Woods Hole Oceanographic Institution, WHOI-2005-05, p. 33.
King, J.E., 1954. Variations in zooplankton abundance in the central equatorial Pacific 1950–1952. In: Symposium in Marine and Freshwater Plankton in the Indo-Pacific. Bangkok-1954, FAO, UNESCO, pp. 10–17.
Klages, M., Boetius, A., Christensen, J.P., Deubel, H., Piepenburg, D., Schewe, I., Soltwedel, T., 2004. The Benthos of Arctic seas and its role for the organic carbon at the sea floor. In: Stein, R., Macdonald, R.W. (Eds.), The Organic Carbon Cycles in the Arctic Ocean. Springer, Berlin, Heidelberg, pp. 139–167.
Kobayashi, F., Takahashi, K., 2002. Distribution of diatoms along the equatorial transect in the western and central Pacific during the 1999 La Nina conditions. Deep-Sea Research Part 2 (49), 2801–2821.
Krishfield, R.A., Honjo, S., Takizawa, T., Hatakeyama, K., 1999. Ice Environmental Buoy Program: Archived Data Processing and Graphical Results from April 1992 through November 1998. Technical Report WHOI-99-12, Woods Hole Oceanographic Institution, 83pp.
Lalande, C., Forest, A., Barber, D.G., Gratton, Y., Fortier, L., 2009a. Variability in the annual cycle of vertical particulate organic carbon export on Arctic shelves: contrasting the Laptev Sea, Northern Baffin Bay and the Beaufort Sea. Continental Shelf Research 29, 2157–2165.
Lalande, C., Belanger, S., Fortier, L., 2009b. Impact of a decreasing sea ice cover on the vertical export of particulate organic carbon in the northern Laptev Sea, Siberian Arctic Ocean. Geophysical Research Letters 36, L21604. doi:10.1029/2009GL040570.
Lisitzin, A.P., 1995. The marginal filter of the ocean. Oceanology 34, 583–590.
Longhurst, A., Sathyendranath, S., Platt, T., Caverhill, C., 1995. Estimate of global primary production in the ocean from satellite radiometer data. Journal of Plankton Research 17, 1245–1271.
Macdonald, R.W., 1996. Awakenings in the Arctic. Nature 380, 286–287.
Macdonald, R.W., Carmack, E.C., 1991. Age of Canadian Basin deep waters: a way to estimate primary production for the Arctic Ocean. Science 254, 1348–1350.
Macdonald, R.W., Carmack, E.C., Wallace, D.W.R., 1993. Tritium and radiocarbon dating of Canada Basin deep waters. Science 259, 103–104.
Macdonald, R.W., Carmack, E.C., McLaughlin, F.A., Falkner, K.K., Swift, J.H., 1999. Connections among ice, runoff and atmospheric forcing in the Beaufort Gyre. Geophysical Research Letters 26, 2223–2226.
Macdonald, R.W., McLaughlin, F.A., Carmack, E.C., 2002. Freshwater and its sources during the SHEBA drift in the Canada Basin of the Arctic Ocean. Deep-Sea Research I 49, 1769–1785.
Macdonald, R.W., Naidu, A.S., Yunker, M.B., Gobell, C., 2004a. The Beaufort Sea: distribution, sources, fluxes and burial rates of organic carbon. In: Stein, R., Macdonald, R.W. (Eds.), The Organic Carbon Cycles in the Arctic Ocean. Springer, Berlin, Heidelberg, pp. 177–193.
Macdonald, R.W., Sakshaug, E., Stein, R., 2004b. The Arctic Ocean: modern status and recent climate changes. In: Stein, R., Macdonald, R.W. (Eds.), The Organic Carbon Cycles in the Arctic Ocean. Springer, Berlin, Heidelberg, pp. 6–21.
Macdonald, R.W., Solomon, S.M., Cranston, R.E., Welch, H.E., Yunker, M.B., Gobeil, C., 1998. A sediment and organic carbon budget for the Canadian Beaufort shelf. Marine Geology 144, 255–273.
Maita, Y., Yamada, M., Takahashi, T., 1999. Seasonal variation in the process of marine organism production based on downward fluxes of organic substances in the Bering Sea. In: Loughlin, T.R., Ohtani, K. (Eds.), Dynamics of the Bering Sea. University Alaska Sea Grant AK-SG-99-03, University of Alaska, Fairbanks, pp. 341–352.
Manganini, S.J., Chandler, C.L., Honjo., S., 2007. JGOFS Program Office, Wood Hole Oceanographic Institution, Woods Hole, MA, USA <http://usjgofs.whoi.edu/mzweb/data/Honjo/sed_traps.html>.
Maslanik, J.A., Serreze, M.C., Agnew, T., 1999. On the record reduction in 1998 western Arctic sea ice cover. Geophysical Research Letters 26, 1905–1908.
Mathis, J.T., Pickart, R.S., Hansell, D.A., Kadko, D., Bates, N.R., 2007. Eddy transport of organic carbon and nutrients from the Chukchi Shelf: impact on the upper halocline of the western Arctic Ocean. Journal of Geophysical Research 112, CO5011. doi:10.1029/2006JC003899.
McCave, I.N., Hall, I.R., Antia, A.N., Chou, L., Dehaires, F., Lampit, R.C., Thompson, L., van Weeering, T.C.E., Wollast, R., 2001. Distribution, composition and flux of particulate material over the European margin at 47–50°. Deep-Sea Research II 34, 267–285.
McGuire, D.A., Anderson, L.G., Christensen, R.R., Dallmore, S., Guo, L., Hays, D.J., Heimann, M., Lorensen, T.D., Macdonarld, R.W., Roulet, N., 2009. Sensitivity of the carbon cycle in the Arctic to climate change. Ecological Monographs 79, 532–555.
McNichol, A.P. et al., 1994. TIC, TOC, DIC, DOC, PIC, POC-unique aspects in the preparation of oceanographic samples for ^{14}C-AMS. Nuclear Instruments and Methods in Physics Research Section B 92, 162–165.
Melnikov, I.A., Kolosova, E.G.H., Welch, E., Zhitina, L.S., 2002. Sea ice biological communities and nutrient dynamics in the Canada Basin of the Arctic Ocean. Deep-Sea Research I 49 (9), 1623–1649.
Moran, S.B., Ellis, K.M., Smith, J.N., 1997. ^{234}Th/^{238}U disequilibrium in the Central Arctic Ocean: implications for particulate organic carbon export. In: Milliman, J.D. (Ed.), Topical Studies in Oceanography, 1994 Arctic Ocean Section. Deep-Sea Research, Part II 44 (8), 1593–1606.
Morison, J., Aagaard, K., Teele, M., 2000. Recent environmental changes in the Arctic: a review. Arctic 53, 359–371.
Moritz, R.E., Perovich, D.K., 1996. Surface Heat Budget of the Arctic Ocean Science Plan. ARCSS/AII Report Number 5, University of Washington, Seattle, 64 pp.
Müller, P.J., 1977. C/N ratios in Pacific deep-sea sediments; effect of inorganic ammonium and organic nitrogen compounds adsorbed by clays. Geochemica Cosmochemica Acta 41, 765–776.
Naidu, A.S., Cooper, L.W., Grebmeleir, J.M., Whiteledge, T.E., Hameedi, M.J., 2004. The continental margin of the North Bering-Chukchi Sea: concentration, sources, fluxes, accumulation and burial rates of organic carbon. In: Stein, R., Macdonald, R.W. (Eds.), The Organic Carbon Cycles in the Arctic Ocean. Springer, Berlin, Heidelberg, pp. 193–204.
Naidu, A.S., Cooper, L.W., Finney, B.P., Macdonald, R.W., Alexander, C., Semiletov, I.P., 2000. Organic carbon isotope ratios (δ^{13}C) of Amerasian continental shelf sediments. International Journal of Earth Science 89, 522–532.
National Geophysical Data Center, NOAA, 2006. Digital Relief of the Surface of the Earth, ETOPO5 Bathimetry Data: Data Announcement 93-MGG-01, Boulder, Colorado. <http://www.ngdc.noaa.gov/mgg/fliers/06mgg01.html>.
Nelson, D.M., Anderson, R.F., Barber, R.T., Brzezinski, M.R., Buesseler, K.O., Chase, Z., Honjo, S., Marra, J., Martin, W.R., Sambrotto, R.N., Sayles, F.L., Sigmon, D.E., 2002. Vertical budgets for organic carbon and biogenic silica in the Pacific sector of the Southern Ocean, 1996–1998. Deep-Sea Research II 49 (9–10), 1645–1674.
Nozaki, Y., Oba, T., 1995. Dissolution of calcareous tests in the ocean and atmosphere carbon dioxide. In: Sakai, H., Nozaki, Y. (Eds.), Biogeochemical Processes and Ocean Flux in the Western Pacific. Terra Scientific Publishing, Tokyo, pp. 83–92.
O'Brien, M.C., Macdonald, R.W., Melling, H., Iseki, K., 2006. Particle fluxes and geochemistry on the Canadian Beaufort Shelf: implications for sediment transport and deposition. Continental Shelf Research 26, 41–81.
Ostrom, W., Kemp, J., Krishfield, R., Proshutinsky, A., 2004. Beaufort Gyre Freshwater Experiment: Deployment Operations and Technology 2003. Technical Report of the Woods Hole Oceanographic Institution, WHOI-2004-01, p. 32.
Overland, J.E., Salo, S.E., Kantha, L.H., Clayson, A.C., 1999. Thermal stratification and mixing on the Bering Sea shelf. In: Loughlin, T.R., Ohtani, K. (Eds.), The dynamics of the Bering Sea. University of Alaska Sea Grant AK-SG-03, University of Alaska, Fairbanks, pp. 129–146.
Parkinson, C.L., Cavarieli, D.J., Gloersen, P., Zwally, H.J., Comiso, J.C., 1999. Arctic sea ice extents, areas, and trends, 1978–1996. Journal of Geophysical Research 104 (C9), 20837–29856.
Perovich, D.K., Andreas, E.L., Curry, J.A., Eiken, H., Fairall, C.W., Grenfell, T.C., Guest, P.S., Intrieri, J., Kadko, D., Lindsay, R.W., McPhee, M.G., Morison, J., Moritz, R.E., Paulson, C.A., Pegau, W.S., Persson, P.O.G., Pinkel, R., Richter-Menge, J.A., Stanton, T., Stern, H., Sturm, M., Tucker III, W.B., Uttal, T., 1999. Year on ice gives climate insights. EOS, Transactions of the American Geophysical Union 80 (481), 485–486.
Pfirman, S., Lange, M.A., Wollenberg, I., Schlosser, P., 1990. Sea ice characteristics and the role of sediment inclusions in deep-sea deposition: Arctic–Antarctic comparisons. In: Bleil, U., Thiede, J. (Eds.), Geological History of the Polar Oceans: Arctic versus Antarctic. Kluwer Academic Publishers, Netherlands, pp. 187–211.
Pfirman, S., Crane, K., deFur, P., 1993. Arctic contaminant distribution. Northern Perspectives 21, 8–15.
Pfirman, S., Kogeler, J., Anselme, B., 1995. Coastal environments of the western Kara and eastern Barents Seas. Deep-Sea Research 42, 1391–1412.
Pilskaln, C.H., Manganini, S.J., Trull, T.W., Armand, L., Howard, W., Asper, V.L., Massom, R., 2004. Geochemical particle fluxes in the Southern Indian Ocean seasonal ice zone: Prydz Bay region, East Antarctica. Deep-Sea Research 51, 307–332.
Proshutinsky, A., Krishfield, R., Barber, D., 2009. Preface to special section on Beaufort Gyre climate system exploration studies: documenting key parameters to understand environmental variability. Journal of Geophysical Research 114, C00A08. doi:10.1029/2008JC005162.
Pry, R.K., Fleming, H.S., 1986. Bathymetry of the Arctic Ocean. Acoustics Division, Naval Research Laboratory MC-56.
Rachold, V., Eicken, H., Gordeev, V.V., Grigoriev, M.N., Hubberten, H.-W., Lisitzin, A.P., Shevchenko, V.P., Schirrmeister, L., 2004. Modern terrigenous organic carbon input to the Arctic Ocean. In: Stein, R., Macdonald, R.W. (Eds.), The Organic Carbon Cycles in the Arctic Ocean. Springer, Berlin, Heidelberg, pp. 35–55.
Reimnitz, E., 2002. Interactions of river discharge with sea ice in proximity of Arctic deltas: a review. Polarforschung 70, 123–134.
Reimnitz, E., Barnes, P.W., 1987. Sea-ice influence on Arctic coastal retreat. In: Kraus, N.C. (Ed.), Coastal Sediments '87: Proceedings of a Specialty Conference on Advances in Understanding of Coastal Sediment Processes, vol. 2. American Society of Civil Engineers, New York, pp. 1578–1591.
Reimnitz, E., Kempema, E.W., Weber, W. S., Clayton, J.R., Payne, J.R., 1990. Suspended-matter scavenging by rising frazil ice. In: Ackley, S.F., Weeks, W.F. (Eds.), Sea Ice Properties and Processes: Proceedings of the W.F. Weeks Sea Ice Symposium Held in San Francisco, California on December 1988. CRREL Monograph 90-1. Cold Regions Research and Engineering Laboratory, Hanover, New Hampshire, pp. 97–100.
Reimnitz, E., McCormick, M., McDougall, K., Brouwers, E., 1993a. Sediment export by ice rafting from a coastal polynya, Arctic Alaska, USA. Arctic and Alpine Research 25, 83–98.
Reimnitz, E., Barnes, P.W., Weber, W.S., 1993b. Particulate matter in pack ice of the Beaufort Gyre. Journal of Glaciology 39, 186–198.

Reimnitz, E., Dethleff, D., Nurnberg, D., 1994. Contrasts in Arctic shelf sea-ice regimes and some implications: Beaufort Sea versus Laptev Sea. Marine Geology 119, 215–225.

Rich, J., Gosselin, M., Sherr, E., Sherr, B., Kirchman, D.L., 1997. High bacterial production, uptake and concentration of dissolved organic matter in the Central Arctic Ocean. Deep-Sea Research II 44, 1645–1663.

Richter-Menge, J., 2008. Arctic: overview. In: State of the Climate in 2007. Special Supplement to the Bulletin of the American Meteorology Society 89 (7), S85–S97.

Rigor, I., 1992. Arctic Ocean buoy program. ARCOS Newsletter 44, 1–3.

Roach, A.T., Aagaard, K., Pease, C.H., Salo, S.A., Weingartner, T., Pavlov, V., Kulakov, M., 1995. Direct measurement of transport and water properties through the Bering Strait. Journal of Geophysical Research 100 (C9), 18443–18457.

Rothrock, D.A., Yu, Y., Maykut, G.A., 1999. Thinning of the Arctic sea ice cover. Geophysical Research Letters 26, 3469–3472.

Sakshaug, E., 2004. Primary and secondary production in the Arctic. In: Stein, R., Macdonald, R.W. (Eds.), The Organic Carbon Cycles in the Arctic Ocean. Springer, Berlin, Heidelberg, pp. 58–81.

Sampei, M., Sasaki, H., Hattori, H., Fukuchi, M., Hargrave, N.T., 2004. Fate of sinking particles, especially fecal pellets, within the epipelagic zone in the North Water (NOW) polynya of northern Baffin Bay. Marine Ecology Progress Series 278, 17–25.

Sampei, M., Forest, A., Sasaki, H., Hattori, H., Makabe, R., Fukuchi, M., Fortier, L., 2009. Attenuation of the vertical flux of copepod fecal pellets under Arctic sea ice: evidence for an active detrital food web in winter. Polar Biology 32 (2), 225–232.

Sapozhnikov, V.V., Arzhanova, N.V., Zubarevichi, V.V., 1993. Estimation of primary production in the ecosystem of the western Bering Sea. Russian Journal of Aquatic Ecology 2, 23–34.

Schell, D.M., Saupe, S., 1989. Primary production, carbon energetic, and nutrient cycling. In: Truett, J.C. (Ed.), Environmental Characterization and Biological Utilization of the North Aleutian Shelf Nearshore Zone. MMS/NOAA OCSEAP Report 60, pp. 99–140.

Shevchenko, V.P., Lisitzin, A.P., 2004. Aeolian input. In: Stein, R., Macdonald, R.W. (Eds.), The Organic Carbon Cycles in the Arctic Ocean. Springer, Berlin, Heidelberg, pp. 53–55.

Smith, K.L., Baldwin, R.J., Ruhl, H.A., Kahru, M., Mitchell, B.G., Kaufmann, R.S., 2006. Climate effect on food supply to depths greater than 4000 m in the northeast Pacific. Limnology and Oceanography 51, 166–176.

Smith, S.L., Schnack-Schiel, S.B., 1990. Polar zooplankton. In: Smith, W.O. (Ed.), Polar Oceanography: Part B. Chemistry, Biology and Geology. Academic Press, San Diego, pp. 527–598.

Springer, A.M., McRoy, C., Flint, M.V., 1996. The Bering Sea green belt: shelf edge processes and ecosystem production. Fish Oceanography 5, 205–223.

Stein, R., 1996. Organic carbon and carbonate distribution in Eurasian continental margin and Arctic Ocean deep-sea surface sediment: sources and passways. In: Stein, R., Ivanov, G.I., Levitan, M.A., Fharl, K. (Eds.), Surface Sediment Composition and Sedimentary Processes in the Central Arctic Ocean and along the Eurasian Continental Margin. Report on Polar Research 212, pp. 243–267.

Stein, R., Fahl, K., 2004. The Laptev Sea: distribution, sources, variability and burial of organic carbon. In: Stein, R., Macdonald, R.W. (Eds.), The Organic Carbon Cycles in the Arctic Ocean. Springer, Berlin, Heidelberg, pp. 213–237.

Stein, R., Macdonald, R.W., 2004. The Organic Carbon Cycle in the Arctic Ocean. Springer, Berlin, Heidelberg.

Stroeve, J., Holland, M.M., Meier, W., Scambos, T., Serreze, M., 2007. Arctic sea ice decline: faster than forecast. Geophysical Research Letters 34, L09501. doi:10.1029/2007GL029703.

Swift, J.H., Jones, E.P., Aagaard, E.C., Carmack, E.C., Hingston, M., Macdonald, R.W., McLaughlin, F.A., Perkin, R.G., 1997. Waters of Makarov and Canada Basin. Deep-Sea Research II 44, 1503–1529.

Sydor, M., 1988. Water Survey of Canada, Unpublished Data.

Takahashi, K., Fujitani, N., Yanada, M., Maita, Y., 1997. Five year long particle fluxes in the Central Subarctic Pacific and the Bering Sea. In: Tsunogai, S. (Ed.), Biogeochemical Processes in the North Pacific. Japan Marine Science Foundation, Tokyo, pp. 249–255.

Takahashi, K., Fujitani, N., Yanada, M., Maita, Y., 2000. Long-term biogenic particle fluxes in the Bering Sea and the central subarctic Pacific Ocean, 1990–1995. Deep-Sea Research I 47, 1723R–1759R.

Taylor, R., McLennan, S.M., 1981. The composition and evolution of the continental crust: rare earth element evidence from sedimentary rocks. Philosophical Transactions of the Royal Society of London 301, 381–399.

Thomsen, L., van Weering, T.C., 1998. Spatial and temporal viability of particulate matter in the benthic boundary layer at the North East Atlantic Continental Margin (Coban Spur). Progress in Oceanography 42, 61–76.

Tréguer, P., Jaques, G., 1992. Dynamics of nutrients and phytoplankton, and fluxes of carbon, nitrogen and silicon in the Antarctic Ocean. Polar Biology 12, 149–162.

Uttal, T., Curry, J.A., McPhee, M.G., Perovich, D.K., Moritz, R.E., Maslanik, J.A., Guest, P.S., Stern, H.L., Moore, J.A., Turenne, R., Heiberg, A., Serreze, M.C., Wylie, D.P., Persson, O.G., Paulson, C.A., Halle, C., Morison, J.H., Wheeler, P.A., Makshtas, A., Welch, H., Shupe, M.D., Intrieri, J.M., Stamnes, K., Lindsey, R.W., Pinkel, R., Pegau, W.S., Stanton, T.P., Grenfeld, T.C., 2002. Surface heat budget of the Arctic Ocean. Bulletin of the American Meteorological Society 83, 255–275.

Vinogradov, M.E., Shushkina, E.Z., Vedernikov, V.I., Nezlin, N.P., Gagarin, V.I., 1997. Primary production and plankton stocks in the Pacific Ocean and their seasonal variation according to remote sensing and field observations. Deep-Sea Research II 44, 1979–2001.

Volk, T., Hoffert, M.I., 1985. Ocean carbon pumps: analysis of relative strength and efficiencies of in ocean-driven circulation atmospheric CO_2 changes. In: Sundquist, E.T., Broecker, W.S. (Eds.), The Carbon Cycle and Atmospheric CO_2: Natural Variations Archean to Present; Proceeding of the Chapman Conference on Natural Variations in Carbon Dioxide and the Carbon Cycle, Geophysical Monograph Series, vol. 32. American Geophysical Union, Washington, DC, pp. 99–110.

Walsh, J.J., Dietele, D.A., 1994. CO_2 cycling in the coastal ocean: I. A numerical analysis of the southeastern Bering Sea, with applications to the Chukchi Sea and the northern Gulf of Mexico. Progress in Oceanography 34, 335–392.

Wassmann, P., 2004. Particulate organic carbon flux to the sea floor of the Arctic Ocean: quantity, seasonality and processes. In: Stein, R., Macdonald, R.W. (Eds.), The Organic Carbon Cycles in the Arctic Ocean. Springer, Berlin, Heidelberg, pp. 131–138.

Wheeler, P.A., Gosselin, M., Sherr, E., Thibaut, D., Kirkman, D.I., Benner, R., Whitledge, T.E., 1996. Active cycling of organic carbon and organic nitrogen in the Central Arctic Ocean. Nature 380, 697–699.

Wefer, G., Fischer, G., 1991. Annual primary production and export flux in the Southern Ocean from sediment trap data. Marine Chemistry 35, 599–613.

Wheeler, P.A., Watkins, J.M., Hansing, R.L., 1997. Nutrients, organic carbon and organic nitrogen in the upper water column of the Arctic Ocean: implications for the source of dissolved organic carbon. Deep-Sea Research II 44, 1571–1592.

Whitehouse, B.G., Macdonald, R.W., Iseki, K., Yunker, M.B., McLaughlin, F.A., 1989. Organic carbon and colloids in the Mackenzie River and Beaufort Sea. Marine Chemistry 26, 371–378.

Wong, C.S., Whitney, F.A., Crawford, D.W., Iseki, K., Matear, R.J., Johnson, W.K., Page, J.S., Timothy, D., 1999. Seasonal and interannual variability in particle fluxes of carbon, nitrogen and silicon from time series of sediment traps at Ocean Station P, 1982–1993: relationship to changes in subarctic primary productivity. Deep-Sea Research II 46, 2735–2760.

Wong, C.S., Whitney, F.A., Tsoy, I., Bychkov, A., 1994. Opal pump and subarctic carbon removal. In: 1994 Sapporo IGBP Symposium (Extended Abstract). Sapporo.

Yunker, M.B., Belicka, L.L., Harvey, H.R., Macdonald, R.W., 2005. Tracing the inputs and fate of marine and terrigenous organic matter in Arctic Ocean sediments: a multivariate analysis of lipid biomarkers. Deep-Sea Research II 52, 3478–3508.

Zernova, V.V., Nöthig, E.-M., Shevchenko, V.P., 2000. Vertical microalgae flux in the northern Laptev Sea (from the data collected by the year-long sediment trap). Oceanology 40, 801–808.